論文 / 著書情報
Article / Book Information

題目(和文)	乱流環境下における匂い源探知戦略の開発と数値流体シミュレーションのフレームワークにおける評価
Title(English)	Development of Odor Source Localization Strategy in Turbulent Environment and its Evaluation under Framework of Computational Fluid Dynamics
著者(和文)	Muis Muhtadi
Author(English)	Muis Muhtadi
出典(和文)	学位:博士(学術), 学位授与機関:東京工業大学, 報告番号:甲第11005号, 授与年月日:2018年9月20日, 学位の種別:課程博士, 審査員:中本 高道,三宅 美博,小野 功,石井 秀明,長谷川 晶一
Citation(English)	Degree:Doctor (Academic), Conferring organization: Tokyo Institute of Technology, Report number:甲第11005号, Conferred date:2018/9/20, Degree Type:Course doctor, Examiner:,,,,
学位種別(和文)	博士論文
Type(English)	Doctoral Thesis

Development of Odor Source Localization Strategy in Turbulent Environment and its Evaluation under Framework of Computational Fluid Dynamics

Muis Muhtadi

A thesis submitted for the degree of

Doctor of Philosophy

of Tokyo Institute of Technology

August 2018

Abstract

An autonomous sensing system has long been envisaged to help in a source localization task. This task has been increasingly important in our modern life for various critical applications, such as searching for chemical leakage in a factory infrastructure, searching for a fire in the early stage inside a building, detecting and searching for drugs in airports and harbors, as well as humanitarian missions such as searching for human victims under building rubles. Hence, advancement of odor source localization is demanded to enable such autonomous sensing system.

Although the idea of an autonomous sensing system has been arising for more than two decades and numerous works have been attempted to build it since then, to date, the system development has not achieved a practical application. The problem of odor source localization is related with the environmental condition and the localization method. The problem related with the environmental conditions is generally owing to the complicated odor distribution. An odor distribution in real world is generally governed by turbulent airflow resulting in temporally and spatially fluctuating distribution of an odor. As for the problem related with the localization method is generally rooted from the limitation of the chemical sensor. One of the limitation of the chemical sensor in general is not able to follow quick changes in the chemical concentration resulting in the sensor response delay which should be considered in odor source localization strategy.

The objective of this study is to develop an odor source localization strategy in computer simulation considering common issues in the study of odor source localization, such as; the real world environment having a turbulent airflow, odor sensors having response delay, inconsistent environment for evaluating localization strategies. The development was carried out gradually in three phases.

The first phase, a localization technique based on Gaussian distribution was studied. A time-invariant testing environment with Gaussian time-averaged odor distribution was created using MATLAB programming. Using this static environment, an odor source location can be estimated remotely by fitting the Gaussian distribution to several sensor responses observed at different locations. The estimation using a formation of multiple sensor nodes was affected by distance between the sensor nodes in the formation, the formation orientation towards wind direction, and the formation position in crosswind direction towards the source location. An odor source localization strategy using multiple sensor nodes was developed for this environment. Using principle of chemotaxis and anemotaxis, the strategy divides the nodes to have two different tasks; leading node and supporting node. The leading node has a task to track the plume toward the source using chemotaxis-anemotaxis strategy, whereas the supporting node moves zigzag while keeps up beside the leading node to collect odor information. The node which finds the highest odor concentration takes the role as the leading node and the others are the supporting nodes. This strategy, as simulated in MATLAB, showed its promising merit.

The second phase, a bio-inspired localization strategy was developed for a dynamic environment. For the testing environment, a turbulent environment was simulated using a Computational Fluid Dynamics (CFD) software. The environment is a closed room with an odor source on the floor and obstacles inside it. The localization strategy comprises searching for the plume centerline according to odor gradient (chemotaxis) and moving upwind along the centerline (anemotaxis). Direction to the plume centerline in crosswind direction is searched by using a zigzag scanning, i.e., collecting odor-concentration information to be used in an odor gradient estimation while moving zigzag. The odor gradient is estimated from a latest frame of time-series odor-concentration information obtained by a sensor node while moving. The estimation employs a regression technique to compute the model function from which the gradient function can be derived. To increase the accuracy of this estimation, a moving average filter is applied to the data before determining the model function. An estimation method based on an adaptive threshold was also developed and the efficacy was compared with the regression-based estimation. The performance evaluation shows that the strategy with regression-based estimation outperforms the strategy with adaptive threshold-based estimation with success rate above 95%.

The final phase, the strategy was further developed to consider odor sensor with response delay. To implement a realistic odor sensor with response delay, a sensor calibration model and a dynamic response model were applied in the sensing method. A new method for estimation of plume centerline was developed to exploit a transient sensor response. Similar regression technique as used in the previous phase was used here to determine the plume edges. The plume start and ending edges along the crosswind direction can be estimated accurately based on the gradient sign. The centerline can be estimated around the central points between the edges. Although the localization used sensor response which does not accurately represent the actual odor concentration, the gradient can still estimate the trend of odor concentration quite accurately and be used to navigate the localization with success rate above 71%.

In this study, the strategy of odor source localization with high efficiency for the dynamic environment with wind turbulence is demonstrated under the framework of computational fluid dynamics even when the sensor response delay is considered.

Acknowledgments

I am grateful to all those who have supported and encouraged me during my PhD study. Foremost, I would like to express my gratitude to my academic supervisor Prof. Takamichi Nakamoto for his expert support and guidance, insightful discussion and meticulous check on my writings.

I would like to thank all members of Nakamoto lab, in alphabetically order, Bartosz Wyszynski, Dani Prasetyawan, Deng Lin, Fan Fu, Gui Ping Qi, Katsuhito Akahane, Kazuki Hashimoto, Kei Ichikawa, Lu Qiaochu, Masaaki Iseki, Misato Takahasi, Parthojit Chakraborty (PJ), Ma Shuhan, Kaoru Nakazawa, Ryo Nagasaka, Ryoji Kurihara, Sawit Na Songkhla, Shingo Kato, Shiori Ito, Sota Kimura, Takayoshi Inuma, Tanoy Debnath, Yasufumi Yokoshiki, Yoshiki Hashimoto, Yosuke Maruno, Yuhei Tsuji, Yuji Nozaki, Yuji Sukekawa, Yuki Harada, Yuta Shuto, Yuta Yasuda, Yuki Kinoshita, and Zhan Wei, who helped directly or indirectly in various academic and daily matters, and made the lab an exiting place for study with their kind friendship. My special thanks to Dr. Totok Mujiono for various encouragements, advises and helps prior to and during this PhD study. My thanks goes also to short-term members of the lab, Ha Nguyen (YSEP exchange student), Li Qun (visiting researcher), Nitikarn Nimsuk (post doctoral researcher), Ollila Sami Iivari (YSEP exchange student), and Yan Lin (JICA trainee), for sharing interesting academical and cultural insights and for their kind friendship. I would like to thank the lab secretaries, Mika Kondo, Sumiyo Imai, and Rika Saijo, who kindly helped in various academics administrative documents.

I would like to thank Prof. Hideaki Ishii, Prof. Isao Ono, Prof. Shoichi Hasegawa, and Prof. Yoshihiro Miyake for their constructive inputs and encouragements during the thesis defense presentations.

I would like to gratefully acknowledge Indonesian Government who supported this study financially through Indonesia Endowment Fund for Education (LPDP) scholarship.

Finally, I would like to thank my family and friends for supporting me throughout my PhD study, especially my parents and my wife Safira who provided me support and understanding during the study.

Contents

List of Figures

Chapter 1

Introduction

Disasters due to man-made cause or nature frequently bring destruction to building in a large scale resulting a lot of victims trapped beneath building rubbles. In such catastrophic circumstances, emergency operation to rescue the survivors need to be performed as quickly as possible to minimize human fatalities especially when considering that the first 24 hour are very critical to rescue a trapped victim. In this case, the first responder team need to find the survivors among building rubbles. In such rescue operation, a trained dog is often used to localize the victims by tracking the odor. Unfortunately, training a dog for rescue operation takes an immense amount of time and human labor. This makes such dog typically a limited resource in a large scale disaster situation. Hence, an autonomous sensing system has long been envisaged which is capable of localizing an odor source as the dog does. When such system is successfully realized into application, it could help not only in a disaster aftermath for localizing human victims but also in a disaster prevention operation, such as to detect dangerous gas leakages, a fire at its initial stage, etc. If the odor source is generalized to be any chemical liquid, then such system has also potentially important contribution for underwater application, for example, searching for contaminant sources and explosive ordnance under the sea, etc.

Although the idea of an autonomous sensing system has been arising for more than two decades and numerous works have been attempted to build it since then, to date, the system development has not achieved a practical application [3]. The problem of odor source localization is combination of *environmental conditions* and *localization method*. The problem related with the environmental conditions is generally owing to the complicated odor distribution. An odor distribution in real world is generally governed by turbulent airflow resulting in temporally and spatially fluctuating distribution of an odor. A deeper discussion about odor distribution is provided in Section 1.3, whereas the problem related with the localization method in most cases is closely associated with the type of odor sensors being used. Each type of sensors has different performance characteristic as described in Section 1.4. There are several performance indicators of sensors, among which *sensitivity*, *selectivity* and *response time* are the main indicators. These main indicators are particularly important considerations for designing a source localization system. As an example, one of the critical issue for odor source localization strategy in turbulent environment is sensor response time. In such environment, odor distribution changes dynamically owing to turbulent airflow. In this case, The localization strategy need to take into account the response delay. A deeper discussion about gas sensing technology is provided in Section 1.4.

1.1 Odor source localization strategy

Odor source localization is essential routine for most animals for foraging, reproductive activities, homing, etc., e.g., lobsters and crabs track scents toward the food [4, 5], male moths locate the females by tracking the emitted pheromone [6], and homing by salmons [7]. These animals employ both chemical and fluid dynamics information to track an odor plume toward the source in turbulent environment [5,8]. Thus, many studies have been carried out to understand and try mimicking the animals plume tracking mechanisms for artificial tracking system [5, 9]. These studies uncovered animal's behavioral mechanisms to track turbulent plumes which generally integrate sort of chemically driven orientation, *chemotaxis*[1] , with a visual or mechanical evaluation of flow condition in order to steer upwind, *anemotaxis*[2]. These mechanisms appear as zigzag pattern movement along odor plume toward the source.

Numerous artificial odor/gas source localization techniques/strategies are developed by taking inspiration from animal's strategy which is known as *bio-inspired* strategy. In order to take advantage of computation technology and distributed system which may not be used in animals strategy, many strategies were developed to employ probabilistic (stochastic) theory, spatial odor mapping, and multiple sensing agents. Lilienthal et al. [10], Kowadlo and Russel [3], and Ishida et al. [11] made comprehensive surveys on chemical source localization strategies. In this thesis, the author developed a simplified classification of the localization strategies mainly based on the utilization method of chemical (chemotaxis) and flow information (anemotaxis) regardless of environmental flow conditions (laminar of turbulent), as shown in Figure 1.1. In this classification, the strategies are classified into five groups: *odor gradient following*, *odor plume tracking*, *odor distribution mapping*, *source estimation or odor tracking using probabilistic method*, and *odor tracking using optimization method*.

[1]Chemotaxis: orientation or movement of an organism or cell in relation to chemical agents (Merriem Webster Dictionary).

[2]Anemotaxis: oriented movement in response to a current of "fluid" (according to the Random House Unabridged Dictionary, where "air" has been generalized to "fluid").

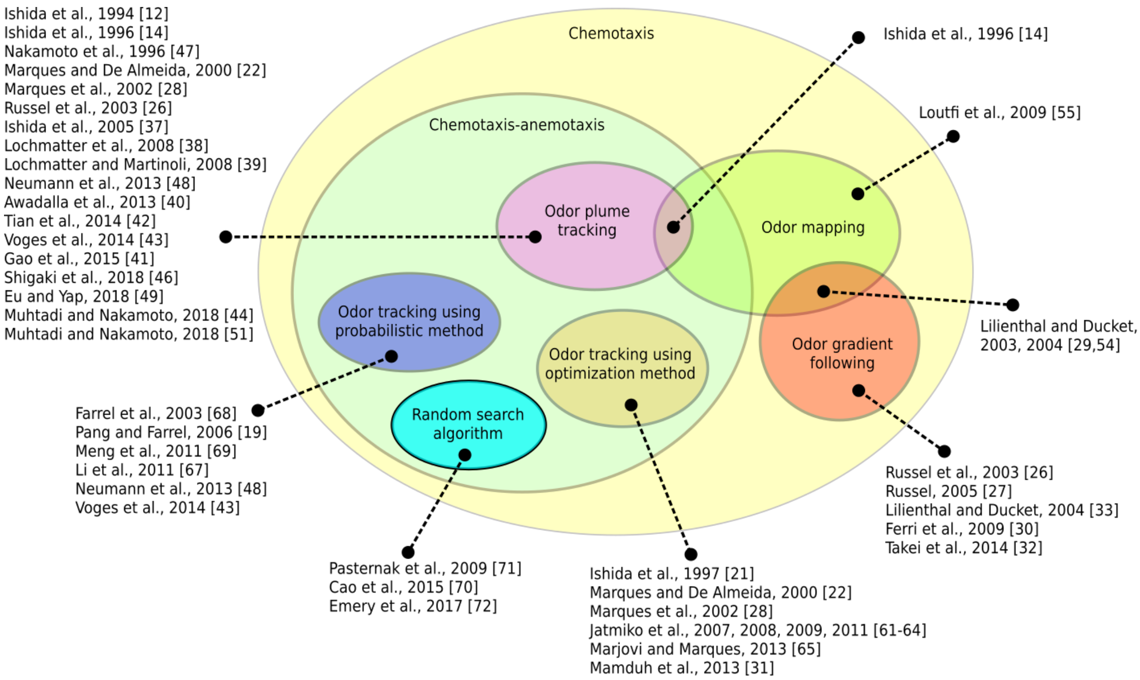

Figure 1.1: Venn diagram of odor source localization strategies.

Extensive works have been made in the last three decades to develop odor source localization strategies suitable for turbulent environment. These works attempted to push the technique development toward real world application by addressing the general characteristics of odor distribution in the real world environment which is governed by turbulent flow. A large number of the localization were developed based on strategy of chemotaxis and anemotaxis (bio-inspired). This strategy comprises searching for a chemical *plume*[3] followed by tracking the plume using chemical and anemometric sensors. The first model of chemotaxis-anemotaxis based localization systems built into localizing robot was reported by Ishida et al. [12–14] and Russel [15]. Inspiration of these systems came from insect's localization behavior, most notably male moth's behavior to track trails of the female's pheromone while flying [6]. In order to achieve higher performance or to address more difficult environment scenarios, some strategies used multiple sensing agents to do localization cooperatively using swarm technique [16–18]. A couple of localization strategies constructed an analytical map of odor or source probability distribution based on previously obtained data to remotely estimate the source location [19–25]. The strategies classified in 1.1 are briefly reviewed in the following sections.

[3]Plume: a long cloud of smoke or vapor resembling a feather as it spreads from its point of origin (Oxford Living Dictionary).

1.1.1 Odor gradient following

The strategy to localize an odor source by following the spatial odor gradient is known as *gradient-following* approach which is classified as a chemotaxis. In this approach, the rate of odor concentration change can be estimated according to some odor concentration information at different locations obtained simultaneously (tropotaxis) or obtained successively (klinotaxis). Then, the localization moves toward direction of gradient increase. Various source localization strategies were designed to use only chemical information for environments without airflow and weak airflow [22, 26–32], as shown in Figure 1.2. Russel [26] demonstrated chemotaxis approach in the *E. coli*-inspired algorithm as ilustrated in Figure 1.2a. Russel [27] reported the application for underground odor source localization. A robot with penetrating probe equipped with a chemical sensor, was designed to move in hexagonal path as illustrated in Figure 1.2b. Lilienthal [33], and Takei [32] implemented a chemotaxis approach using Braitenberg robots as illustrated in Figure 1.2c. Ferri [30] reported the implementation using a robot moving in spiral pattern as illustrated in Figure 1.2d. More detailed information of these reported experiments are summarized in Table 1.1.

Chemotaxis combined with anemotaxis has been implemented successfully with various method: odor plume tracking, source odor tracking using optimization method, and estimation or odor tracking using probabilistic method. Chemotaxis combined with spatial information processing has also widely investigated for odor mapping (plume mapping) to support odor source localization or for environmental monitoring application. These strategy approaches are explained in the following sections.

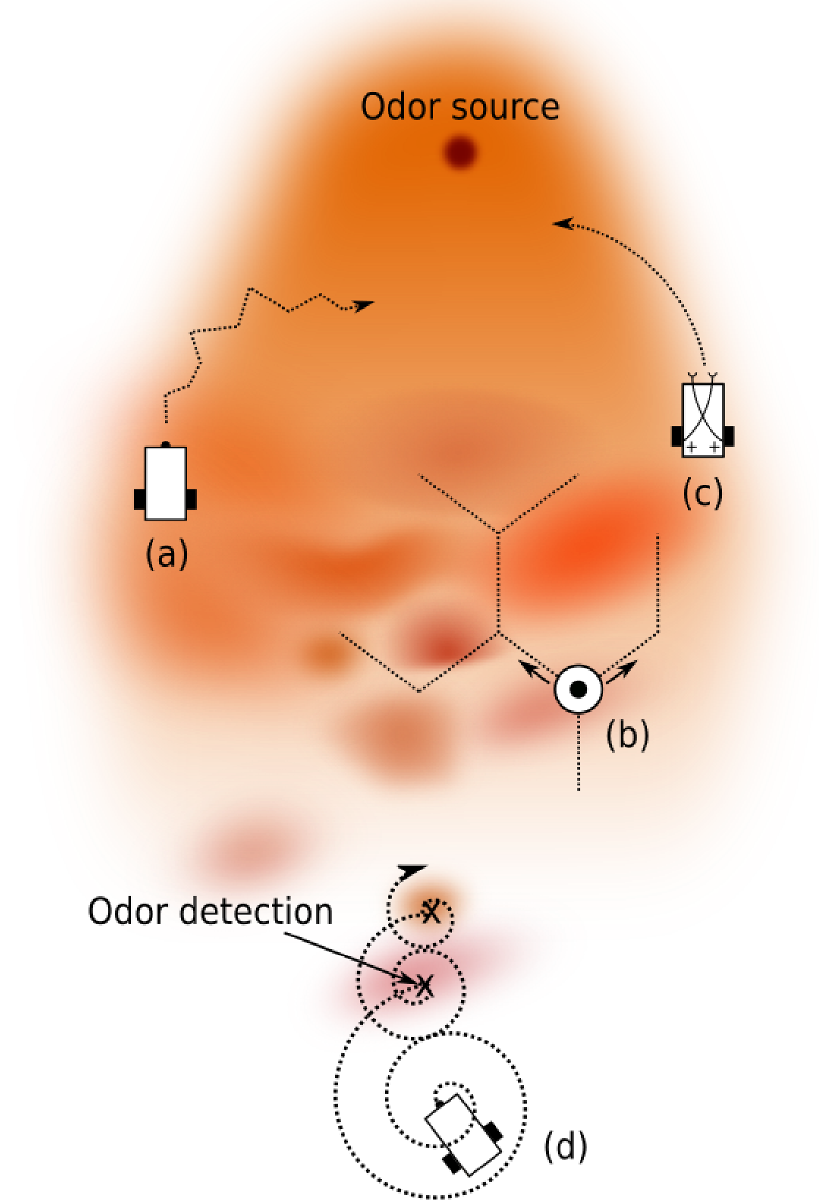

Figure 1.2: Various approaches of gradient-following strategy. (a) *E. coli*-based strategy, (b) strategy with hex-path movement, (c) Braitenberg-based strategy, and (d) spiral-based strategy.

Table 1.1: Odor gradient following strategy.

Approach	Methodology	Testing environment	Publication
Odor gradient following using random walk style.	Four strategies were investigated including pure chemotaxis and chemotaxis-anemotaxis. In simulation: a robot node equipped with an ideal gas sensor. In real experiment: a mobile robot was equipped with two polypyrrole-based gas sensors mounted on bilateral fixed positions, an airflow sensor. The odor gradient was estimated using tropotaxis method.	In simulation: environment without obstacle having a smooth chemical distribution. In real experiment, indoor environment without obstacle having turbulent airflow with an odor source on the ground.	Russel et al., 2003 [26]
Odor gradient following and hex-path movement pattern.	A mobile robot equipped with sand penetrating sensing probe containing a metal oxide gas sensor. The odor gradient was estimated using *klinotaxis*[4] method.	The environment was the surface of an area of dry coarse sand. An odor source was located underground.	Russel, 2005 [27]
Odor gradient following using Braitenberg style.	A mobile robot carried a portable e-nose comprising 6 tin oxide sensors of 3 different types. The sensors with different types were mounted into two tubes which equipped with a suction fan each. The odor gradient was obtained using *tropotaxis*[5] method. Two Braitenberg strategies (positive and negative tropotaxis) were investigated.	Indoor environment with turbulent and convective flow condition. An odor source on the ground.	Lilienthal and Duckett, 2004 [33]
	A mobile robot equipped with two metal oxide gas sensors; The robot used Braitenberg navigational control. The odor gradient was estimated using tropotaxis method.	Indoor environment. An odor source on the ground.	Takei et al., 2014 [32]
Odor tracking using spiral movement.	A mobile robot equipped with a metal oxide gas sensor. Chemotaxis was carried out using repetitive spiral movement. The spiral was restarted upon detecting odor. The odor gradient was estimated using klinotaxis method.	Indoor environment with no strong airflow and an odor source on the ground.	Ferri et al., 2009 [30]

1.1.2 Odor plume tracking

Most odor source localization strategies are main implemented by means of plume tracking as inspired by the biological strategy. The tracking incorporates chemotaxis to search for the plume and move toward it and anemotaxis that is to move upwind direction inside the plume. There are diverse implementations of the plume tracking on numerous reported studies for different target environment. Most of these studies implement a robotic tracking system for on-the-ground environment [12, 14, 22, 26, 28, 37–46]. These tracking systems mostly used odor and flow information across 2D spatial domain as the mobility of the robot is limited on the surface of the environment. However, some studies designed a localization system with capability of tracking plume in 3D space. Nakamoto et al. [47] proposed a portable odor compass which can be mounted to mobile robot or carried by human. Neuman et al. [48], and Eu et al. [49] developed a system for tracking an airborne odor above the ground using a flying drone. Tian et al. [42] investigated tracking strategy for underwater environment in a simulation and the validation in a real experiment.

Various strategies of tracking an odor plume mainly inspired by a flying moth strategy were reported. These strategies are illustrated in Figure 1.3. A tracking strategy employing a series of zigzags across the plume with a turning angle α toward upwind direction was introduced by Ishida [12, 14] and investigated by Russel [26], and Tian [42], as illustrated in Figure 1.3a. A tracking strategy combining an upwind surge zigzag movements and loops (spiral) was reported by Marques and De Almeida, 2000 [22], Marques et al. [28], Voges et al. [43], and Shigaki et al. [46], as illustrated in Figure 1.3e. An upwind surge combined with spiral was investigated by Lochmatter et al. [38, 39], Voges et al. [43] and Yap [49], as illustrated in Figure 1.3d. An upwind surge with zigzag search to acquire a plume was employed by Awadalla [40] and Eu and Yap [49], as illustraged in Figure 1.3f. An upwind surge combined with crosswind cast was introduced by Lochmatter and Martinoli [39, 50], as illustrated in Figure 1.3b. A tracking based on a pseudo gradient was introduced by Neumann et al. [48], as illustrated in Figure 1.3c.

In our study reported in the first journal publication [44], we developed an algorithm of upwind surge along the centerline for indoor closed room environment as illustrated in Figure 1.3g. In this environment, the plume is relatively continues and the odor gets accumulated by the time. As the result, the baseline concentration level is increasing by the time. Upon losing the plume, the algorithm checks crosswind gradient to estimate direction toward the centerline using a zigzag scanning. This algorithm works well assuming that the obtained odor information is accurate or an ideal odor sensor is used. When the sensor is not ideal, there is a response delay resulting in inaccurate odor information. Therefore the zigzag scanning does not result in accurate direction toward the centerline. To tackle this problem, we developed an algorithm of upwind surge along the centerline with plume edges search, as illustrated in Figure 1.3h. This algorithm is reported in our second paper which has been accepted for journal publication. In this algorithm, the centerline is determined from two edges of the plume along the crosswind direction. The plume tracking strategies from these reports are summarized in Table 1.2.

Plume identification is an integral part of plume tracking. The plume can be identified by simple concentration threshold or gradient. The threshold can be used to mark the assumed concentration level at the edges of the plume at crosswind direction, the centerline and the vicinity of the source. This way of plume identification is popular among the reported studies [12, 14, 22, 28, 37–42, 45]. Despite the simplicity, determining the proper threshold value is difficult in the real world application since the concentration at the plume centerline or the source is generally unknown. Instead of using a threshold, in our first journal paper [44], we introduced an identification method of plume centerline by an estimated odor gradient calculated using regression method. In our second journal paper [51], we applied the regression method to identify plume edges which is then used to estimate the centerline. In this report, a sensor model with response delay was used in the simulation. Owing to the response delay, an odor gradient is not reliable for identifying the centerline.

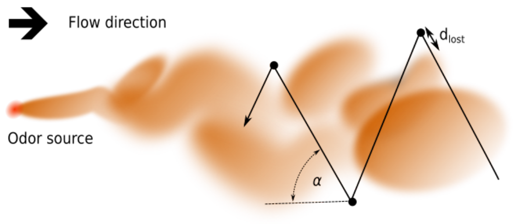

(a) Zigzag algorithm.

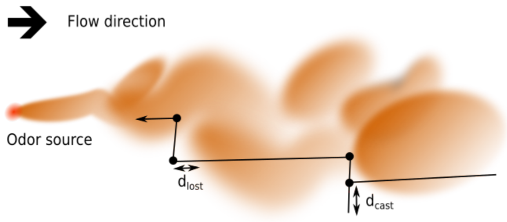

(b) Surge-cast algorithm.

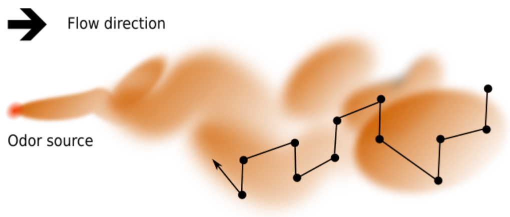

(c) Pseudo gradient-based algorithm.

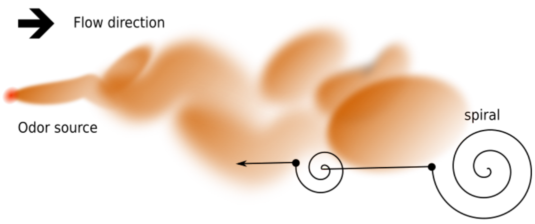

(d) Spiral algorithm.

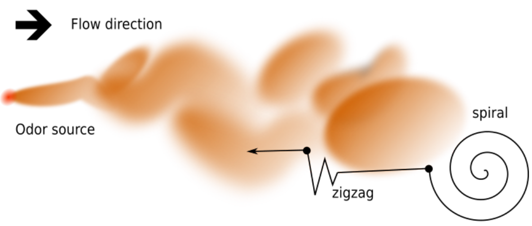

(e) Spiral-upwind-zigzag algorithm.

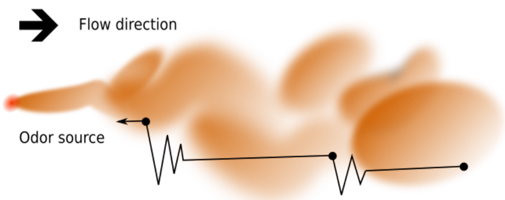

(f) Upwind surge with zigzag search algorithm.

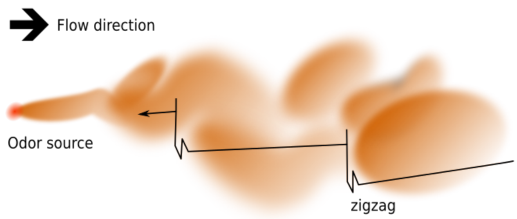

(g) Centerline-upwind surge algorithm.

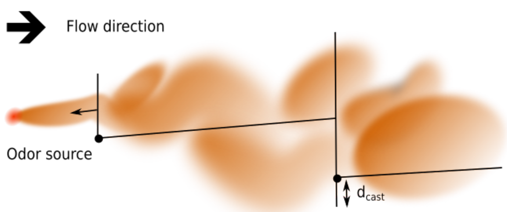

(h) Centerline-upwind surge with edges detection algorithm.

Figure 1.3: Various tracking strategies.

Table 1.2: Odor plume tracking strategy.

<table>
<tr><th>Approach</th><th>Methodology</th><th>Testing environment</th><th>Publication</th></tr>
<tr><td rowspan="2">Odor plume search and upwind surge along the plume (plume tracking).</td><td rowspan="2">4 metal oxide gas sensors for sensing ethanol information and 4 thermistor anemometric sensors for sensing wind direction are mounted at fixed positions on a mobile robot. The odor gradient was estimated using tropotaxis method.</td><td>Wind tunnel, turbulent airflow, small wind fluctuation. An odor source.</td><td>Ishida et al., 1994 [12]</td></tr>
<tr><td rowspan="2">Indoor environment without obstacle. Air ventilation was managed by 2 air supplies in the ceiling and 2 exhausts near floor outside the experiment space. An odor source on the ground.</td><td>Ishida et al., 1996 [14]</td></tr>
<tr><td>Active sampling</td><td>3D odor compass equipped with 4 metal oxide gas sensors and a suction fan. 2D odor compass equipped with 2 metal oxide gas sensors and a suction fan. The odor gradient was estimated using tropotaxis method.</td><td>Nakamoto et al., 1996 [47]</td></tr>
<tr><td rowspan="2">Odor plume search and upwind surge along the plume (plume tracking).</td><td>A mobile robot uses a sensing modality. E-nose and simple gas sensors were compared for the sensing modality. The odor gradient was estimated using tropotaxis method.</td><td>Indoor environment with obstacles and turbulent airflow condition and with two odor sources.</td><td>Marques and De Almeida, 2000 [22]
Marques et al., 2002 [28]</td></tr>
<tr><td>Silkworm-inspired and dung beetle-inspired strategies which consider upwind direction.
In simulation: a robot node equipped with an ideal gas sensor.
In real experiment: a mobile robot was equipped with two polypyrrole-based gas sensors mounted on bilateral fixed positions, an airflow sensor. The odor gradient was estimated using tropotaxis method.</td><td>In simulation: environment without obstacle having a smooth chemical distribution. In real experiment, indoor environment without obstacle having turbulent airflow with an odor source on the ground.</td><td>Russel et al., 2003 [26]</td></tr>
</table>

Table 1.2: Odor plume tracking strategy.

Approach	Methodology	Testing environment	Publication
	3 metal oxide gas sensors for sensing ethanol information and 2 thermistor anemometric sensors for sensing wind direction are mounted at fixed positions on a mobile robot. The odor gradient was estimated using tropotaxis method.	Indoor environment without obstacle and with an odor source on the ground. Airflow field was created using a fan. Air ventilation was managed by an air supply an exhaust outside the experiment space.	Ishida et al., 2005 [37]
	A mobile robot equipped with a volatile organic compound sensor and a wind sensor. Two strategies for reacquiring a plume were compared: casting (zig-zagging) and spiral-surge. The chemotaxis use binary odor information; detect odor or do not detect odor.	An indoor environment without obstacle. The airflow has laminar characteristic. An odor source.	Lochmatter et al., 2008 [38]
	A simulated mobile robot equipped with an ideal odor and wind direction sensors. Three strategies for reacquiring a plume were compared: casting (zig-zagging), surge-spiral and surge-cast. The chemotaxis use binary odor information; detect odor or do not detect odor.	Odor distribution used advection-diffusion model [52]. The airflow has laminar characteristic. An odor source is located on the ground.	Lochmatter and Martinoli, 2008 [39]
	An aerial drone equipped with an inertial measurement unit for estimating wind direction, an e-nose containing up to 4 metal oxides gas sensors and an electrochemical cell, and a gas detector containing a catalytic sensor, electrochemical and infrared sensors. Strategies using binary odor information and using tropotaxis gradient following were compared.	Outdoor aerial environment without obstacle has an odor source on the ground.	Neumann et al., 2013 [48]

Table 1.2: Odor plume tracking strategy.

Approach	Methodology	Testing environment	Publication
	A simulated mobile robot equipped with an ideal gas and flow sensor. The odor gradient was estimated using klinotaxis method.	A small scale model of indoor structured building containing rooms and corridors. An odor distribution was simulated in steady state mode using a CFD application. An odor source is located above the ground level.	Awadalla et al., 2013 [40]
	In simulation, a tracking robot equipped with chemical and flow sensing modality. In real experiment, an autonomous underwater vehicle equipped with multiple sensors, including an underwater fluorometer and a Doppler velocity log. The chemotaxis use binary odor information; detect odor or do not detect odor.	In simulation: an environment with a turbulent plume simulation model [53]. In real experiment: underwater ocean environment. An odor source underwater was searched using an autonomous underwater vehicle (AUV).	Tian et al., 2014 [42]
	A mobile robot equipped with an alive moth for the chemical sensing modality. In chemotaxis-anemotaxis, combinations with spiral and zigzag searches were investigated. The chemotaxis use binary odor information; detect odor or do not detect odor.	Indoor environment with turbulent flow condition. An odor source is located on the ground.	Voges et al., 2014 [43]
	A simulated sensor node equipped with 4 ideal gas sensors. The odor gradient was estimated using tropotaxis method. The focus is on the plume tracking.	Simulated environment with diffusive airflow condition; An odor source above the ground.	Gao et al., 2015 [41]
	The behavior of silkworm moth was analyzed to be mimicked for a chemical plume tracking using a ground robot. The robot was equipped with two ethanol sensors. An auto-regressive with exogenous input (ARX) model was used to estimate the sensor response timing.	Indoor environment with an odor source on the ground. Airflow field was created using a fan.	Shigaki et al., 2018 [46]

Table 1.2: Odor plume tracking strategy.

Approach	Methodology	Testing environment	Publication
	A 3D chemical plume tracking was implemented using a quadrotor. The quadrotor was equipped with 4 metal oxide gas sensors. A sensing algorithm using certainty factors and evidential reasoning was used to estimate the trend of transient sensor response.	Indoor environment with an odor source on the ground.	Eu and Yap, 2018 [49]
	A simulated sensor node equipped with an ideal an odor sensor and an anemometric sensor. The odor gradient was estimated using klinotaxis method.	Simulated indoor environment with an obstacle. An odor source is located on the ground.	Muhtadi and Nakamoto, 2018 [44]
	A simulated sensor node equipped with an odor sensor with response delay model and an ideal anemometric sensor. The odor gradient was estimated using klinotaxis method.	Simulated indoor environment with multiple obstacles. An odor source is located on the ground.	Muhtadi and Nakamoto, 2018 [51]

1.1.3 Odor mapping

The priority of odor distribution mapping is typically not to search for the odor source, but to collect odor information across a targeted area. In this case, localizing an odor source is a secondary task. Some studies carried out this mapping for environment monitoring purpose [29,54,55]. Therefore, the time required to localize an odor source in this task is generally long. This odor map can indicate also the likely location of odor source.

Some studies incorporated the mapping into the source localization system to improve the performance. Ishida et al. [14] used a latticed map (gridmap) for memorizing the previously searched area, as illustrated in Figure 1.4a. Similarly, a gridmap was also build by Lilienthal and Duckett [29, 54] collected odor information obtained during a source tracking for building a concentration map. Here a Gaussian weighting was used to model the decreasing likelihood of odor concentration around a measured point. In the report, Lilienthal and Duckett also investigated strategies to collect odor data for the gridmap; using a predefined path and using a reactive gas source tracking. Two predefined paths were proposed; a rectangular spiral path, as illustrated in Figure 1.4b, and a sweeping path, as illustrated in Figure 1.4c. The odor mapping strategies from these reports are summarized in Table 1.3.

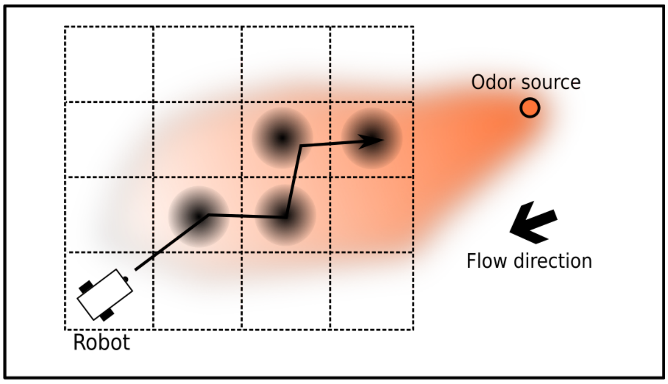

(a) Odor gridmap.

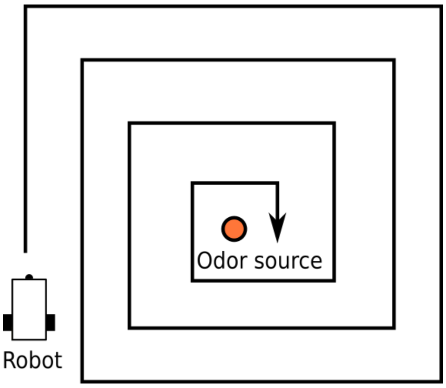

(b) Rectangular spiral path.

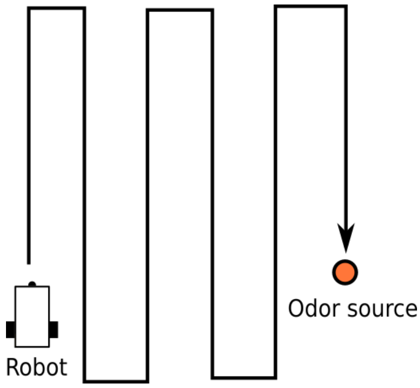

(c) Sweeping path.

Figure 1.4: Data acquisition strategy for odor mapping.

Table 1.3: Odor mapping strategy.

Approach	Methodology	Testing environment	Publication
Odor mapping on sub-divided cells of the search area.	The map is used to mark the searched area. The active cell including the stage position and the eight surrounding cells are marked every second.	Indoor environment without obstacle. Air ventilation was managed by 2 air supplies in the ceiling and 2 exhausts near floor outside the experiment space. An odor source on the ground.	Ishida et al., 1996 [14]
Kernel extrapolation gas distribution mapping.	6 semiconductor sensors of 3 different types were used. Two sets of sensors with different types were installed into two different tubes with a suction fan each. Two methods of data acquisition were investigated: predefined path and reactive gas source tracing.	Indoor environment without obstacle contains no dominant constant flow and an odor source on the ground.	Lilienthal and Duckett, 2003, 2004 [29, 54]
	Two e-noses in which each contains 4 semiconductor sensors with different types and a suction fan.	Four connecting corridors (semi-outdoor space) with 2 odor sources.	Loutfi et al. 2009 [55]

1.1.4 Odor tracking using optimization method

The plume in the real world environment is generally not regularly shaped. The turbulent airflow makes the plume meandering in random manner and thus the odor concentration in it is fluctuating temporally and spatially. However the time-averaged odor distribution in general is well predicted through Gaussian model [56]. This Gaussian distribution model is explained in

Section 1.3.1. Making use this Gaussian distribution model, Ishida et al. [21, 57] introduced a remote estimation of the source location by fitting the distribution model to its sensor response data using Nonlinear optimization algorithms, the gradient descent method [58] and Kalman filtering method [59]. The model fitting is performed after collecting some data while moving toward the source based on zigzag algorithm. Marques et al. [22, 28] also reported utilization optimization techniques based on a Gaussian odor distribution model in the plume tracking. Different from the Ishida's work which used pure gradient vector to determine the direction toward the source location, in Marques' works, the direction was defined as a linear combination of the gradient and the upwind vectors. This remote estimation of odor source is illustrated in Figure 1.5a.

Employing a Swarm Optimization approach [60], Jatmiko et al. [61–64], Marjovi and Marques [65], and Mamduh [31] investigated a localization strategy using multiple search agents, as is illustrated in Figure 1.5b. Multiple search agents having simple behavior and capability individually but organize well as a swarm based on simple rules can perform intelligent source localization collectively in a complex environment. Each search agent collects odor information and evaluates the best local position in term of highest ever found concentration and communicates with other agents to determine the best global position out of the best local positions. The formation of the agents are maintained according to a virtual repulsive-attractive force that is applied between each agent to its neighboring agents. As an example, in Figure 1.5b, a repulsion force is applied at two agents, e.g. between Robot1 and Robot 2, when their in-between distance is less than R_2. An attraction force is applied at two agents, e.g. between Robot 1 and Robot 4, when their in-between distance is more than R_1. Between Robot 1 and Robot 3, no force is applied. This force formulation maintains the formation of the swarm agents. The optimization method-based odor tracking strategies from these reports are summarized in Table 1.4.

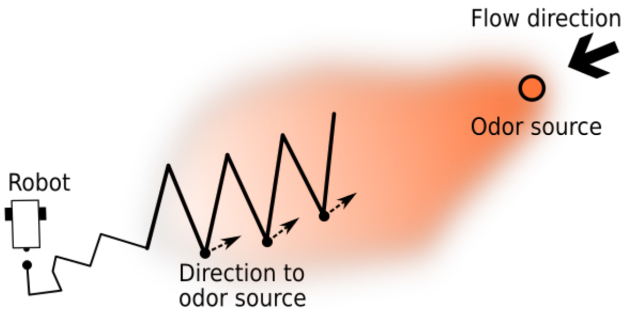

(a) Remote estimation of odor source.

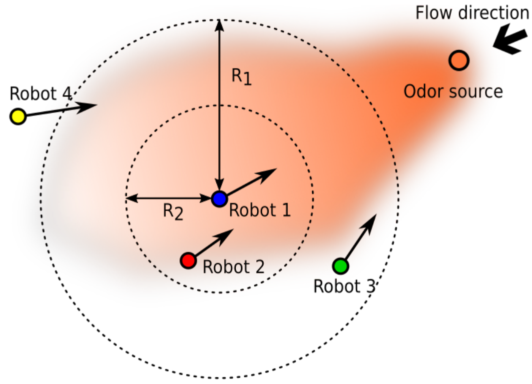

(b) Swarm optimization.

Figure 1.5: Various approach of odor tracking using optimization method.

Table 1.4: Strategy of odor tracking using optimization method.

Approach	Methodology	Testing environment	Publication
Remote source estimation using Gaussian odor distribution optimization and zigzag movement.	A mobile robot used a metal oxide gas sensor and 4 anemometric sensors for sensing modality. The Gaussian model of gas distribution was used as a reference to estimate the location of the source. Direction to odor source location was estimated using nonlinear optimization algorithms, the gradient descent method and the Kalman filtering method.	Indoor environment without obstacle. Air ventilation was managed by 2 air supplies in the ceiling and 2 exhausts near floor outside the experiment space. An odor source on the ground.	Ishida et al., 1997 [21]
	A mobile robot uses a sensing modality. E-nose and simple gas sensors were compared for the sensing modality. The odor gradient was estimated using tropotaxis method. The Gaussian model of gas distribution was used as a reference to estimate the location of the source. Direction to odor source location was estimated by a linear combination of the concentration gradient and the upwind vector.	Indoor environment with obstacles and turbulent airflow condition and with two odor sources.	Marques and De Almeida, 2000 [22] Marques et al., 2002 [28]
Odor plume search and upwind surge along the plume was combined with Swarm Optimization	The PSO was modified to include Coulomb law and chemotaxis-anemotaxis theory. Multiple simulated robots were each equipped with an ideal odor and wind sensor. The direction of robot movement is determined by taking into account the best local postion (the position with highest concentration found by each robot) and the global position (the position with highest concentration from all the best local positions), upwind vector, Coulomb force among the robots, and a random variable.	A 2D simulated environment with obstacles and advection-diffusion model odor distribution [52] in [61–63] and a small scale indoor environment in [64]. On the ground, an odor source in [61,62,64] and multiple odor sources in [63] were used.	Jatmiko et al., 2007, 2008, 2009, 2011 [61–64]
	The Swarm optimization applies a virtual forces to maintain the formation of the swarm sensor network. Multiple simulated robots were each equipped with an ideal odor and wind sensor. Direction of robot movement is determined by linear combination of the estimated odor concentration gradient and the upwind vector.	3D simulated environment; Turbulent airflow-generated odor distribution was simulated using CFD framework. The environment has obstacles.	Marjovi and Marques, 2013 [65]
	Simulated single robot and multiple cooperative robots were compared for localization. Each robot was equipped with two gas sensors and a wind direction sensor. The robot navigation incorporated Braitenberg control. The odor gradient was estimated using tropotaxis method.	2D simulated environment without obstacle with an odor source. The gas distribution used Farrel model [52].	Mamduh et al., 2013 [31]

1.1.5 Odor tracking using probabilistic method

In a large scale environment with strong turbulent airflow, odor distribution by airflow produces intermittently scattered plume. The turbulent airflow tears and stirs the plume into odor pockets. In this case, using only odor gradient is not reliable to indicate the direction to the source.

Addressing this problem, numerous localization strategies employed probabilistic methods to map likelihood of chemical detection, the likelihood source location and the likelihood of path between two points to result in odor detection. *Hidden Markov* and *Bayesian* methods were employed to map the likelihood of the source location in turbulent environment [19, 20, 66], as illustrated in Figure 1.6a. In these works, the probability distribution of the source location is mapped by fixed grid points on the search area. The likelihood map is initialized with a prior uniform distribution and then updated iteratively as the new data obtained. Similar approach were developed by Li et al. [67] and Neumann et al. [48] using *Particle Filters* method, as illustrated in Figure 1.6b. In contrast to fixed distribution points in the map based on Hidden Markov and Bayesian methods, particle filters method represents the probability distribution as weighted particles. The particles number changes dynamically. The particles are resampled when necessary and the weights are iteratively updated [48] [67]. The probabilistic method-based strategies from these reports are summarized in Table 1.5.

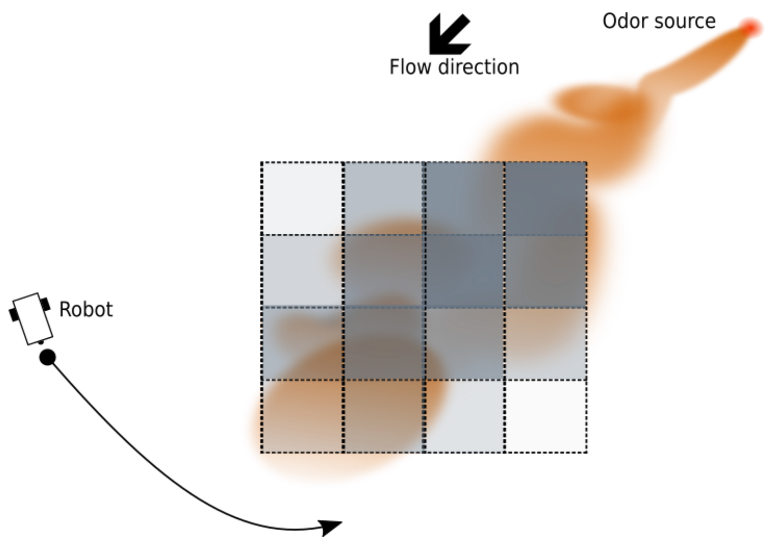

(a)

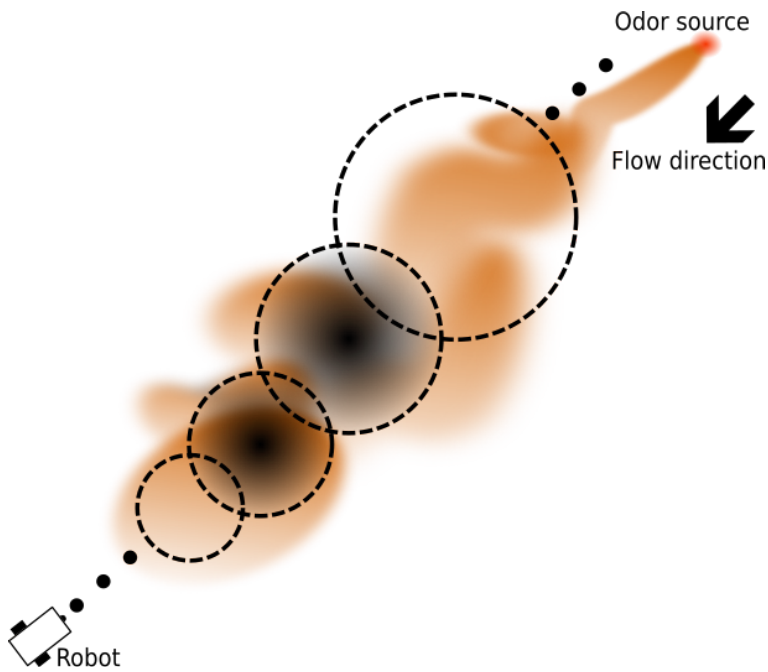

(b)

Figure 1.6: Various probabilistic methods for odor tracking and source estimation. (a) Likelihood odor map represents probability of measured odor at a cell originated from another cell. This likelihood is indicated by the gray-scale cell, where darker cells have higher probability of containing a plume. (b) Likelihood of odor distribution is represented as a weighted particles. The circles represent probability densities of the origin location of measured odor at the robot's location with different possible release time.

Table 1.5: Strategy of odor tracking using probabilistic method.

Approach	Method	Testing	Publication
A source probability map was developed using hidden Markov methods (HMMs).	A plume tracing vehicle equipped with ideal odor and wind sensing modality.	Simulated environment has turbulent flow and an odor source on the ground.	Farrel et al., 2003 [68]
A source probability map was developed using Bayesian methodology.	An autonomous underwater vehicle equipped chemical sensor (fluorometer) and Doppler flow sensor.	Data of chemical sensor and flow sensor were used for testing the algorithm in a simulation. The data were obtained from an experiment for tracking an odor source underwater [20].	Pang and Farrel, 2006 [19]
A source probability map was developed using Bayesian methodology.	Multiple mobile robots equipped with a gas and flow direction sensor each perform gas source probability estimation individually resulting probability map. The maps resulted from different robots were then combined into a single map. In simulation, each robot was equipped with a gas and flow sensor. In real experiment, each robot was equipped with a 2D ultrasonic anemometer and a metal oxide gas sensor.	In simulation, odor distribution used advection-diffusion model [52]. In real experiment, indoor environment without obstacle. Turbulent flow field was created using a fan. An odor source is located on the ground.	Meng et al., 2011 [69]
	A mobile robot equipped with an alive moth for the chemical sensing modality.	Indoor environment with tubulent flow condition. An odor source is located on the ground.	Voges et al., 2014 [43]
The source location was estimated using particle filters (PF) based method.	A mobile robot equipped with a metal oxide gas sensor and an anemometric sensor.	Outdoor environment without obstacle. An odor source is located on the ground.	Li et al., 2011 [67]
	An aerial drone equipped with an inertial measurement unit for estimating wind direction, an e-nose containing up to 4 metal oxides gas sensors and an electrochemical cell, and a gas detector containing a catalytic sensor, electrochemical and infrared sensors. Strategies using binary odor information and using tropotaxis gradient following were compared.	Outdoor aerial environment without obstacle has an odor source on the ground.	Neumann et al., 2013 [48]

1.1.6 Odor source localization using random search algorithm

This localization strategy is inspired from the biased random walk of *E. coli*. It is originally designed to performs a plume searching when no odor information is not available or scarce, as illustrated in Figure 1.7. The strategies in this category are Brownian Walk, Correlated Random Walk, Lévy Walk, and Lévy-taxis. The random movements are controlled through the distribution model for generating the turning angles (TAs), i.e. the angles used for each new step of movement, and the move lengths (MLs), i.e. the length of each movement steps. The typical distribution models are Gaussian distribution, wrapped Cauchy distribution and Lévy distribution. The odor source localization strategies from these reports are summarized in Table 1.6.

Cao et al. [70] reported experimental comparison of random search strategies for multi-robot odor source localization. Brownian Walk, Correlated Random Walk, and Lévy Walk were tested in the localization. The test showed that Correlated Random Walk and Lévy Walk are more time-efficient than Brownian Walk. Pasternak et al. [71] introduced Lévy-taxis and compared the performance to that of Brownian Walk, Correlated Random Walk, and Lévy Walk under simulated environment. Under particular condition of the simulation, Lévy-taxis outperformed the other random search strategies. Emery et al. [72] proposed an adaptive Lévy-taxis and compared the performance to that of moth-inspired strategies. The adaptive Lévy-taxis proved to show consistent performance in different environmental conditions.

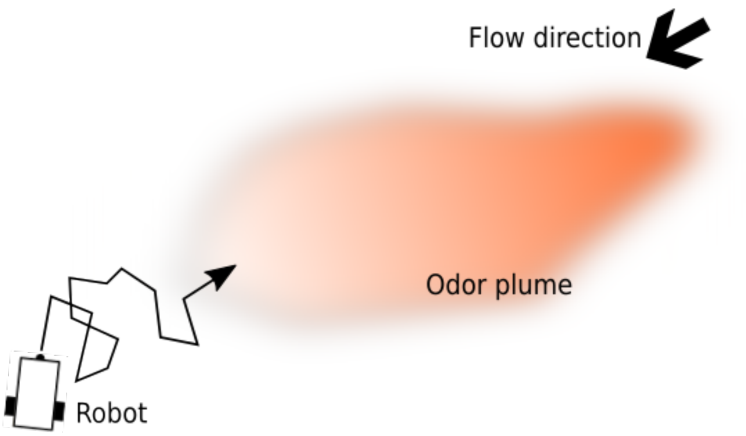

Figure 1.7: Random search algorithm.

Table 1.6: Various approach of random search algorithm.

Approach	Methodology	Testing environment	Publication
Brownian walk	It utilizes Gaussian distribution for the MLs and a uniform distribution for TAs. It does not have directional persistence (DP).	Multiple robots. Artificial potential field was applied at each robots to avoid collision between them and to attract them toward their goal position.	Cao et al, 2015 [70]
Correlated random walk	It utilizes wrapped Cauchy distribution for TAs and Gaussian distribution for MLs. DP is controlled through WCD of TAs.		
Lévy walk	It utilizes Lévy distribution for MLs and uniform distribution for TAs. DP is controlled through Levy distribution of MLs.		
Lévy-taxis	A simulated searching agent was equipped with chemical sensing with a minimum detection threshold and a flow direction sensing modalities. It utilizes Lévy distribution for MLs and wrapped Cauchy distribution centered on the upwind angle for TAs.	A simulated environment with flow-dominated river-like was developed based on simulator software by Farrel [52]. An odor source was located on the ground.	Pasternak et al., 2009 [71]
	The standard Lévy-taxis strategy is improved by making the movement decision at each step is based on measured gradient of the plume. A mobile robot equipped with a volatile organic compound sensor and a wind sensor. Key parameters of standard Lévy-taxis were dynamically changed.	A wind tunnel of $20 \times 4 \times 2$ m^3 with wind speed ranging from 0.1 m/s to 1.0 m/s. A single odor source was ethanol vapor emitted through a thin pipe. The robot and the source were place at the center of wind tunnel, initially 7 m distance between each other. An odor source on the ground.	Emery et al., 2017 [72]

1.2 Simulated experiment

There is no single best strategy would work optimally for all kind of localization problems. Most of the strategies are designed with different methodologies to address specific problems (environmental conditions, hardware limitations). Therefore, for the purpose of investigating the fittest strategy and methodology for a given localization problem and its evaluation, it is more economical and efficient to use a computer simulation in the early design phase before the implementation on a real experiment. Table 1.7 lists some investigations on localization strategies carried out using simulations.

Table 1.7: Summary of simulated experiments.

Environment	Methodology	Publication
Static environment	CFD framework; Indoor structured building.	Awadalla et al. (2013) [40]
Dynamic environment	Farrel's odor distribution model [52]	Farrel et al. (2003) [20]
		Jatmiko et al. (2007) [61]
		Meng et al. (2011) [69]
		Mamduh et al. (2013) [31]
	Odor detections and flow velocities were obtained from real underwater chemical plume tracking.	Pang and Farrel (2006) [19]
	Digitalized real-world water flow and chemical plume.	Pasternak et al. (2009) [71]
	A simulation environment using a Lagrangian particle random walk model. Under water environment.	Tian et al. (2014) [42]
	CFD framework; Indoor room with multiple obstacles and a ventilation to let air flows in and out; Search area is varied from 4×6 m^2 to 30×40 m^2.	Marjovi and Marques [65,73]
	CFD framework; Closed room model with an obstacle and an odor source on the ground; Search area is approximately 5.6×3.2 m^2; Evaluation was conducted over 404 initial positions; Localization time limit: 300 s.	Muhtadi and Nakamoto (2018) [44]
	CFD framework; Closed room model with multiple obstacles and an odor source on the ground; Evaluation was conducted over 404 initial positions; Localization time limit: 600 s.	Muhtadi and Nakamoto (accepted for pulication on June 2018)

1.3 Odor distribution

The effectiveness and efficiency of odor source localization depends on how well the selected algorithm is suitable for the environmental condition which determines how the odor is dispersed. Odor dispersal characteristics can be predicted using *Reynolds* number of airflow that carry the odor:

$$Re = \frac{inertial\ force}{viscous\ force} = \frac{\rho \mathbf{v} L}{\mu} = \frac{\mathbf{v} L}{\nu} \tag{1.1}$$

where ρ is the density of the fluid (kg/m^3), $\mathbf{v}$ is the mean velocity of the object relative to the fluid (SI units: m/s), L is characteristic linear dimension (traveled length of the fluid; hydraulic diameter when dealing with river systems), μ is the dynamic viscosity of the fluid (Pa·s or N·s/m^2 or kg/(m·s)), ν is the kinematic viscosity ($\nu = \mu/\rho$) (m^2/s).

1.3.1 Time-averaged Gaussian odor distribution

At low Reynolds numbers[6], laminar flow occurs where viscous force is dominant factor in odor transport. This condition results in smooth gradient of chemical concentration with the peak at the source and decreases monotonically radially according to a Gaussian distribution [56]. In this case, the time-averaged odor distribution in 3D space domain can be represented by

$$C_0\left(x,y,z\right) = \frac{q}{4\pi K}\frac{1}{d}exp\left[-\frac{U}{2K}\left(d-x\right)\right] \tag{1.2}$$

where $C_0\left(x,y,z\right)$ is odor concentration at coordinate position $\left(x,y,z\right)$, q is emission rate of odor, K is turbulent diffusion coefficient of odor and U is flow speed, and

$$d = \sqrt{(x^2+y^2+z^2)}.$$

When the source is located near the floor, the odor concentration is given by

$$C_0\left(x,y,z\right) = \frac{q}{4\pi K}\frac{1}{d_1}exp\left[-\frac{U}{2K}\left(d_1-x\right)\right] + \frac{q}{4\pi K}\frac{1}{d_2}exp\left[-\frac{U}{2K}\left(d_2-x\right)\right] \tag{1.3}$$

where

$$d_1 = \sqrt{x^2+y^2+(z-h)^2},$$

and

$$d_2 = \sqrt{x^2+y^2+(z+h)^2}.$$

These conditions will only be encountered by extremely small robots, the size of microscopic organisms, or where there is no background fluid flow [74, 75]. At medium to high Reynolds numbers, turbulent flow occurs where inertial force is the dominant factor.

1.3.2 Turbulent flow-generated odor distribution

By assuming that odor is passive and neutrally buoyant, its distribution in an environment is governed by the characteristic of the fluid flow transporting it. The fluid flow in real world is generally turbulent. Airflow in outdoor environment and inside buildings, vehicles are turbulent. Also movement of low viscosity liquid such as water tends to be turbulent. Turbulence is more easily created in low viscosity fluid, but more difficultly created in high viscosity fluid. There is no clear definition of turbulent flow, however it has some characteristic as follows [76]:

Irregularity. Turbulent flow is irregular and chaotic. The flow consists of turbulent eddies.

[6]The Reynolds number (Re) is a dimensionless quantity in fluid mechanics used to help predict flow patterns in different fluid flow situations. The concept was introduced by Sir George Stokes in 1851, but the Reynolds number was named by Arnold Sommerfeld in 1908 after Osborne Reynolds (1842–1912), who popularized its use in 1883 (Wikipedia).

Diffusivity. Mass diffusivity is increased by turbulent flow. The turbulence increases the exchange of momentum, the resistance (wall friction) and heat transfer in internal flow such as in channel and pipes.

Large Reynolds numbers. Turbulence degree increases as the increase of Reynolds number. However, the Reynolds number for the turbulence to start occurring is different for different shape and dimension of the containing room. For example, in pipes, the turbulence starts to occur at $Re_D \simeq 2300$, and in boundary layers at $Re_x \simeq 500,000$. A case of transition of laminar to turbulent flow is shown in Figure 1.8

Three-dimensional. Turbulent flow is always occurs in three dimensional and is unsteady.

Dissipation. In turbulent flow, kinetic energy in small eddies are transformed into thermal energy.

Continuum. Turbulent scales in the flow are always much larger than the molecular scales. Therefore, the flow can be treated as a continuum[7].

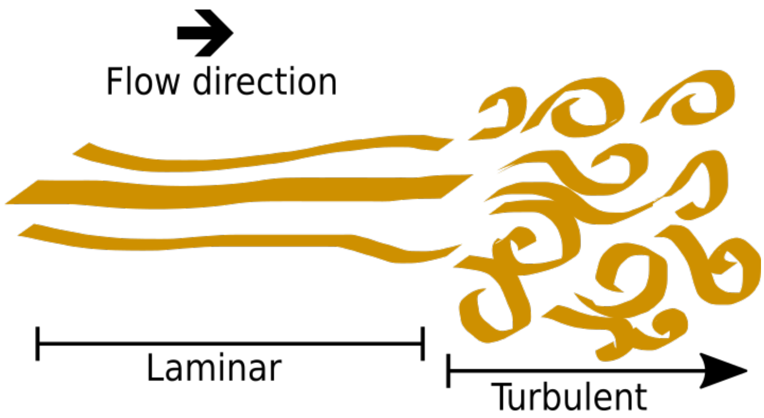

Figure 1.8: Transition of flow from laminar to turbulent.

Even though turbulence may seem random and chaotic it is deterministic and is described by the Navier-Stokes[8] equations. Unfortunately, a complete time-dependent solution of Navier-Stokes equations for high Reynolds number has not been attained at the moment. However, a number of solvable time-averaged models of Navier-Stokes equations are available which is known as family of The Reynolds-averaged Navier-Stokes (RANS) equations. A model of the RANS equation which is most commonly used in Computational Fluid Dynamics (CFD) to simulate mean flow characteristics for turbulent flow is the standard $k - \varepsilon$ model. This model is expressed by the turbulent kinetic energy k and its dissipation ε [76].

[7]Continuum: a continuous series or whole, no part of which is noticeably different from its adjacent parts, although the ends or extremes of it are very different from each other (Wiktionary).
[8]The Navier–Stokes equations, named after Claude-Louis Navier (a French engineer and physicist) and George Gabriel Stokes (an Irish physicist and mathematician), describe the motion of viscous fluid substances (Wikipedia).

The k equation is given by

$$\frac{\partial k}{\partial t} + \bar{v}_j \frac{\partial k}{\partial x_j} = \nu_t \left(\frac{\partial \bar{v}_i}{\partial x_j} + \frac{\partial \bar{v}_j}{\partial x_i} \right) \frac{\partial \bar{v}_i}{\partial x_j} + g_i \beta \frac{\nu_t}{\sigma_\theta} \frac{\partial \bar{\theta}}{\partial x_i} - \varepsilon + \frac{\partial}{\partial x_j} \left[\left(\nu + \frac{\nu_t}{\sigma_k} \right) \frac{\partial k}{\partial x_j} \right] \tag{1.4}$$

and the ε equation by

$$\frac{\partial \varepsilon}{\partial t} + \bar{v}_j \frac{\partial \varepsilon}{\partial x_j} = \frac{\varepsilon}{k} c_{\varepsilon 1} \nu_t \left(\frac{\partial \bar{v}_i}{\partial x_j} + \frac{\partial \bar{v}_j}{\partial x_i} \right) \frac{\bar{v}_i}{\partial x_j} + c_{\varepsilon 1} g_i \frac{\varepsilon}{k} \frac{\nu_t}{\sigma_\theta} \frac{\partial \bar{\theta}}{\partial x_i} - c_{\varepsilon 2} \frac{\varepsilon^2}{k} + \frac{\partial}{\partial x_j} \left[\left(\nu + \frac{\nu_t}{\sigma_\varepsilon} \right) \frac{\partial \varepsilon}{\partial x_j} \right]. \tag{1.5}$$

The turbulent viscosity is computed as

$$\nu_t = c_\pi \frac{k^2}{\varepsilon} \tag{1.6}$$

We used the standard values for the coefficient

$$\left(c_\mu, c_{\varepsilon 1}, c_{\varepsilon 2}, \sigma_k, \sigma_\varepsilon \right) = (0.09, 1.44, 1.92, 1, 1.3). \tag{1.7}$$

This model assumes that the turbulent viscosity is isotropic which means that the ratio between Reynolds stress and mean rate of deformation is the same in all directions. This model is robust, reasonably accurate and widely used model for industrial application. As the turbulent environment is simulated using ANSYS software, this model implementation is performed by the software.

1.4 Odor sensing technology

An odor sensor is the key component in an odor source localization system. Although an odor can refer to any chemical fluid including diluted chemical in water, in this section, since the odor source localization strategy investigated in this work is evaluated with ethanol vapor as the odor, the discussion about odor sensing technology is limited to the technology for sensing airborne odor (gas). There are a lot of gas sensors available in the market for different chemical target. These sensors have different sensing methods and performance characteristics. MRIGlobal [77] and Liu et al. [1] made excellent surveys of the gas sensor and the sensing technology. The gas sensing technology can be classified into two groups of method; based on electrical properties change and the other properties as shown in Figure 1.9.

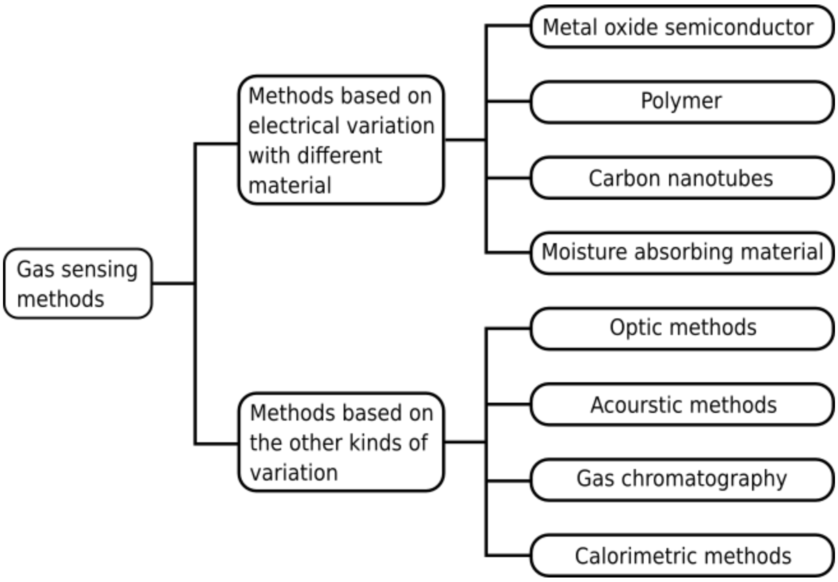

Figure 1.9: Classification of gas sensing methods (figure is reproduced from Liu et al. [1]).

1.4.1 Methods based on variation of electrical properties

1.4.1.1 Metal oxide semiconductor

Metal oxides semiconductors-based sensors have been widely used to detect wide range of gas. The metal oxide-based sensors are based on metal oxide sensing layer between two electrodes on top of dielectric substrate layer as shown in Figure 1.10. These sensors utilize metal oxides semiconductors as the sensing layer because of its conductivity characteristic i.e. when a semiconducting oxide is exposed to air, the adsorption of water and/or oxygen from the atmosphere modifies the band structure of the material at the surface with respect to the bulk which in turn change the conductivity [78]. When the sensing layer of the sensor is exposed to an analyte gas, the oxygen and water vapor molecules in the layer swap with the gas molecules which change the conductivity of the layer. This conductivity change is measured as a response toward the analyte gas. These sensors operate at high temperatures. This high temperature is required to increase gas molecule adsorption on the sensing layer surface which would capture ions of the sensing materials. In essence, the sensitivity of this sensor is controlled by the temperature. To achieve this temperature, the sensitive layers often need to be heated to an optimum temperature for the target analyte using a heating filament. Tin dioxide (SnO_2) is the most understood type of metal oxides semiconductor for gas sensors. For SnO_2-based sensors, the operating temperature is from 25°C to 500°C.

The requirement for high temperature is a disadvantage for metal oxide-based sensors. This causes high operational cost and demands complicated configuration for the application. Another disadvantage is the long recovery time after each gas exposure resulting in a response delay which makes it generally not suitable for real-time sensing application. However, numerous studies successfully used this kind of sensor for odor source localization systems. With appropriate design consideration to the response delay, this sensor can be used in the localization system for a plume tracking, odor distribution mapping, etc.

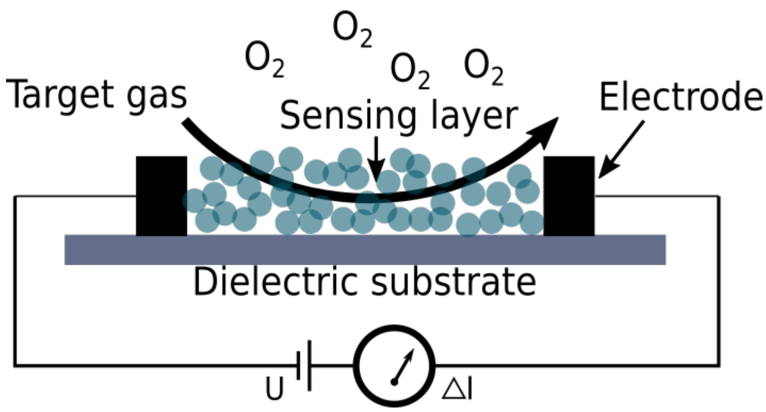

Figure 1.10: Schematic of metal oxide-based sensor.

1.4.1.2 Polymer

Polymer-based sensors are mostly used to detect a wide range of volatile organic compounds (VOCs) such as alcohols vapor, aromatic compounds and halogenated compounds. Similar to metal oxide semiconductors, when the polymer layers are exposed to an analyte gas, the absorption of the gas into the layers changes the physical properties of the layers such as their mass, dielectricity, acoustic variables etc. According to the different change in physical properties, sensing polymers can be grouped into two types: conducting polymers and non-conducting polymers [1]. In conducting polymers, the electrical conductivity changes upon exposure to wide range of organic and inorganic gases. This conductivity is too low to be transduced into a response signal. The polymer then requires a doping by redox reactions or protonation to improve the conductivity. Conducting polymers commonly used as gas sensing materials are polypyrrole (PPy), polyaniline (PAni), polythiophene (PTh) and their derivatives. Non-conducting polymers have been widely used as sorptive coating on various sensor devices such as mass-sensitive (e.g., Quartz Crystal Microbalance (QCM), Surface Acoustic Wave (SAW) and Surface Transverse Wave (STW)), capacitive (dielectric) and calorimetric sensors. Different polymers absorve selectively to different gases.

Polymer-based gas sensors have advantages such as high sensitivities and fast response. These sensors consumes low energy as they operate at room temperature. However, they have disadvantages such as instability for long time usage, irreversibilty, and poor selectivity.

1.4.1.3 Carbon nanotubes

Carbon nanotubes (CNTs) draw great attention for their characteristics such as large adsorptive capacity, high surface-area-to-volume ratio and short response time upon an analyte exposure, which in turn improve their electrical characteristic such as capacitance and resistance [1]. Having these features, CNTs are capable to detect extremely little amount of gases such as alcohol, amonia (NH_3), carbon dioxide (CO_2) and nitrogen oxide (NO_x) at room temperature. To improve their selectivity and sensitivity as sensing materials, CNTs are often mixed with other materials.

1.4.1.4 Moisture absorbing material

Moisture absorbing materials find their application in humidity sensing system. These materials are embedded with radio frequency identification (RFID) tag for measuring humidity level in the surrounding air. If active RFID tags are covered with moisture absorbing materials like paper, absorbed water changes the resonance frequency of the RFID which can be detected by RFID reader. For passive RFID tags, amount of absorbed water determines the minimum power level required by RFID reader to power up the tags. The moisture absorbing material-based tags are cheap thus suitable for mass production.

1.4.2 Methods based on the other kinds of variation

1.4.2.1 Optic methods

Optical methods for gas sensing is mostly realized using molecular absorption spectroscopy. Absorption spectroscopy refers to spectroscopic techniques that measure the absorption of radiation, as a function of frequency or wavelength, due to its interaction with a sample (Wikipedia). The sample absorbs energy, i.e., photons (light), from the radiating field. The intensity of the absorption varies as a function of frequency, and this variation is the absorption spectrum. Infrared and ultraviolet-visible are particularly popular spectrum used in spectroscopy for analytical applications.

Gas sensors based on optical absorption allow fast responses (time constants below 1s are possible), minimal drift and high gas specificity, with zero cross-response to other gases provided their design is carefully considered [79]. Their applications are limited owing to miniaturization problem and high cost.

1.4.2.2 Acoustic methods

Acoustic methods gas sensing is based on sound absorption phenomenon when it propagates through a gas. The intensity of sound propagating through a gas is attenuated to different degrees

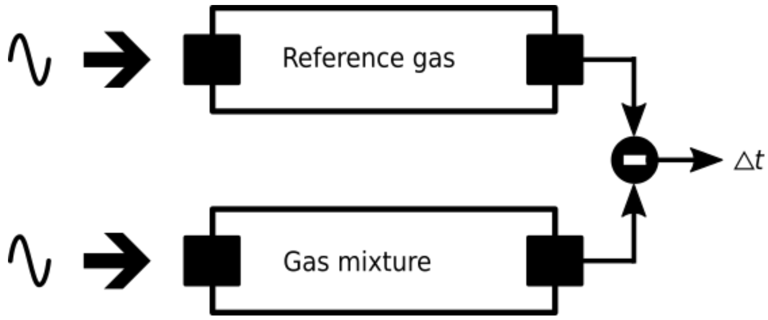

Figure 1.11: Method of ultrasonic detection.

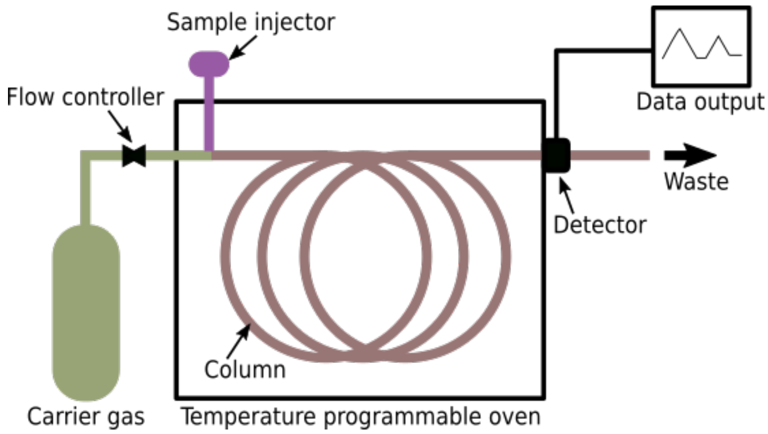

Figure 1.12: Gas chromatography diagram .

depending upon the composition of the gas. The sound absorption was discussed by Strutt and Rayleigh [80] and experimentally investigated by Angona [81]. Measurement parameters of this acoustic method are classified into three categories [1]: (1) speed of sound; (2) attenuation; (3) acoustic impedance.

Acoustic techniques for gas composition sensing have several advantages [82], such as: (1) acoustic technology is simple and rugged, resulting in sensors that are durable and repeatable;. (2) acoustic properties can be measured in real time without calibration; (3) acoustic sensors do not require prior treatment of the target gas; (4) acoustic sensors can be configured for static or flowing test set up. The working principle of acoustic methods is described in Figure 1.11. Two identical channels, with one contains a reference and another contains gas mixture, measure ultrasonic propagation parameters, such as time difference $\triangle t$ or wave phase. The concentration of gas of interest in the gas mixture is determined by the time difference or phase shift.

1.4.2.3 Gas chromatography

Chromatography is the process of separating a mixture into individual components. Through the separation process, each component in the sample can be identified (qualitatively) and measured (quantitatively). Gas chromatography (GC) is widely used analytical method for organic compounds in solid, liquid or gas phase. GC is used for compounds that are thermally stable and volatile (or can be made volatile). Because of its simplicity, sensitivity and effectiveness in separating components, GC is one of the most important analytical tools in chemistry [83]. The working principle of GC is described in Figure 1.12. The sample analyte gas is injected into a flowing inert gas, a carrier gas, which flows through a column. As the gas passes through the column, the sample components move at different speeds according to the degree of interaction of each component with the stationary phase in the column. As the components pass the detector, each of them can be identified and quantified by the detector.

1.4.2.4 Calorimetric methods

The calorimetric gas sensor is a gas sensor that uses calorimetry as the transduction basis i.e. by measuring the heat of a reaction on the sensor surface. This devices category, in various sensing configurations is also known by the names pellistor, catalytic bead, catalytic gas sensor, combustible gas sensor, or thermometric gas sensor [84]. Calorimetric gas sensors will detect the presence of any combustible gas as long as oxygen is also present for the necessary reaction to take place.

The advantages of calorimetric gas sensors include low sensor cost, small size and portability, low power consumption, established utility in a decade's market, and long operating life. The main drawbacks are the susceptibility to poisoning of the catalyst when certain gases are present, and the need for re-calibration.

1.4.3 Summary of odor sensing

The important advantages, disadvantages and the applications of the gas sensing technology are summarized in Table 1.8. There are numerous gas sensors product on the market with various sensing technology. As the localization strategy is aimed for turbulent environment and the localization process includes movement of sensor node toward the source, the ideal sensor for the odor source localization strategy being developed should at least has some criterion including: appropriate sensitivity and selectivity, short response time, small size and robust against physical disturbance as well as preferably low cost. These criterion have excluded some class of sensor from the possible options such as sensor based on optic methods, gas chromatography and calorimetric methods owing to their bulky size. Sensors based on moisture absorbing material is not likely suitable for this mission owing to the limited range of detectable gases/chemicals. Depend on the target odor and environmental conditions, the suitable sensors for the localization task are sensors based on metal oxide semiconductor, polymer, carbon nanotubes and acoustic methods. When considering low cost criteria, sensors based on metal semiconductor and polymer are the best options.

Table 1.8: Summary of basic gas sensing method (from Liu et al. [1]).

Materials	Advantages	Disadvantages	Target Gases and Application Fields
Metal Oxide Semiconductor	Low cost; Short response time; Wide range of target gases; Long lifetime.	Relatively low sensitivity and selectivity; Sensitive to environmental factors; High energy consumption.	Industrial applications and civil use
Polymer	High sensitivity; Short response time; Low cost of fabrication; Simple and portable structure; Low energy consumption.	Long-time instability; Irreversibility; Poor selectivity.	Indoor air monitoring; Storage place of synthetic products as paints, wax or fuels; Workplaces like chemical industries.
Carbon Nanotubes	Ultra-sensitive; Great adsorptive capacity; Large surface-area-to-volume ratio; Quick response time; Low weight.	Difficulties in fabrication and repeatability; High cost.	Detection of partial discharge (PD)
Moisture Absorbing Material	Low cost; Low weight; High selectivity to water vapor.	Vulnerable to friction; Potential irreversibility in high humidity.	Humidity monitoring
Optical Methods	High sensitivity, selectivity and stability; Long lifetime; Insensitive to environment change.	Difficulty in miniaturization; High cost.	Remote air quality monitoring; Gas leak detection systems with high accuracy and safety; High-end market applications.
Acoustic Methods	Long lifetime; Avoiding secondary pollution.	Low sensitivity; Sensitive to environmental change.	Components of Wireless Sensor Networks
Gas Chromatography	Excellent separation performance; High sensitivity and selectivity.	High cost; Difficulty in miniaturization for portable applications.	Typical laboratory analysis
Calorimetric Methods	Stable at ambient temperature; Low cost; Adequate sensitivity for industrial detection (ppth range).	Risk of catalyst poisoning and explosion; Intrinsic deficiencies in selectivity.	Most combustible gases under industrial environment; Petrochemical plants; Mine tunnels; Kitchens.

1.5 Comparison of strategies and methodologies

Obviously there is no single methodology works optimally for any environmental conditions. In addition, criterion not related to performance are often taken into consideration for selecting the strategy, method of an odor source localization, as well as how the study is carried out. Table 1.9 outlines the strategies characteristics in general. Table 1.10 outlines the advantages of using a single odor sensor and multiple odor sensors. Table 1.11 outlines the advantages of using real experiment and simulation in the study of odor source localization strategies.

Table 1.9: Comparison of odor source localization strategies.

Criteria	Gradient following (chemotaxis)	Plume tracking (chemotaxis-anemotaxis)	Odor distribution mapping (chemotaxis-anemotaxis)	Source estimation or plume tracking using probabilistic method (chemotaxis-anemotaxis)	Odor tracking using optimization method (chemotaxis-anemotaxis)
Suitable fluid flow	weak/without flow	laminar and turbulent flow	laminar and turbulent flow	laminar and turbulent flow	laminar and turbulent flow
Computation and memory resource	low	low	high	high	low
Advantage	simple	robust for turbulent flow	spatial information is obtained	remote estimation of the source	PSO: better coverage. odor distribution-based: odor distribution estimation
Disadvantage	approach the source slowly	dynamic flow can lead to inefficient track	approach the source slowly	difficult to follow a dynamic environmental changes	difficult to follow a dynamic environmental changes

Table 1.10: Comparison of single and multiple sensors.

Criteria	Single sensor	Multiple sensor
Complexity	lower	higher
Gradient estimation	klinotaxis: good at following low to high spatial gradient	tropotaxis: good at following high spatial gradient
Cost	cheaper	more expensive

Table 1.11: Comparison of real experiment with simulation.

Criteria	Real experiment	Computer simulation
Problem category	actual	virtual
Repeatability	no	yes
Development	difficult	easy
Accuracy of odor distribution	not available	depends on model

There are a wide range of environments targeted by the application of odor source localization strategies. Whereas there have been various odor source localization techniques and strategies proposed and studied in typically simplified real or simulated testing environments and searching scenarios. Developing a best-fit strategy for a particular environment is a challenge since the reported strategies and techniques were usually claimed to have good performance or outperforms the others, with respect to the testing environments. Understanding these different traits of strategies and the methodologies helps in determining the optimal and cost-effective strategies and methodologies for a targeted odor source localization task.

The approach of this thesis is described in Figure 1.13. We take some considerations in this study which determine the selection of research methodology, environmental condition, and the localization strategy.

First, testing the strategies in real experiment faces difficulty in building the realistic and representative real environment because it is simply not practical and expensive. Therefore we learn the importance of testing the strategies in computer simulation, especially in the early stage of study, which can be carried out relatively faster than a real experiment and enable consistent environment for evaluation of different strategies which can not be achieved with a real experiment. Thus, this study carries out the experiment in computer simulation.

Second, odor source localization is generally aimed for a time critical mission, such as to search for human victims under building rubbles, a source of a dangerous gas leakage, a fire when it is still small, etc. In such mission, the dynamic characteristic of target environment should be address by the localization. Therefore, a time-variant environment is generally required for evaluating an odor source localization strategy.

Third, there are various kinds of environment for the target of the application. However most of the environments has fluid flow with turbulent characteristics. Therefore, we focus our study to develop a localization strategy for turbulent environment.

Fourth, there are various strategies were proposed in this area. However, we were interested to explore the moth-inspired chemotaxis-anemotaxis strategy further, as it proves to be effective in turbulent environment. As the commercial chemical sensors is far inferior to the moth's olfaction system, the moth strategy is not completely replicated using our current technology. Therefore, the implementation of this strategy using a chemical sensor is still an open issue.

Finally, in searching for an odor source in a large scale environment, a strategy with multiple multiple sensor nodes or a sensor networks is an advantage compared to a strategy with single sensor. However, when the environment is too large compared to the number of sensor nodes or search robots with multiple odor sources, it is wiser to set the robots at different part of the environment to perform individual odor search. Therefore, we explore the strategy with a single sensor node. In this single sensor node, we used a chemical sensor since with with an appropriate sensing method, it can be used effectively to track an odor plume.

1.6 Research purpose

The objective of this PhD thesis is to develop an odor source localization strategy for indoor turbulent environment and to evaluate it under simulation framework of CFD. Through this thesis, the main challenges of development and implementation of odor source localization are addressed i.e.:

- *The real world environment has a turbulent airflow*. In this work, the testing environment is embodied as a closed room with an odor source located on the floor. Inside the room, a convective airflow created owing to difference in temperature at a window in a wall and the other parts of the room. The airflow has turbulent characteristics. The airflow mainly governs the odor distribution which produces dynamic odor plume. In addition, the environment has obstacles which disturb the airflow and produce irregularly complicated plume shape.

- *An odor sensor exposed to a target odor typically requires a time to produce a response corresponding to the actual concentration which is known as a response delay*. This delay characteristic limits the practical application for real-time sensing tasks. Tracking an odor plume in a time-variant environment requires ideally an odor sensor with real-time response. To solve this problem, a method is required to estimate the odor information accurately (to a certain extent) from the obtained sensor response information with a delay. In this work, the source localization task is carried out using a single odor sensor.

- *A consistent environment for testing the localization strategy can not be attained in the real experiment*. It is necessary to evaluate the performance of the localization strategy in a consistent environment so that the development process can be managed according to valid basis and different strategies can be fairly compared. To attain a consistent environment, the closed room environment is simulated using a Computational Fluid Dynamics (CFD) framework. The result from the CFD simulation is then used to test the localization strategy in a simulation.

Some studies has used CFD framework to simulate a realistic environment. However, to the best of the author's knowledge, this thesis address quite unique environmental condition which has not been addressed in the other source localization strategies, that is the closed room environment in which the odor continuously released from the source gets accumulated by the time. As the baseline odor concentration level increases by the time, a threshold value commonly used to identify the plume or proximity to the source is not applicable. In this thesis, the plume and the source are identified by the odor gradient which liberates from the requirement for a threshold value.

Therefore, the contribution of this thesis is the localization strategy using a regression technique for estimation of the plume centerline and edges. This estimation does not require for a threshold value therefore it is applicable for dynamic environment with any baseline odor concentration level.

1.7 Thesis structure

This research work is managed in phases as described in Figure 1.14. The phases are compiled into this PhD thesis with the structure as follows:

Chapter 2 explains the development of odor source localization strategy using multiple sensor nodes for an environment with a Gaussian time-averaged odor distribution.

Chapter 3 explains the development of simulation environment under CFD framework.

Chapter 4 explains the development of odor source localization strategy using a single odor sensor without time constant in a dynamic environment.

Chapter 5 explains the development of odor source localization strategy using a single odor sensor with time constant in a dynamic environment.

Chapter 6 concludes the outcome of this research work and suggests the future works.

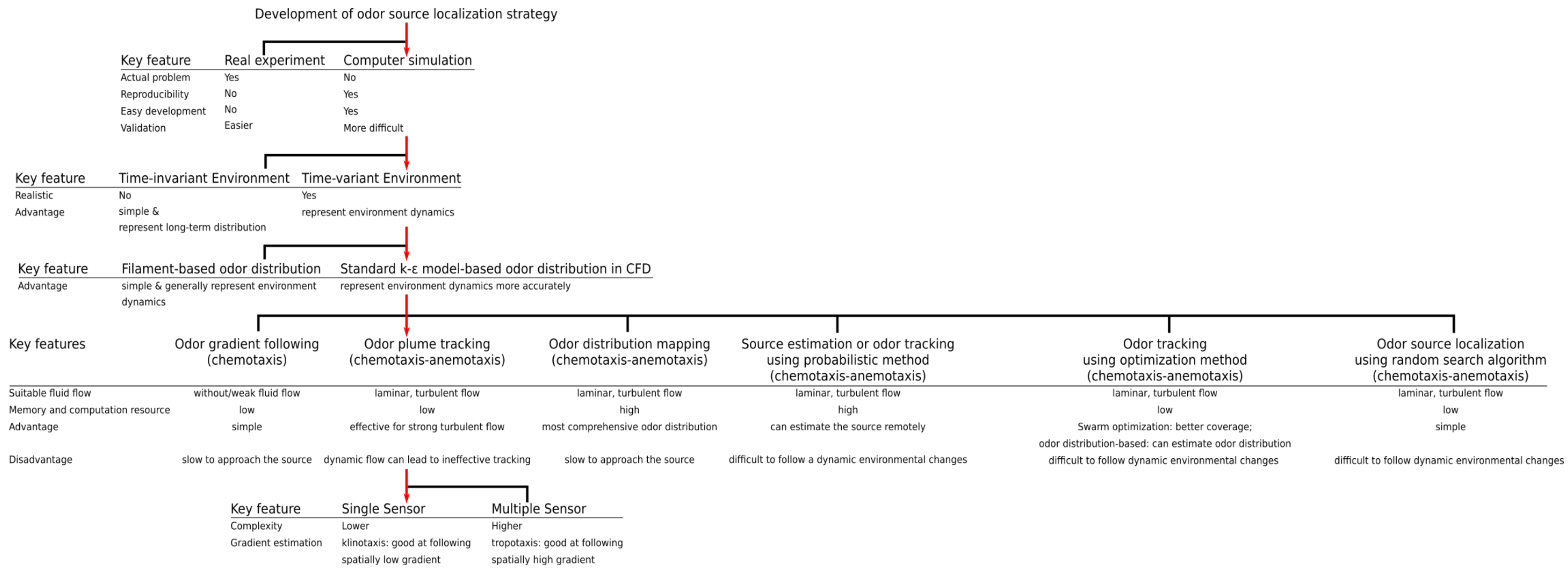

Figure 1.13: Classification of research strategy.

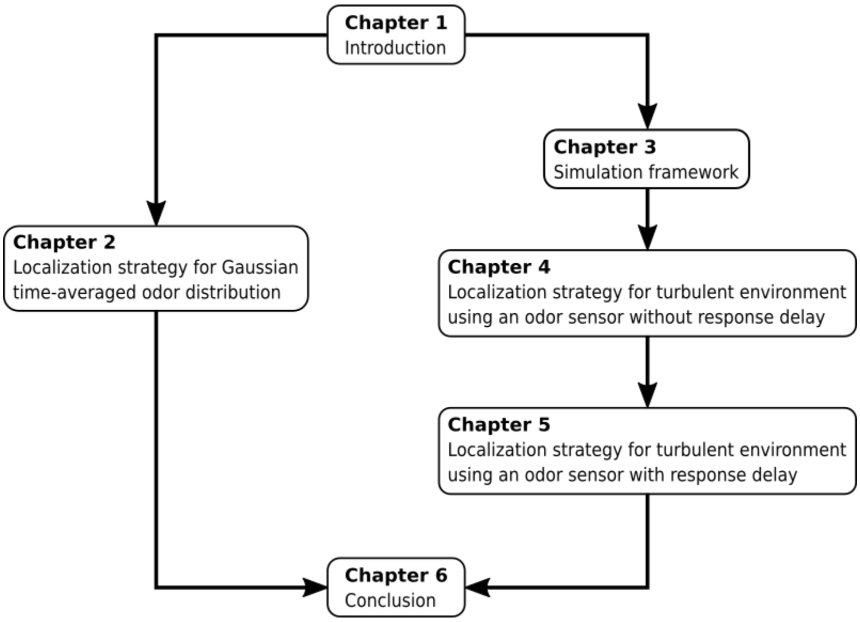

Figure 1.14: Thesis structure.

Chapter 2

Localization strategy for Gaussian time-averaged odor distribution

Utilization of multiple sensor nodes compared to single one for odor source localization proposes faster and more robust performance for task distribution and collaboration among the nodes. In this multiple sensing system, nodes formation and orientation are optimized.

2.1 Optimal arrangement of multiple sensor nodes for source localization

We started the development of the source localization strategy by looking into our previous work on odor source localization using optimization technique. This technique is able to estimate source location remotely by comparing measurement data collected by spatially distributed sensor nodes. The number of sensor nodes and their measurement position contributed to the accuracy of source location estimation. This understanding motivated us to simulate the effect of nodes spatial positions on estimation accuracy as described in Section 2.1.2.

2.1.1 2D Gaussian distribution

Although the algorithm is intended for time-variant environment with turbulent airflow, we simplified the problem at initial development. We assume that the environment has unidirectional airflow, constant wind speed, without turbulence and the odor source is located near the floor. Under these assumptions, time-averaged odor concentration distribution in 3D space can be represented as Gaussian distribution model as described in Equation 1.2.

Here, as the localization strategy is aimed for searching an odor source on the ground, only 2D odor distribution across horizontal plane near the ground is required. Derived from Equation 1.2, the 2D Gaussian distribution can be represented by [57]

$$C_0\left(x,y\right) = \frac{2q}{4\pi K}\frac{1}{d_s}e^{\left[\frac{-U}{2K}\left(d_s - \Delta x\right)\right]} \tag{2.1}$$

where $C_0\left(x,y\right)$ is odor concentration at coordinate position $\left(x,y\right)$, q is gas emission rate, K is turbulent diffusion coefficient, U is wind speed and θ is wind direction angle from x-axis to the upwind direction,

$$d_s = \sqrt{\left(x_s - x\right)^2 + \left(y_s - y\right)^2},$$

and

$$\Delta x = \left(x_s - x\right)cos\theta + \left(y_s - y\right)sin\theta.$$

Figure 2.1 shows an example of odor concentration distribution in two dimensional space, while Figure 2.2 shows the effect of wind direction angle on horizontal orientation of odor plume.

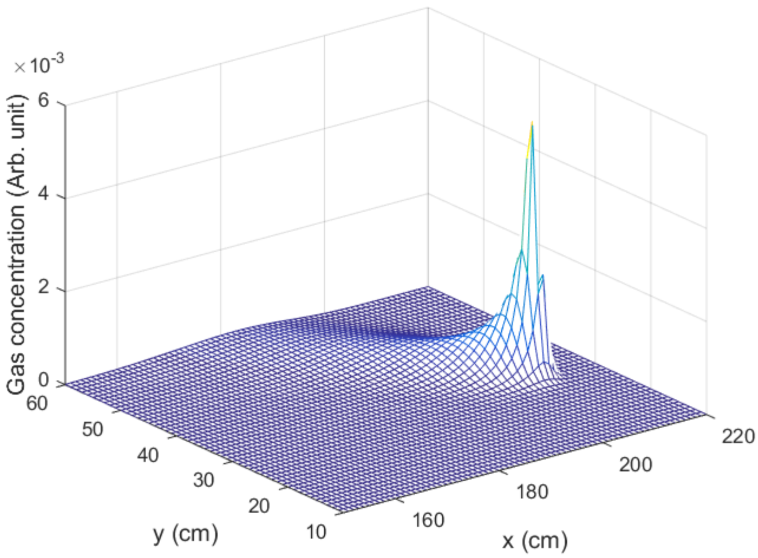

Figure 2.1: Dispersion of odor (ethanol) concentration in two dimensional space $x \times y$ for $q = 37.5$ ml/min, $K = 15.2$ cm^2/s, $U = 20$ cm/s, $x_s = 210$ cm, $y_s = 31$ cm, $\theta = -45°$.

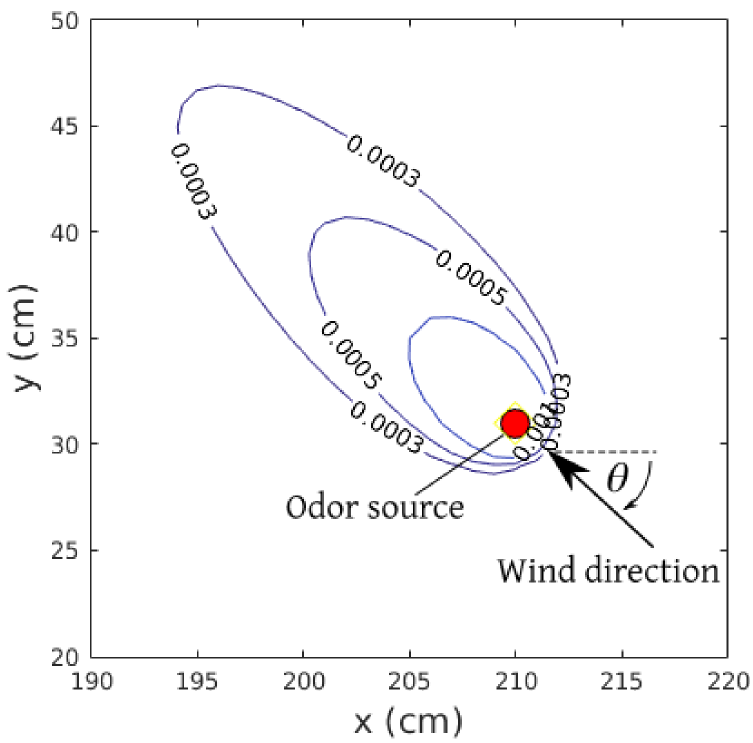

Figure 2.2: The effect of wind direction angle θ on horizontal orientation of gas distribution. Contour line indicates the location with the same concentration. A value on contour line is gas concentration (arb. unit).

2.1.2 Methodology

Investigation for optimum sensor nodes arrangement was carried out using three sensor nodes. The sum of odor concentration difference is calculated between the concentration caused by the presumed source and the concentration caused by the real source at the nodes positions

$$\triangle C = \sum_{i=1}^{n} \left| C_{s(0,0)}\left(x_i, y_i\right) - C_{s(x,y)}\left(x_i, y_i\right) \right| \tag{2.2}$$

where n is number of sensor nodes, $C_{s(x,y)}\left(x_i, y_i\right)$ is concentration measured by the node at(x_i, y_i) caused by the presumed source at (x, y), and $C_{s(0,0)}\left(x_i, y_i\right)$ is concentration measured by the node at (x_i, y_i) caused by the real source at $(0, 0)$. The sum is mapped at (x, y) as shown in Figure 2.3 where three sensor nodes were used. The smaller concentration difference indicates that the presumed source location is closer to the real source location. To aid observation of the estimation accuracy, a contour line of concentration difference based on a threshold value is plotted on the Figure. The white dashed line is the location with concentration difference 10^{-4}. It is used to help mark a likelihood area containing the source. The smaller area means that each point within the area has the higher probability density for being the odor source location. In other word, the smaller area, the more accurate estimation of odor source location (source estimation).

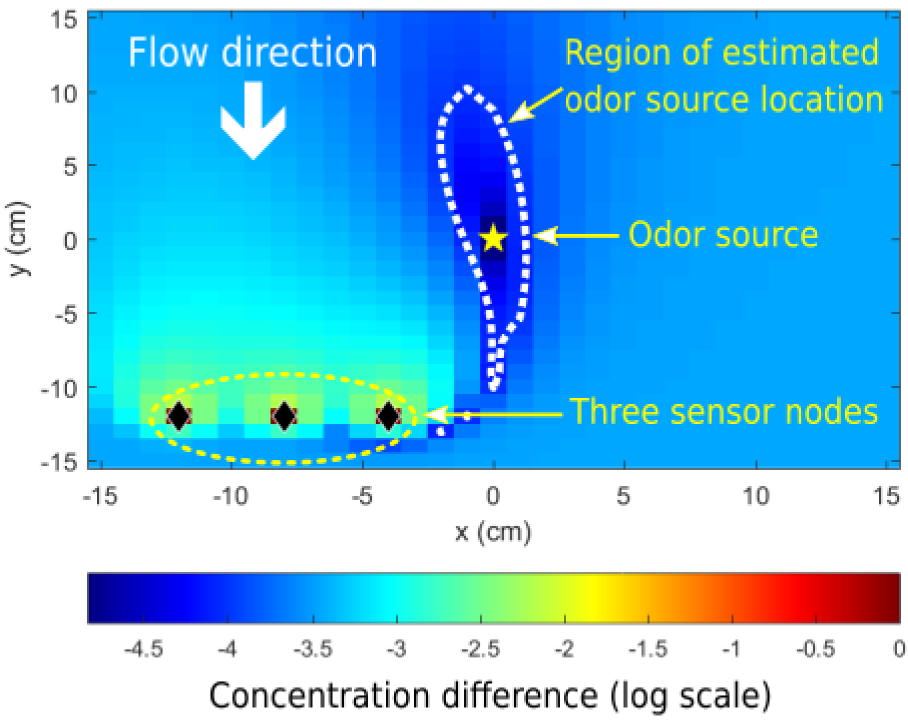

Figure 2.3: Variation of sensor node positions and the region of estimated odor source location. Odor source is at (0,0) coordinate.

It is intuitive to think that arranging the nodes in a straight line formation would give the optimal estimation which is supported by the study of Marjovi and Marques [73]. The next investigation is to evaluate the accuracy of the source estimation with variation on the position of the line formation in crosswind direction, gap size between the nodes and the angular orientation of the line formation.

2.1.3 Result

The evaluation results are shown in Figures 2.4, 2.5, and 2.6.

2.1.3.1 Crosswind position

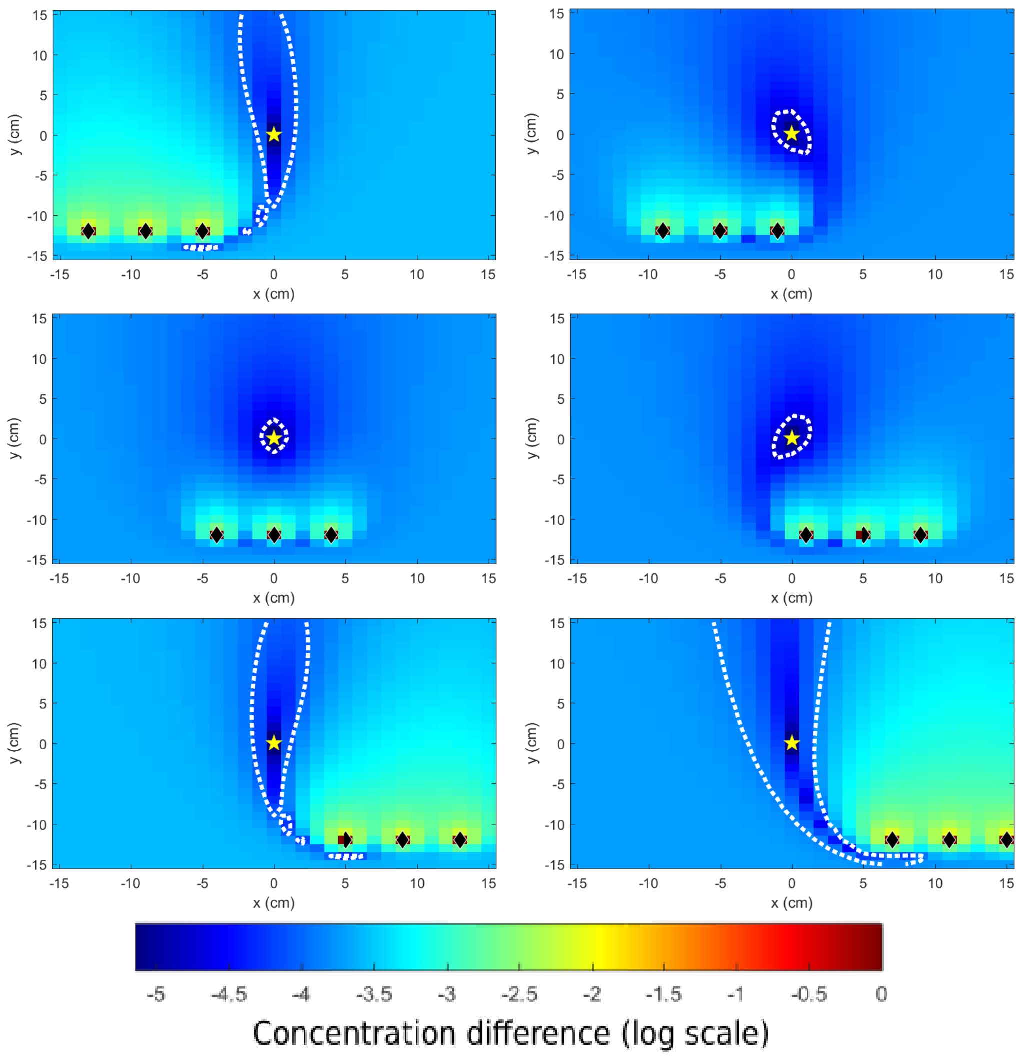

Figure 2.4: Variation of crosswind position and the effect to the accuracy of the source estimation.

It is confirmed that the best accuracy is obtained when the node line-formation is at the downwind of the source as shown in Figure 2.4.

2.1.3.2 Gap between nodes

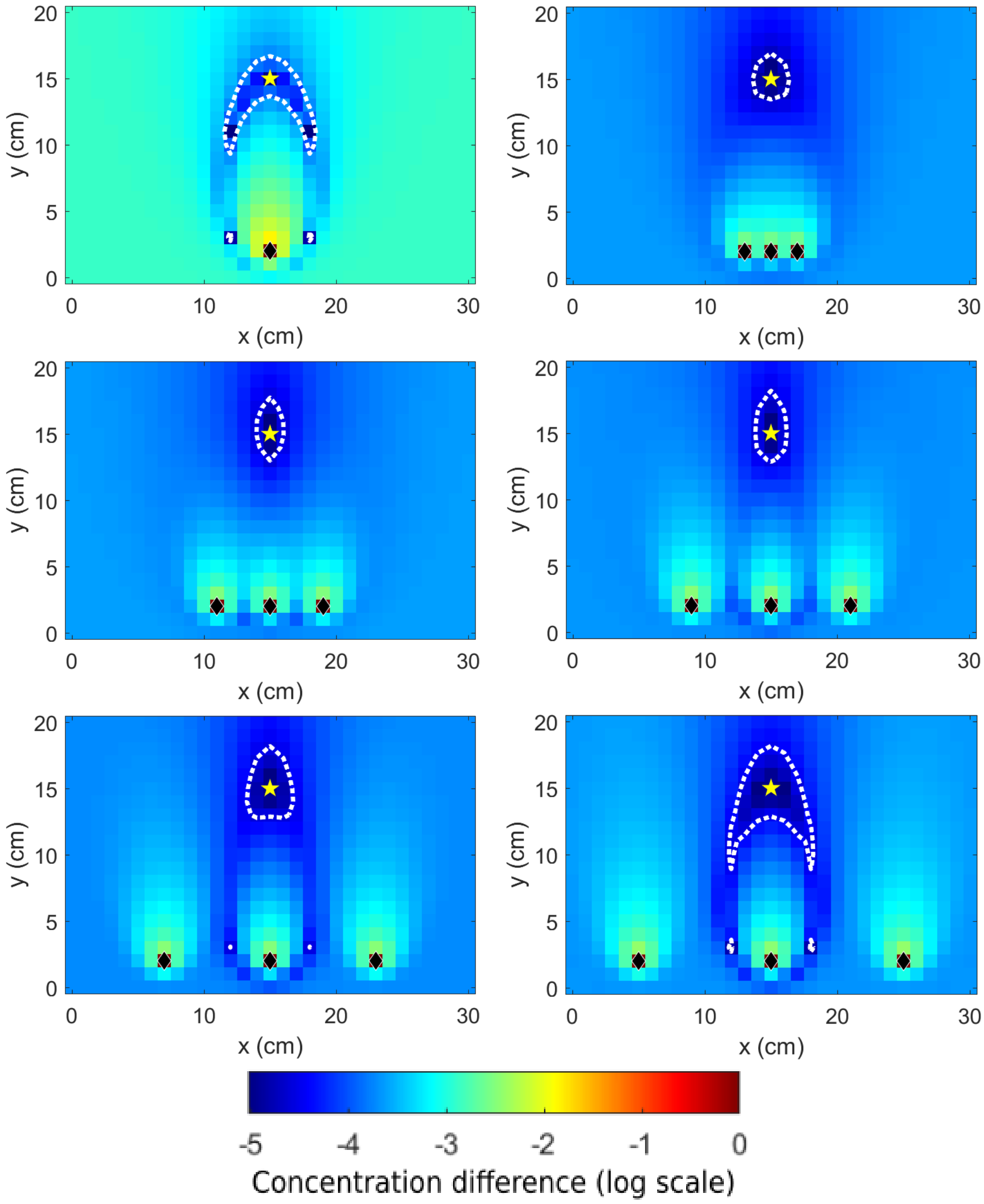

Figure 2.5: Variation of gap between nodes and the effect to the accuracy of the source estimation.

Figure 2.5 shows different accuracy for different gap size. The optimal size is likely to depend on the crosswind width of the plume.

2.1.3.3 Angular orientation

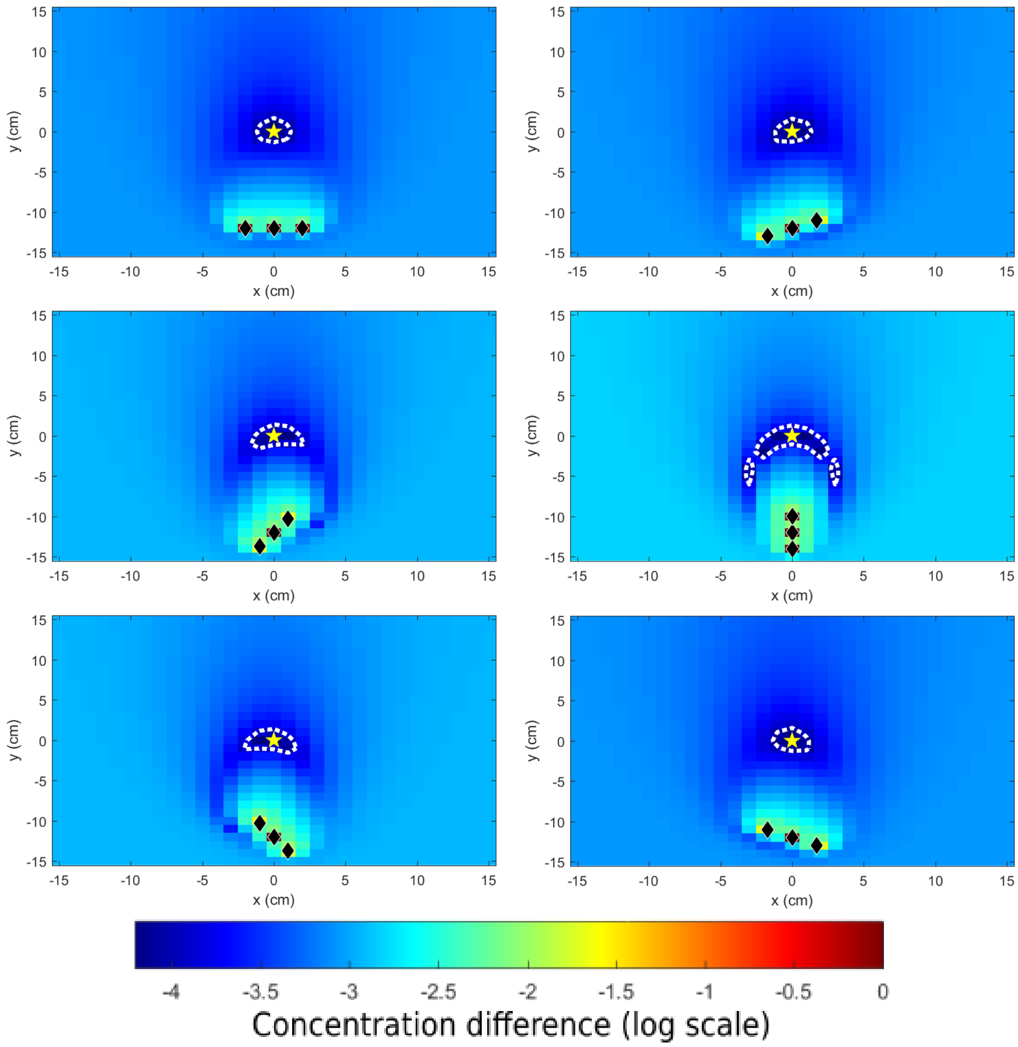

Figure 2.6: Variation of angular orientation and the effect to the accuracy of the source estimation.

It is confirmed that the best orientation is along crosswind direction or perpendicular to the wind direction as shown in Figure 2.6.

In general, we can conclude that the best accuracy was obtained when the formation is distributed along the crosswind line around the center of odor plume. This knowledge is then exploited to design a chemotaxis-infotaxis-based plume tracking strategy using multiple sensor nodes as described further in Section 2.2.

2.2 Cooperative strategy

The basic behavior of each sensor node when searching for odor plume is based on chemotaxis-anemotaxis strategy. This strategy is implemented as zigzag movement along crosswind in attempt to search for the plume and moving toward upwind direction to track the plume toward the source.

The information collected by the nodes is used to construct odor map locally on a rectangular region. This map becomes an infotaxic reference for the sensor nodes to determine the direction of searching and to avoid unnecessary overlapping scanning area among the nodes.

A cooperative strategy is devised here to minimize losing the plume while tracking it. The strategy divides the nodes to have two different roles; *leading node* and *supporting node*. The leading node has a task to track the plume toward the source using chemotaxis-anemotaxis strategy. Whereas the supporting moves zigzag while keeps up beside the leading node to collect odor information. The node which finds the highest odor concentration takes the role as the leading node and the others are the supporting nodes. The zigzag movement by the supporting node here is considered necessary to collect odor information around the plume and build an odor map which can be used to navigate the leading node tracking a dynamic plume. When the leading node loses plume, the supporting nodes which still in contact with the plume or measures the highest odor concentration can switch role to become the leading node. Figure 2.7 illustrates this cooperative strategy using three sensor nodes. In this illustration, there is a leading node and two supporting nodes. This strategy can be scale up to have more than a leading node when more sensor nodes are employed.

Figure 2.8 shows the flowchart of our strategy for this simulation. Two phases are defined in this source searching task i.e plume exploration and source localization. Plume exploration is the phase when no odor information is available. Thus the localization task is started with plume exploration. In this phase all nodes move zigzag toward upwind direction measuring reading odor concentration continuously. The nodes start the zigzag movement with small amplitude and increase the amplitude when the nodes do not find odor information. This zigzag amplitude is limited by another nodes' amplitudes. When at least one node detects odor concentration, the phase changes to source localization.

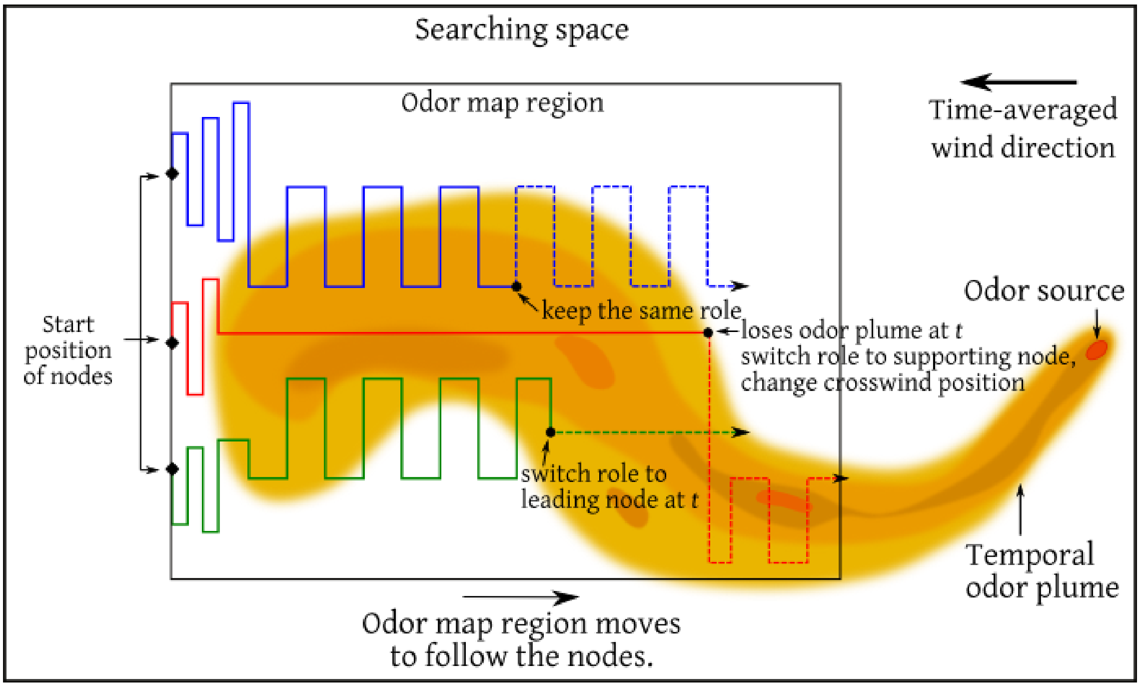

Figure 2.7: Sensor node role definition for system implementation using three sensor nodes. Solid lines (blue, red, green) are nodes' trajectory before role switch at time t and the dashed lines are after the switch.

2.2.1 Odor distribution map

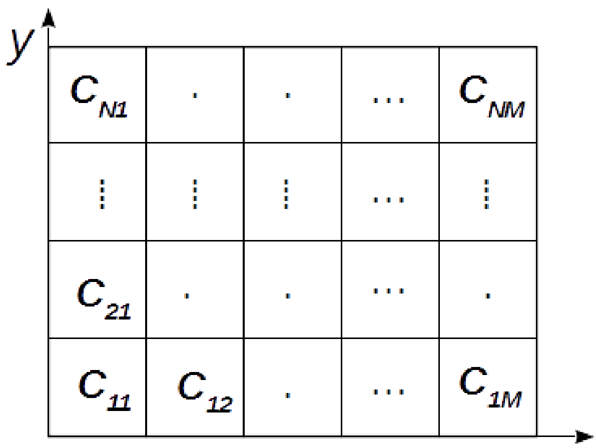

Figure 2.9: Cellular division of map region to be searched.

A map of odor distribution is constructed on a rectangular region of interest that covers all supporting nodes position. In order to represent odor information into spatial map, $M \times N$ cellular divisions is defined as illustrated in Figure 2.9. The cell matrix with its element C_{ij} $(i = 1, ..., N, j = 1, ..., M)$ indicates whether the cell has already been searched or not. This cell representation also means that all area within the cell is assumed to have uniform distribution of concentration. Thus, when an odor concentration is measured at a cell, the entire area of the cell is assumed to contain the

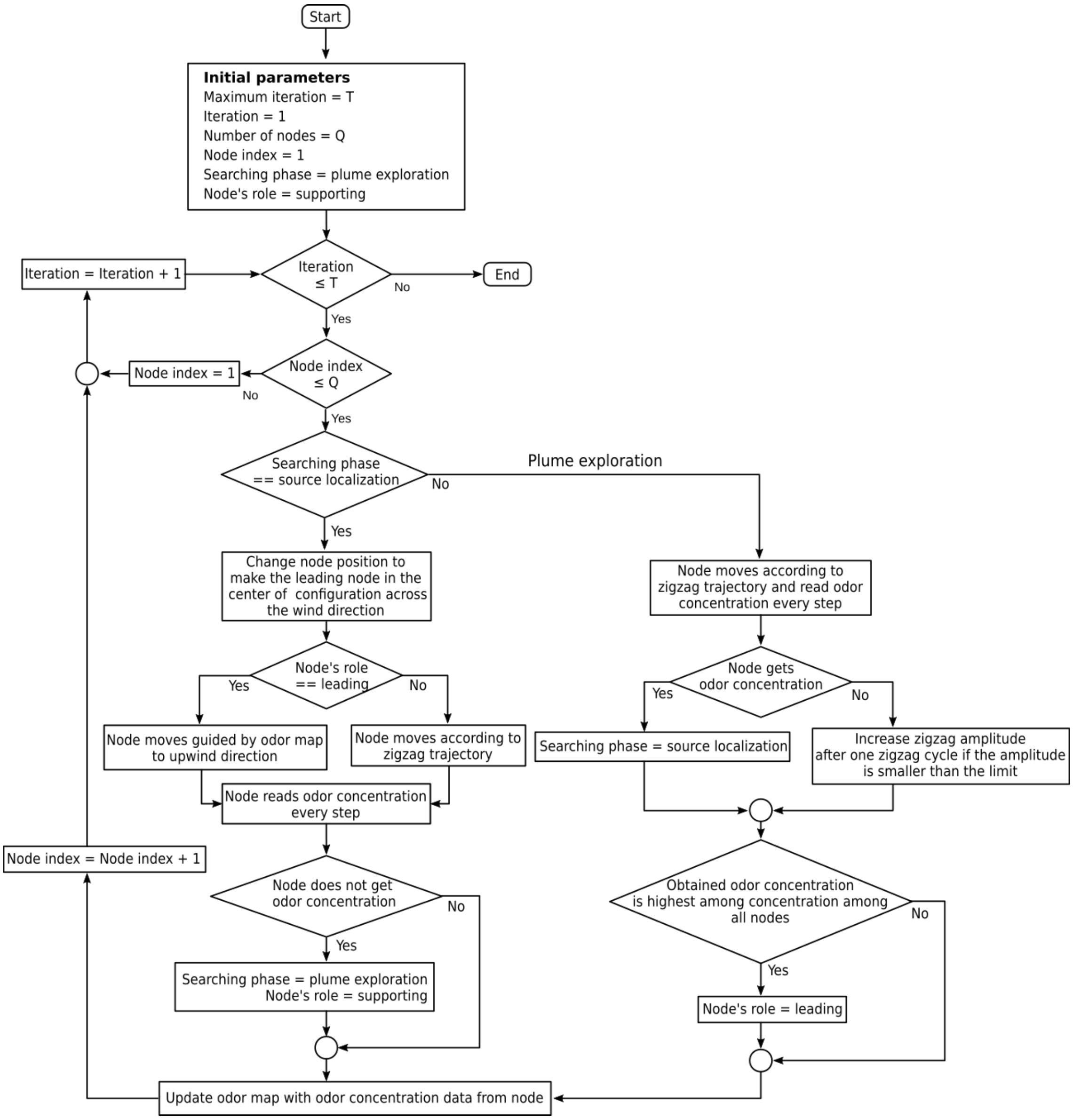

Figure 2.8: Flowchart of system implementation

same concentration.

2.2.2 Simulation

We implemented this strategy using MATLAB simulation. The assumptions adopted here are the same as those mentioned in Section 2.1. In this simulation, we implemented the localization algorithm using three sensor nodes. As illustrated in Figure 2.10, three sensor nodes at the beginning are aligned in crosswind direction. This odor nodes formation is 900cm away from odor source. Distance between the nodes is 180cm, map region is 300×600cm^2, searching space is 1000×800cm^2 and cell dimension is 20×20cm^2. Odor source localization is terminated when at least one node finds location of odor source or searching time is out.

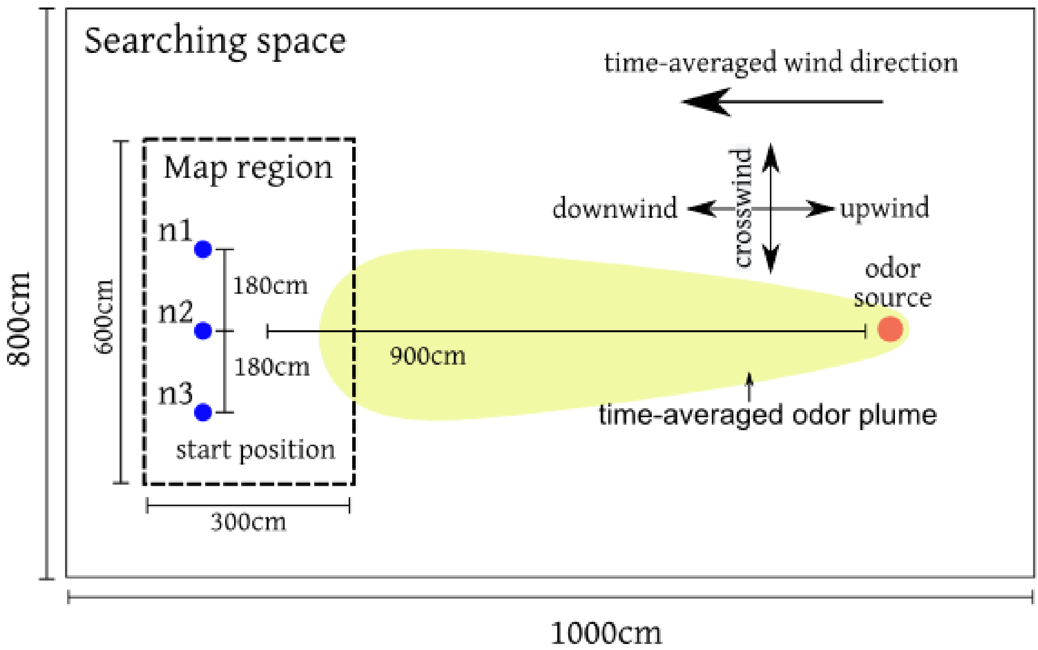

Figure 2.10: Simulation set up of odor source localization.

Figure 2.11 shows the result of simulation. The trajectories of three nodes are indicated by black, red and blue lines (trajectories). The symbols (+) on the lines are the positions where the nodes read odor concentration and the small tiles that cover the symbols are the cells, the small areas that are assumed to have uniform concentration within the cell. The red circle at the right side of the figure is the odor source location. We varied the crosswind position of odor source to show how the strategy works. The odor localization starts with exploration phase.

Figure 2.11a shows the case when the node which finds the highest concentration thus become leading node is initially in the edge of formation (black trajectory). The supporting nodes (indicated by red and blue trajectories) then need to change their crosswind position to let the leading in the crosswind center of formation. In this experiment, the odor source was actually passed (localized) by the leading node (with black trajectory). However the localization was continued to demonstrate when the leading node (black trajectory) lost the plume (more precisely, passed the source) and therefore the supporting node sensing the highest concentration needed to take the leading role, in this the node with the blue trajectory.

Figure 2.11b shows the case when the node which finds the highest concentration is at the center of the formation. Therefore supporting nodes keep their positions at the edge of formation. The simulation reveals that the odor source was successfully localized in both cases.

The rectangular covering trajectories of three nodes is odor map region, where only odor information within this area is assumed to be up to date thus relevant for source localization. The map is designed to have smaller area rather than the entire searching space to limit the memory usage of processing unit. The map moves to keep up with the supporting nodes while they progress upwind.

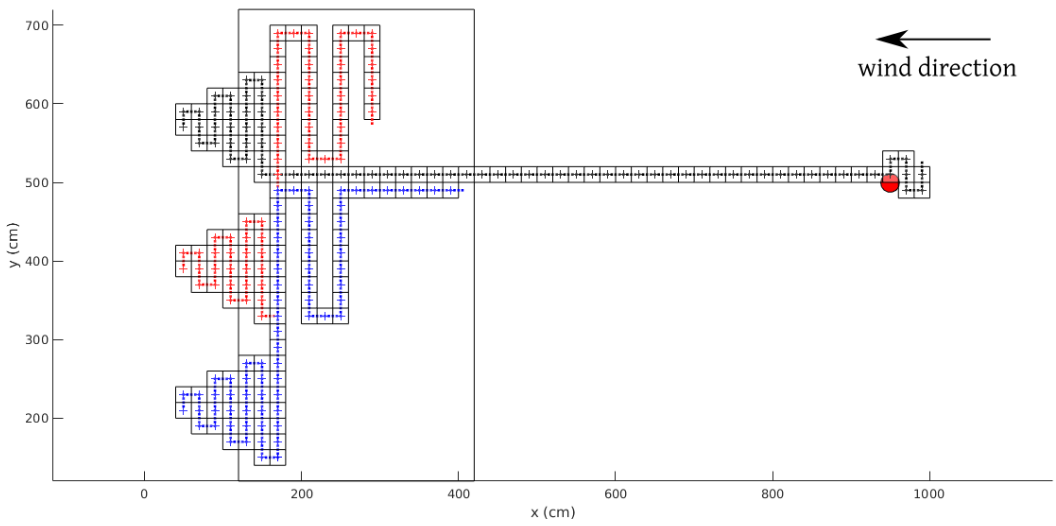

(a)

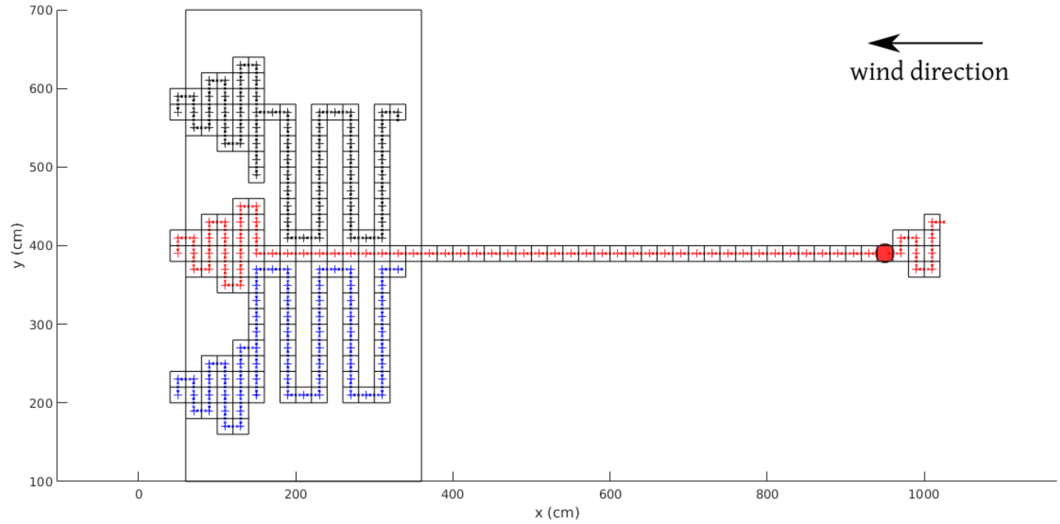

(b)

Figure 2.11: Simulation result with various positions of odor source location. Lateral position of supporting nodes may change to let the leading node in the crosswind center of formation. This strategy is to maximize the probability of odor reading by supporting nodes. Center of sensor nodes formation is (a) away from plume axis and (b) close to plume axis.

2.3 Summary

The result confirmed that the proposed odor source localization strategy using multiple sensor nodes works well. This simulation has not yet shown the true advantage of using multiple sensor nodes as the environment is still ideal (unidirectional airflow, constant wind speed and without airflow turbulence). In spite of the simplified situation, we can demonstrate how this strategy is implemented using three sensor nodes. This map at the moment serves as guidance for the nodes to minimize overlapping of searching area among the nodes. However there is potential of utilizing the map to estimate source location remotely that can be useful for the leading node as a guidance to localize odor source.

This strategy is built from predefined actions of sensor node to respond to the existence of odor information by considering nodes formation and position, and many other variables. Therefore the performance of this strategy highly depends on how well we anticipate every possible conditions and implement the effective actions to respond to them. However in this research we make several assumptions and simplifications to avoid excessive complexity. With these assumptions and simplifications, this simulation confirmed the capability of the strategy for the odor source localization using multiple sensor nodes. Since we realize that the performance of this strategy still needs to be evaluated under more realistic environment, the next work would be to test this strategy in an environment with turbulent airflow condition.

Chapter 3

Simulation environment

Testing odor source localization systems or strategies in a real experiment is a challenge owing to the stochastic nature of odor distribution. Odor distribution in the real-world environment is mostly governed by turbulent airflow. With such stochastic nature, it is not possible to get repeatable environmental conditions for repetitive test of the strategies. Therefore, in this research, a virtual environment was developed as a target environment for the localization strategy. As the virtual environment is completely repeatable, the localization strategy can be repeatedly evaluated under consistent environmental conditions.

This virtual environment was simulated using a Computational Fluid Dynamics (CFD) software package, ANSYS Fluent 17.2. The required data obtained from this simulation were then integrated into an odor source localization simulation in MATLAB programming. The phases of this ANSYS-MATLAB simulation framework is shown in Fig. 3.1.

Phases and configuration of the environment simulation in ANSYS is explained in Sections 3.1. A validation of a simulated environment by comparing with the real experiment is explained in Section 3.2. The pre-processing of the environment data obtained from ANSYS simulation before being integrated into the odor source localization simulation in MATLAB is explained in Section 3.3.

3.1 Environment modeling in ANSYS

The virtual environment was developed based on a real physical model [2]. Two variants of environment were used in this study. These two environments differ in the number of obstacle and emission rate of the odor from the source as explained in Table 3.1. These environments are each used for development and evaluation of two different localization strategies which are explained in Chapter 4 and Chapter 5, respectively.

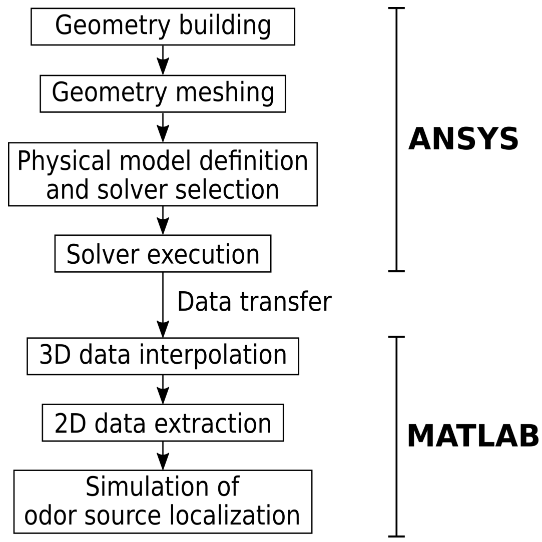

Figure 3.1: Simulation phases in ANSYS and MATLAB.

Table 3.1: Variants of testing environment.

Variants name	Emission rate (ml/min)	Number of obstacle
Single-obstacle-environment model	500	1
Three-obstacles-environment model	50	3

This environment simulation in ANSYS was performed in several development phases, including:

- Geometry building.
- Geometry meshing.
- Physical model definition and solver selection.
- Solver execution.
- Data post processing and analysis.

Some details of these phases are described in the following sections.

3.1.1 Geometry building

This model is asymmetric closed room of 5.9 m long, 3.2 m wide and 2.7 m high with a window at the width side as shown in Fig. 3.2. A gas inlet with a surface area of 25 cm^2 serving as the odor source is located on the floor near the window at coordinate (1.025, 1.625). The single-obstacle-environment model has a screen of 180 cm high and 90 cm wide as the obstacle, whereas the three-obstacles-environment has three screens of 180 cm high and 50 cm wide. Those obstacles stand 2 m from the window at middle-width of the room to obstruct the airflow and create complicated odor plume.

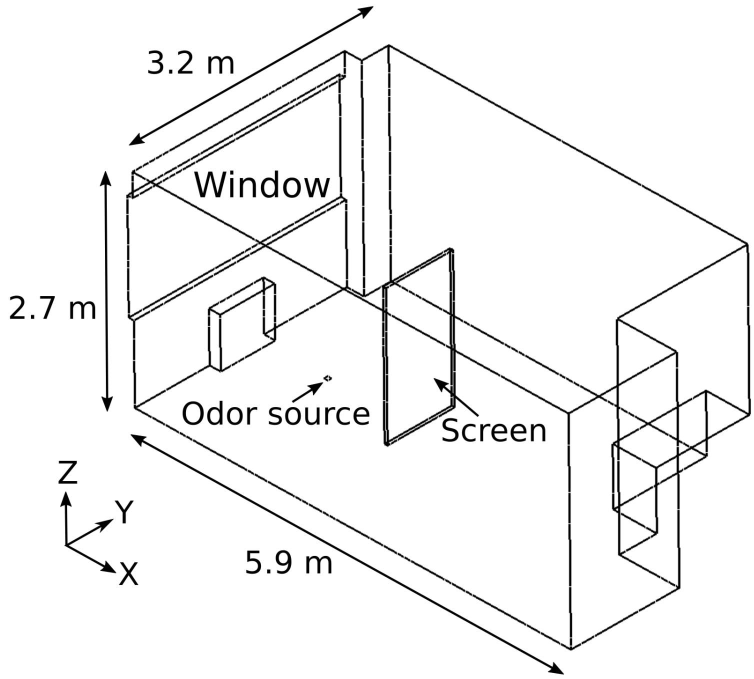

(a)

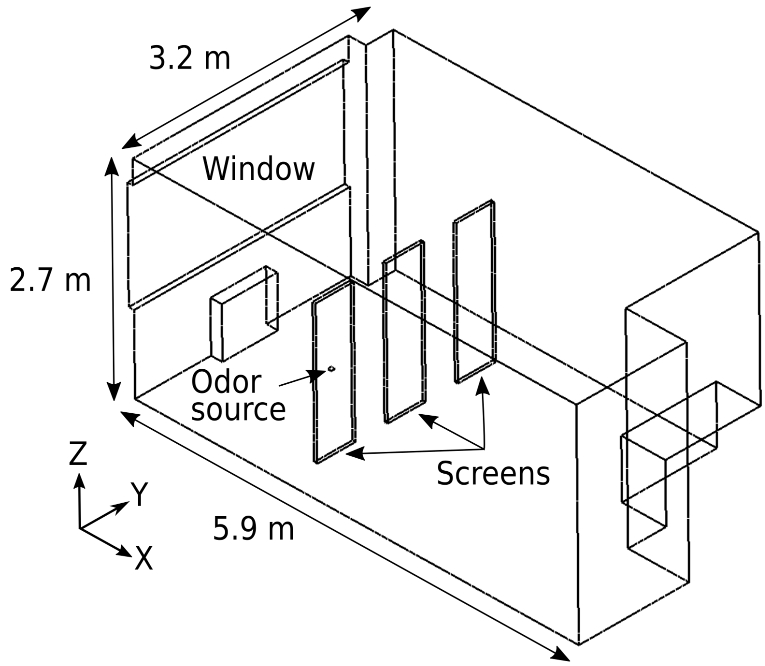

(b)

Figure 3.2: Geometry of the closed room model with (a) a single obstacle and (b) with three obstacles.

3.1.2 Geometry meshing

A structured mesh was generated on the geometry volume using automatic method. The mesh size around floor level, screen and window was set to have smaller size because we expected these areas to have more dynamic airflow and odor fluctuations. Thus the calculation around these areas is required to be more precise. The parameter of meshing and statistics are shown in Table 3.2.

Table 3.2: Meshing parameter.

Parameter		Single-obstacle-environment	Three-obstacles-environment
Sizing	Size function	Curvature	
	Relevance center	Medium	
	Smoothing	High	
	Transition	Slow	
	Span Angle Center	Fine	
	Minimum edge length	4.e-002 m	
Inflation	Inflation option	Smooth transition	
	Inflation algorithm	Pre	
Statistics	Nodes	114492	136821
	Elements	616049	740738

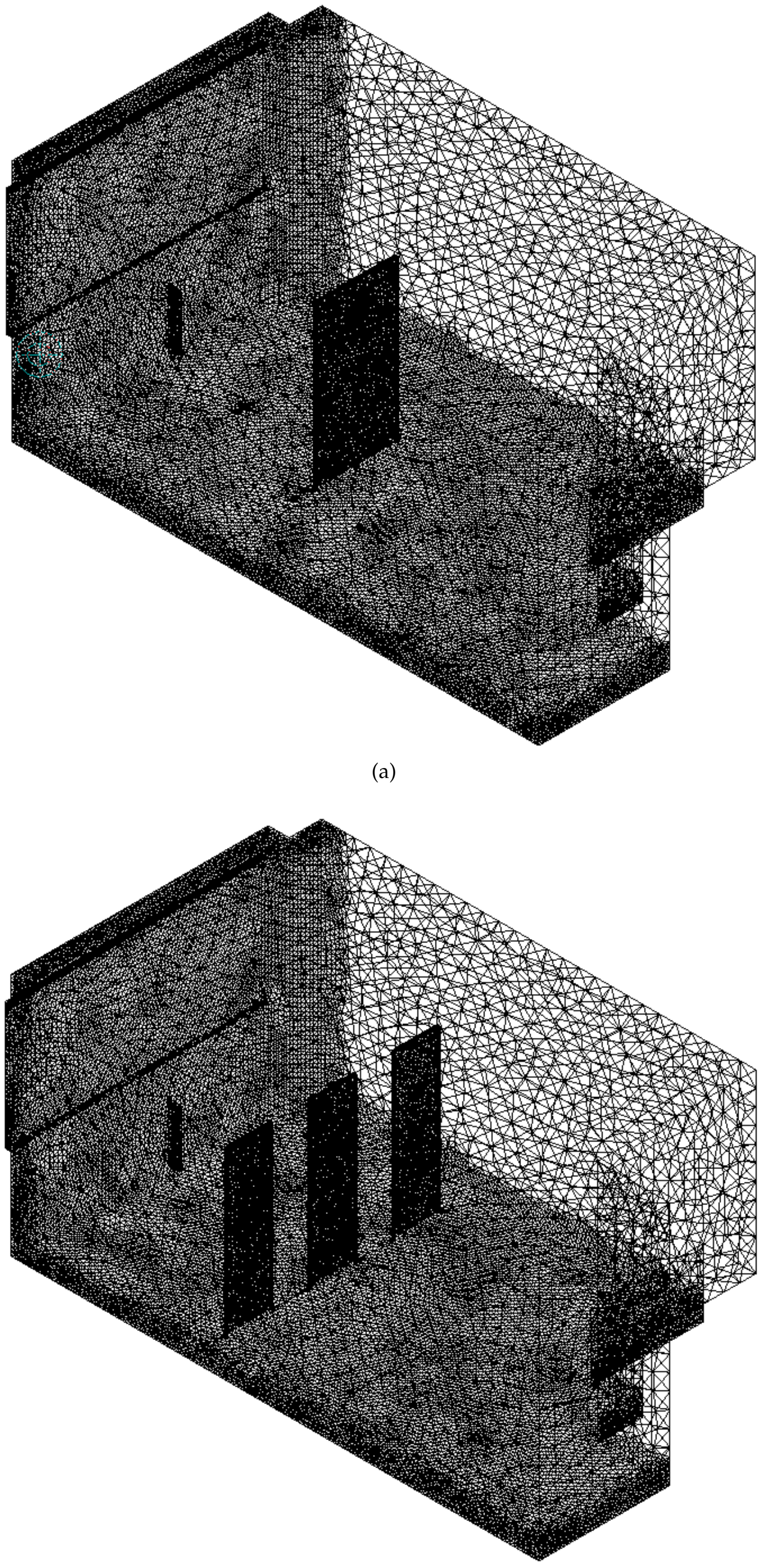

(a)

(b)

Figure 3.3: Geometry meshing. (a) Room with single obstacle. (b) Room with three obstacles.

Table 3.3: Simulation parameters.

Parameter	Single-obstacle-environment	Three-obstacles-environment
Odor source	Ethanol gas (C_2H_5OH)	
• Emission rate	500 ml/min	50 ml/min
Material		
• Room boundaries	aluminum	
• Fluid	mixture of ethanol and air	
Temperature		
• Window	10°C	
• Others	15°C	
Flow model	Standard $k - \varepsilon$ model	
Time step	0.1 s	
Output	Coordinate, ethanol mass fraction and flow velocity	

3.1.3 Physical model definition and solver configuration

Odor source was modeled as ethanol gas (C_2H_5OH) emitted from the gas inlet. Ethanol was chosen here since it was oten used in the experimenst of odor source localization. Turbulent airflow was simulated using standard $k - \varepsilon$ model. The evolution of modeled environment was calculated every 0.1 s. This time step was chosen to match the sensing frequency of odor sensor in the odor source localization. the Upon the starting of the simulation, it was assumed that there was no initial airflow. The physical parameters required for calculation are shown in Table 3.3. After setting these parameters, the calculation of the modeled environment was executed.

3.1.4 Solver execution

In this study, the environment model is calculated in transient mode. As illustrated in Fig. 3.4, the environment simulation was executed in two phases: Firstly, the simulation was proceeded without odor release for 600 s. During this, convective turbulent airflow was gradually developed due to difference between temperature at the window (10°C) and the one at another part of the room (15°C). Secondly, it was then continued with the odor (ethanol) release from gas inlet until the maximum time of simulation. The maximum time of simulation with a single obstacle is 900 s, whereas that of simulation with three obstacles is 1200 s. These two phases resulted in 3D time series data. This data contains ethanol mass fraction and flow velocity at every coordinate point in the simulation domain. The data were then integrated into MATLAB programming to simulate the dynamic environment. Depending on the computation resource (CPU processor, memory, etc.), this solver computation can take several days.

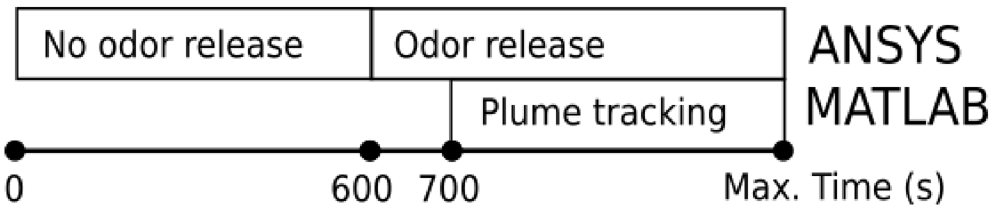

Figure 3.4: Simulation phases.

3.1.5 Data post processing and analysis

For the purpose of analysis and visual presentation, the resulted data can be expressed as image or video of modeled environment. Fig. 3.6a and 3.7a show the instantaneous modeled environment with a single obstacle and three obstacles, respectively, at time step 700 s whereas Fig. 3.6b and 3.7b show the evolution of ethanol concentration over time at points A and B as shown in Fig. 3.6a and 3.7a, respectively, at 5 cm above the floor. These figures show that irregular and fluctuated airflow field was created as the convective airflow was obstructed by the obstacles. This flow was relatively slow as it had maximum flow speed around 16 cm/s for the room with a single obstacle and 13 cm/s for the room with three obstacles. These flows created relatively low frequency fluctuations of odor distribution.

3.2 Validation of the simulated environment

One of crucial issues in in this simulation of the virtual environment is to validate the environment model, meaning to prove that the model is accurate to certain extent compared with the real environment. For this validation, we need to check the characteristics or qualities of interest of virtual environment in comparison to the data of real experiment for the odor source localization, which, in this case are odor distribution and airflow profile.

An experiment to assess the odor distribution and airflow profile in the closed room with an ethanol source is shown in literature [2]. In that experiments, the airflow profile on the vertical plane at the mid-width of the room was measured using an ultrasonic anemometer. The 2D distribution of ethanol on the horizontal plane at 20 cm above the floor was measured using eight metal oxide gas sensors (TGS2620, Figaro Engineering). The sensors measured at different positions at a

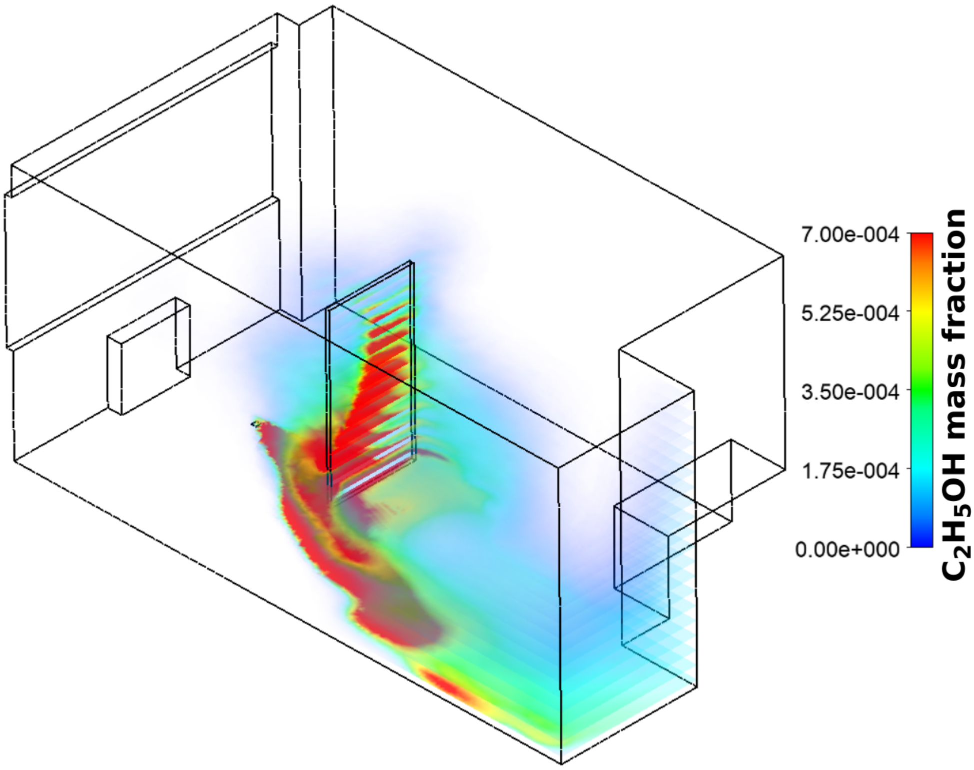

(a)

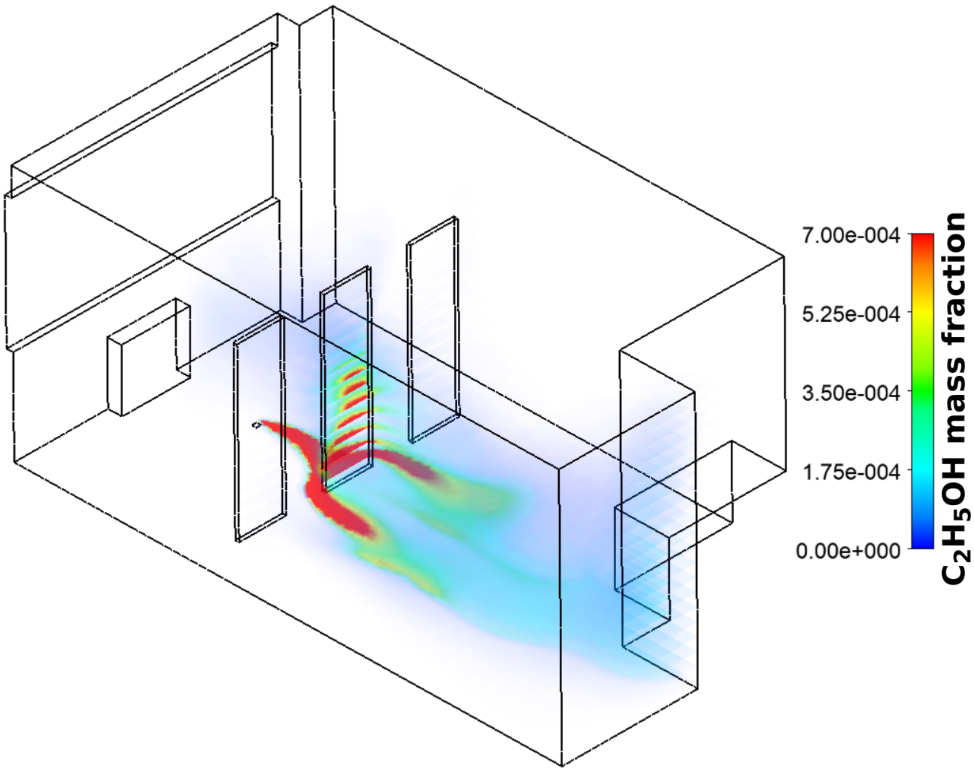

(b)

Figure 3.5: 3D odor distribution at time step 700 s of simulation. (a) The room with single obstacle. (b) The room with three obstacle.

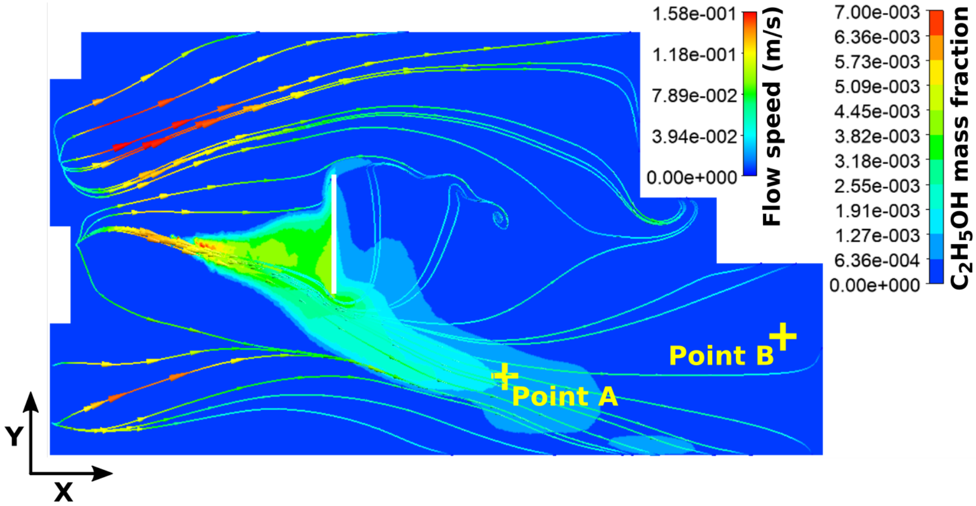

(a)

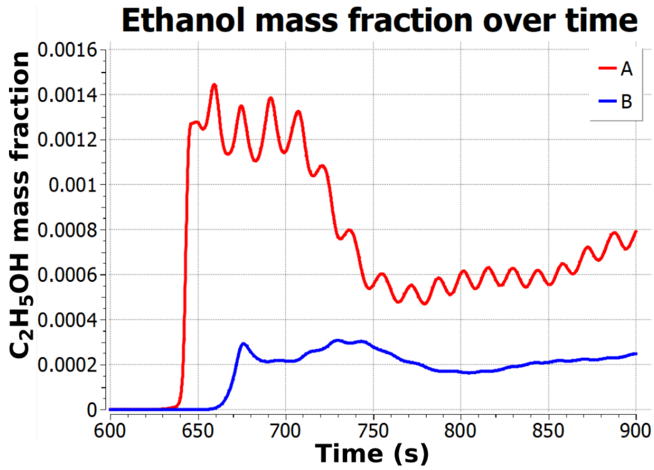

(b)

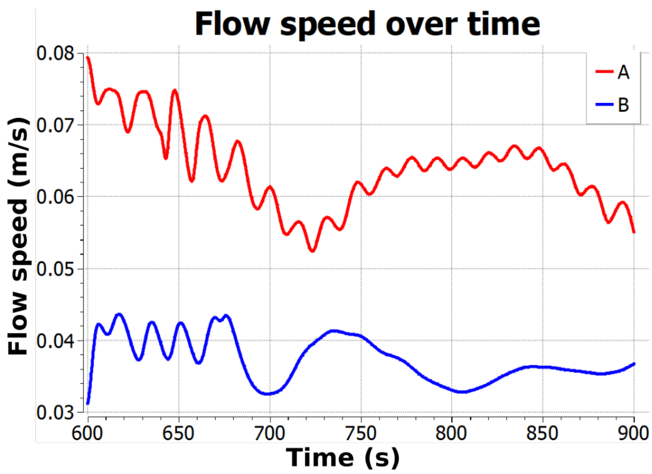

(c)

Figure 3.6: Room with single obstacle. (a) 2D airflow and odor distribution profile at 5 cm above floor at 700 s in ANSYS. (b) at points A and B (as shown in figure (a)) at 5 cm above the floor.

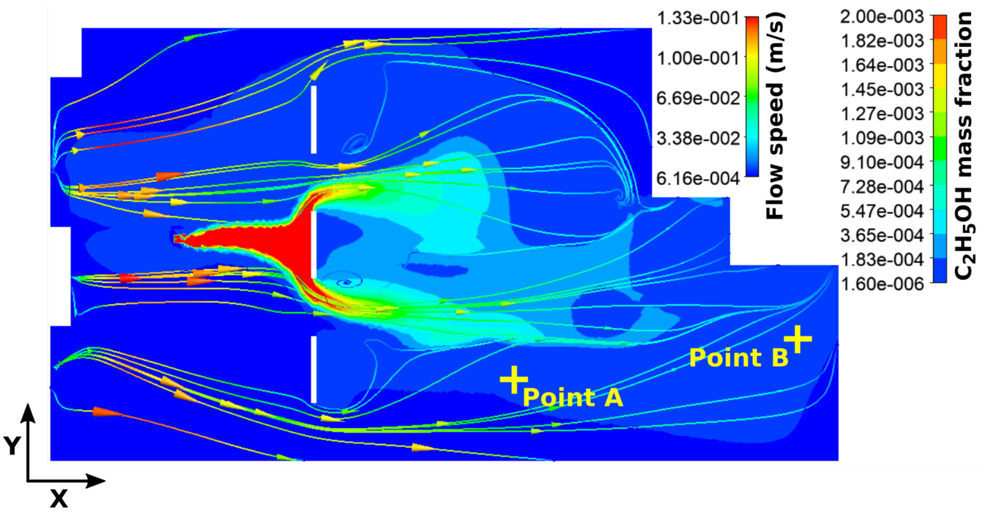

(a)

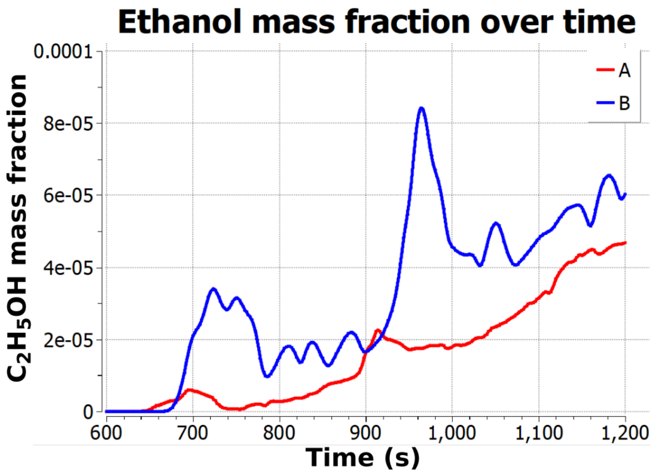

(b)

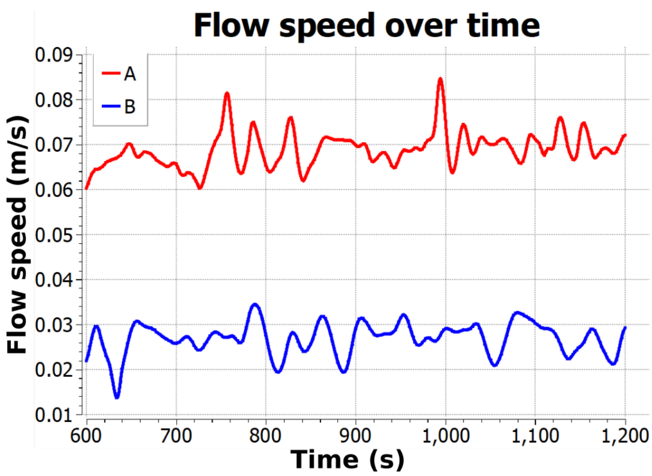

(c)

Figure 3.7: Room with three obstacles. (a) 2D airflow and odor distribution profile at 5 cm above floor at 700 s in ANSYS. (b) at points A and B (as shown in figure (a)) at 5 cm above the floor.

time, and the averages of the concentration values for one minute were calculated. The room was then completely cleaned with fresh air. Afterward, the same measurement procedure was repeated for another positions until covering the entire room's floor. The measured airflow profile and odor distribution is shown in Fig. 3.9. The similar room setting was simulated in ANSYS. The airflow in the simulation is shown in Fig. 3.10. Comparing the real and simulated data, the airflow and distribution of the real room setting agree the simulated one qualitatively.

As the experiment was carried out without obstacle, we could not validate the simulated closed room model with obstacle directly. However, we could expect that the agreement of the closed room model with obstacle in the simulation and real experiment still hold.

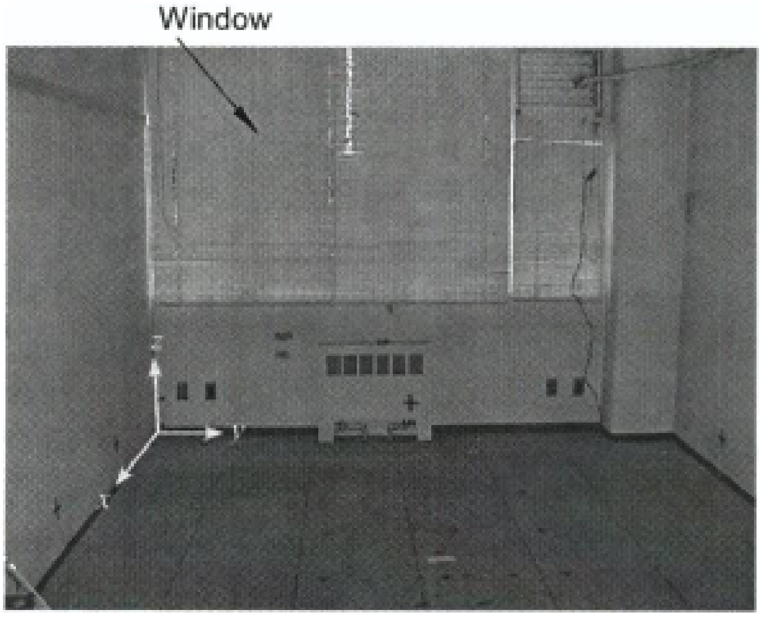

(a)

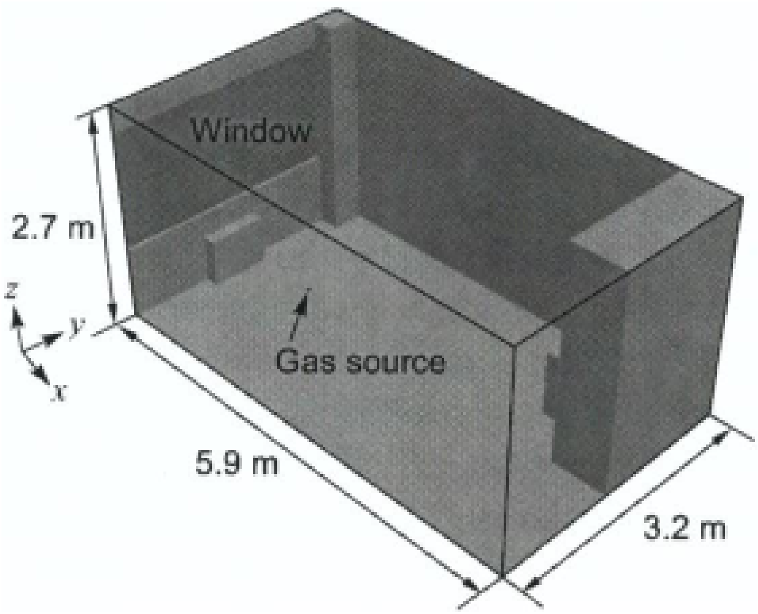

(b)

Figure 3.8: Experiment of odor distribution mapping in a natural convective airflow in a closed room [2]. (a) The picture of the closed room. (b) The geometry of the closed room.

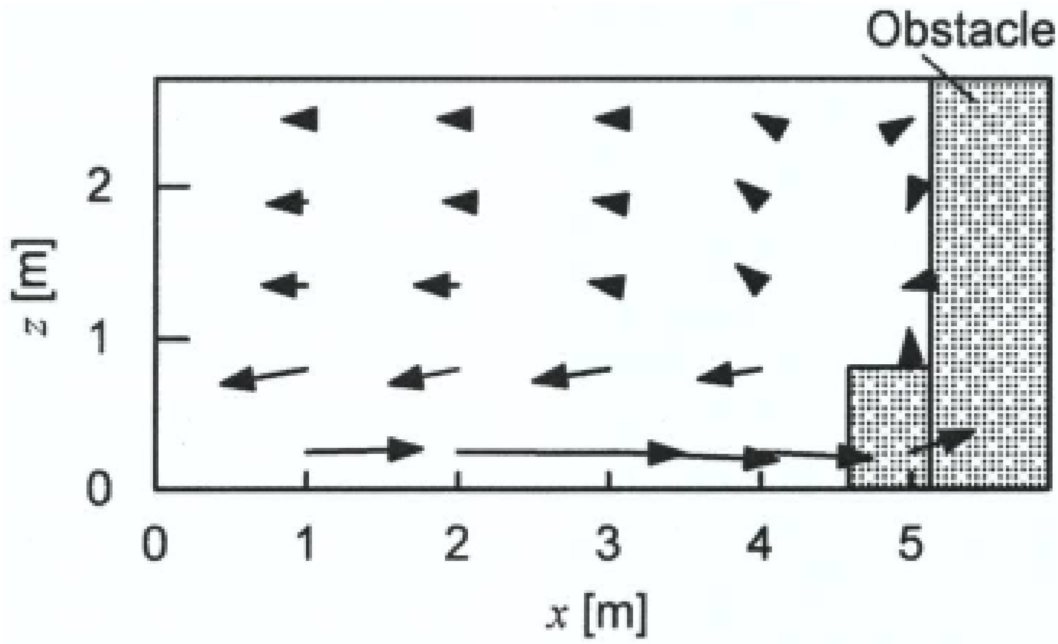

(a)

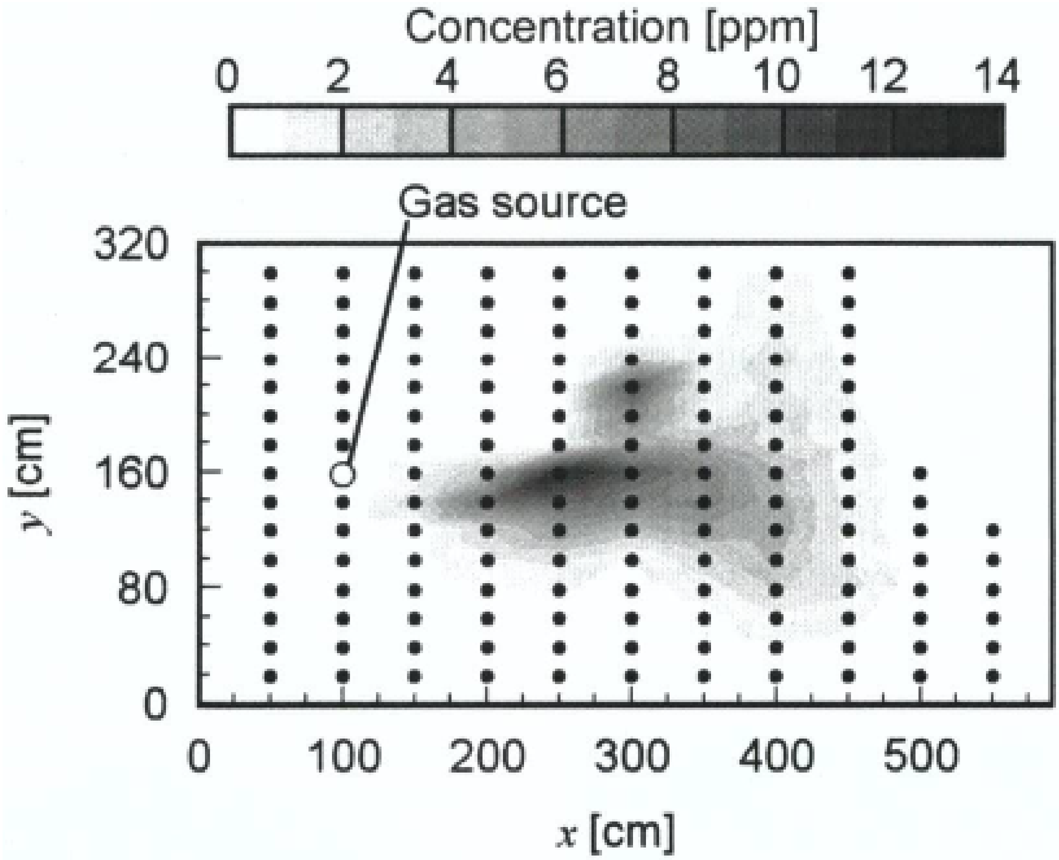

(b)

Figure 3.9: Experiment result. (a) Airflow and (b) odor distribution profile obtained from real experiment [2].

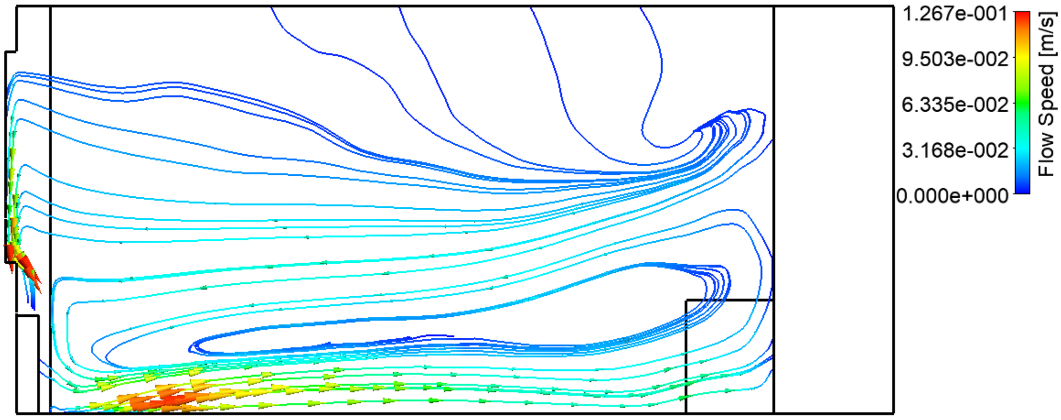

(a)

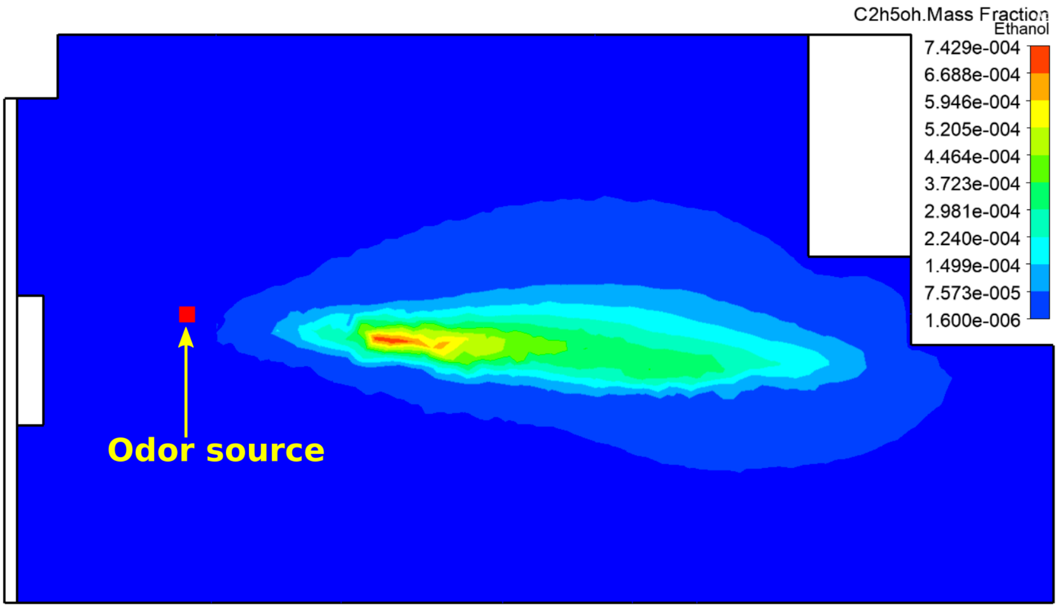

(b)

Figure 3.10: Simulation result. (a) Airflow and (b) odor distribution profile obtained from ANSYS simulation.

3.3 Data processing in MATLAB

Data of the virtual environment from ANSYS, i.e. odor concentration (ethanol mass fraction) and flow velocity, is not uniformly distributed in 3D space. Therefore, it needs grid-based interpolation for convenient data processing before being integrated into tracking algorithm. The interpolation grid size is 5 cm. Although the data from ANSYS is in 3D format, in this simulation, only 2D data throughout a horizontal plane at 5 cm above the floor is used by plume tracking algorithm to localize the source. Moreover, only the data when odor has been released is required for the simulation and thus integrated into MATLAB programming.

3.4 Summary

This simulation framework was developed to provide repeatable testing environment for the source localization strategy. Using state-of-the-art physical simulation CFD application, we can build different models of realistic environment in faster and more economical way than to build the real environment. The model's characteristics agree with the real one qualitatively, provided that the simulation configurations are appropriately set.

There are several ways of improving the accuracy of the simulation in ANSYS including reducing the mesh size, selecting appropriate materials and characteristics of the boundaries (wall, floor, ceiling, window, and obstacles), setting the appropriate model of flow and the parameters (there are several models beside standard $k - \varepsilon$ model). However, the simulation of higly accurate model demands high computational and memory resource as well.

Chapter 4

Localization strategy for turbulent environment using an odor sensor without response delay

In this chapter, an estimation method of temporal odor concentration profile is proposed to determine concentration trend of fluctuated odor data for plume tracking. This estimation is applied to time series of odor data obtained during a plume tracking using a single tracking node, e.g. mobile robot or device. This estimation method is embedded into a bio-inspired plume tracking strategy to localize an odor source. This strategy employs chemotaxis-anemotaxis approach in which the tracking is guided by chemical and fluid flow information. The tracking strategy was developed and evaluated in consistent virtual environment using an ANSYS-MATLAB simulation framework.

4.1 Plume tracking strategy

4.1.1 Tracking phase

Our tracking strategy is designed to exploit odor concentration and flow direction information to localize the source location. As described in Figure 4.1, the strategy has 4 phases:

Upwind tracking. The plume tracking is started in *upwind tracking*. In this phase, the tracking node moves following upwind direction while performing odor sensing as well as recording its position at every specified time interval. During this phase, estimation of temporal odor concentration trend is calculated every time new odor concentration is obtained. Trend here means tendency of odor to increase or decrease indicated by the gradient of the obtained time-series data. The estimation method will be explained in Section 4.2. This upwind tracking phase remains as long as the trend does not decrease or the node does not lose the odor trace. When the tracking detects trend decrease or loses odor trace, the phase switches to *zigzag scanning*. This decreasing trend indicates that the node possibly moves away from the plume centerline or the source location.

Zigzag scanning. The *zigzag scanning* phase aims to estimate direction to the plume centerline. The method of *zigzag scanning* phase will be explained in Section 4.1.2. After finishing one cycle of *zigzag scanning*, estimation of odor concentration trend along crosswind direction is calculated. The direction pointed by increasing trend of concentration leads to the estimated centerline of plume. Subsequently, the phase switches to *crosswind tracking* toward the estimated centerline.

Crosswind tracking. During the *crosswind tracking*, the node climbs up the odor gradient. When the node finds a decreasing trend after an increasing one previously, it means that an odor concentration peak location might have been passed. Then, it can be assumed that the plume centerline is found at the peak location thus the phase switches to *return to the peak location*.

Return to the peak location. In this phase, the node simply moves to the estimated centerline. Information on odor concentration and flow velocity is ignored during this phase. When the node has reached the estimated centerline, the phase switches to *upwind tracking*.

This tracking strategy is illustrated in Figure 4.2. The sequence of tracking phases is repetitive until a termination condition is met: the tracking has arrived nearby the source location or the allocated time for the source localization is over. The nearness criteria used in this simulation for a successful odor source localization is explained in Section 4.3.1.

4.1.2 Searching for plume centerline

Zigzag scanning phase is entered when tracking node obtained decreasing trend of concentration or lost odor trace completely. The purpose of this phase is to find plume centerline. If $c(t)$ is odor concentration sampled at time t, the zigzag scanning in case of odor frame size 5 data points is described in Figure 4.3. The selection of frame size will be explained in Section 4.3.2. The width of zigzag can be varied in order to obtain the same number of data points as the one used in data frame along the middle span of zigzag ($c(t+2T)$ to $c(t+6T)$).

As illustrated in the figure, *zigzag scanning* phase starts after the node at position $c(t)$ and ends at position $c(t+8T)$. Odor concentration c and position is recorded at black dots every time T

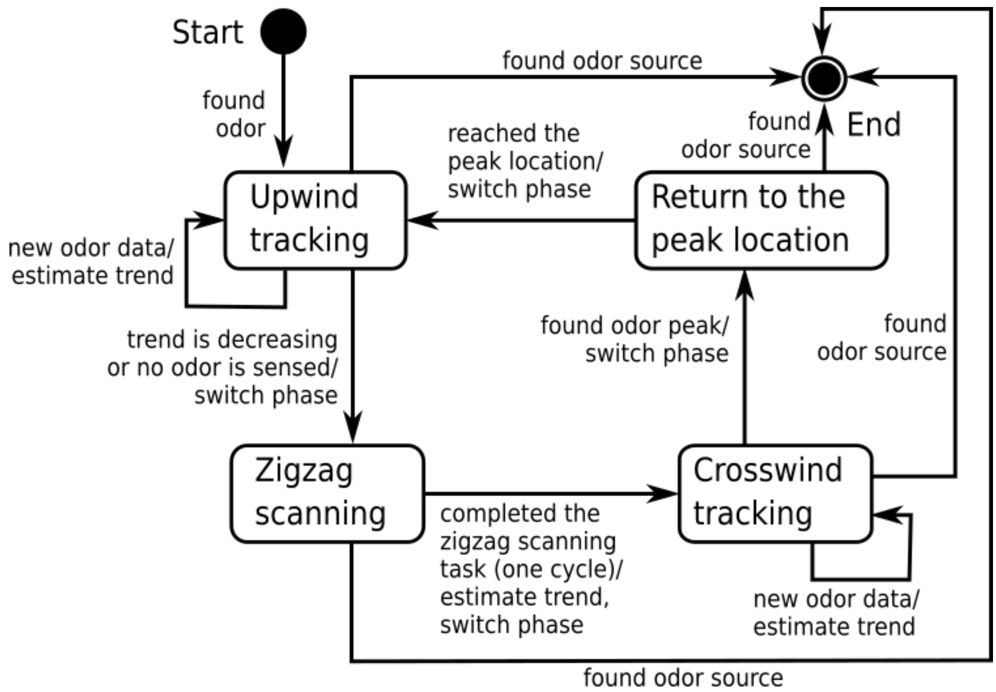

Figure 4.1: Phases of plume tracking strategy.

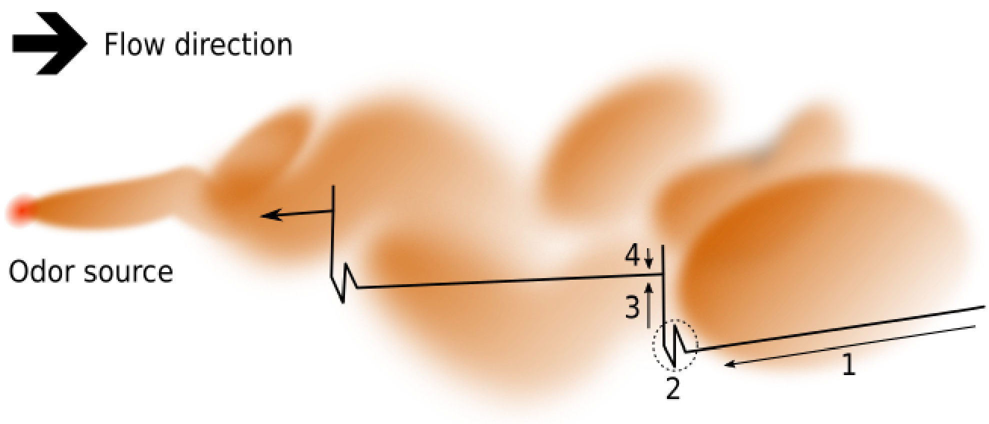

Figure 4.2: Illustration of a plume tracking. The tracking is carried out in cycles of successive phases: (1) *upwind tracking*, (2) *zigzag scanning*, (3) *crosswind tracking*, and (4) *return to the peak location*.

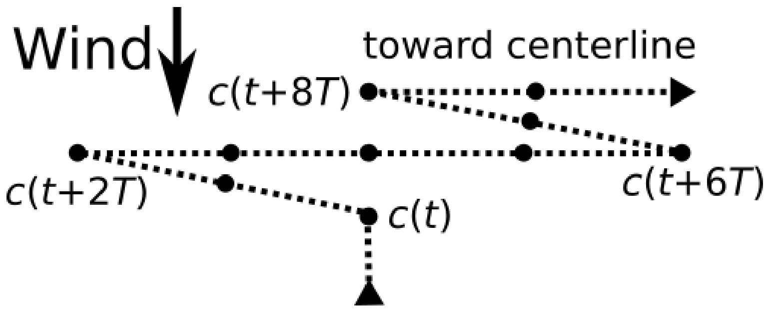

Figure 4.3: Zigzag scanning in case of odor frame size 5 data points.

interval. The zigzag movement shape is made so that the middle span, from $c(t+2T)$ to $c(t+6T)$, is perpendicular (crosswind) to local flow direction at $c(t)$. The odor data obtained from $c(t+2T)$ to $c(t+6T)$ is used to estimate temporal odor concentration trend along crosswind direction. Direction to centerline is indicated by increasing trend of concentration along crosswind direction.

4.1.3 Obstacle avoidance

Since there is possibility that the tracking node moves toward an obstacle, the tracking strategy also includes an obstacle avoidance mechanism. The mechanism works when an obstacle is detected by the ultrasonic sensor within 5 cm and 180° ahead of the tracking node. In general, the avoidance is made by turning the tracking direction 90° away from the obstacle as illustrated in Figure 4.4.

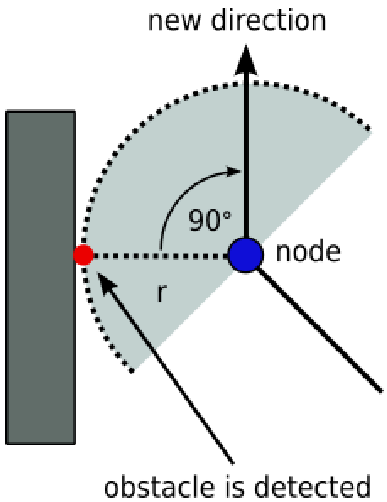

Figure 4.4: Obstacle avoidance.

4.2 Estimation of temporal odor concentration profile

In general, plume tracking is performed by moving toward area with higher odor concentration. For this purpose, the tracking requires to estimate the odor concentration trend during *upwind tracking* and *crosswind tracking* and in the end of *zigzag scanning* as shown in Figure 4.1.

An estimation method of temporal odor concentration profile is proposed to determine concentration trend of fluctuated odor data over time. This method combines odor data smoothing and concentration trend estimation using regression (smoothing-regression concentration trend estimation). The smoothing and the trend estimation method are applied to time series odor concentration data (concentration profile). This trend is explained by the gradient of regression function of odor concentration. The method of odor data smoothing and trend estimation using regression will be explained in Section 4.2.1 and 4.2.2 respectively.

For the purpose of evaluation of the trend estimation using regression in comparison with an established method, we also developed trend estimation using adaptive threshold. This trend estimation method will be explained in Section 4.2.3.

4.2.1 Odor data smoothing

The tracking node measures odor concentration at discrete times resulting in a record of odor concentration $\{\boldsymbol{c}\,(t_i)\}_{i=1}^{k}$. As this is obtained from dynamic environment, the record elements exhibit fluctuation in the magnitude. To get the general picture of odor distribution in the searching area, it is considered necessary to minimize the fluctuation. For this purpose, $\{\boldsymbol{c}\,(t_i)\}_{i=1}^{k}$ is filtered using a moving average filter

$$\bar{c}\,(t_k) = \frac{1}{n} \sum_{i=k-n+1}^{k} c\,(t_i) \tag{4.1}$$

where $\bar{c}(t_k)$ is averaged concentration at present time t_k and $c(t_i)$ is concentration detected at t_i. Here t_i is uniformly distributed. The averaging calculation at t_k is performed over a frame of n data points.

4.2.2 Trend and peak estimation using regression

The concentration trend estimation is applied to the latest n data points$\{\bar{\mathbf{c}}(t_i)\}_{i=k-n+1}^{k}$ obtained from moving average filter as illustrated in Figure 4.5. The regression function is obtained by modeling the relationship between t and $\bar{c}$ using second order polynomial regression technique

$$\hat{c}(t_i) = w_2 t_i^2 + w_1 t_i + w_0 \tag{4.2}$$

where $\hat{c}(t_i)$ is expected concentration at t_i, while w_0, w_1 and w_2 are coefficients. This quadratic function fits approximately to odor data within the frame as illustrated in Figure 4.6. The second order polynomial was used in this regression considering that the frame size used here is short. In this study, the frame size is varied for 3, 5, 7, and 9 data points. Thus, the data variation within this

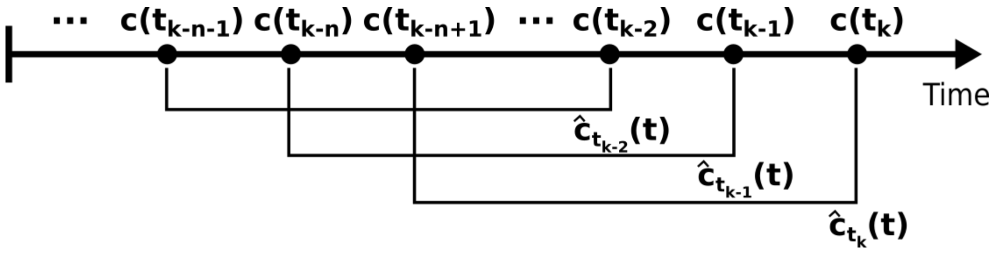

Figure 4.5: Trend estimation on the latest n data points. This process is performed every time a new data is obtained.

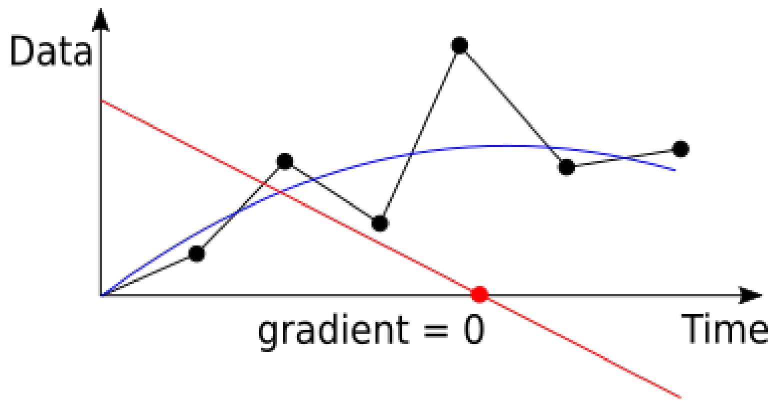

Figure 4.6: Trend and peak estimation. The black dots are the time series odor data obtained from sensor measurement. The blue line is the graph of fitting function obtained using the regression technique. The red line is the gradient graph. Estimated odor peak is found at time when the gradient equals to 0.

frame should be sufficiently approximated using the second order polynomial regression.

The temporal concentration gradient function which describes the rate of concentration change over time is obtained from derivative of equation 4.2, $d\hat{c}(t)/dt$. The gradient function is calculated every time the new data is obtained. The aim of this trend evaluation is to look for a data point with zero derivative within time frame of n data points. If the data point has the maximum value within the frame, then it is the estimated concentration peak.

During *upwind tracking* phase, when the peak has not been found, the node keeps moving upwind. In this phase, the concentration trend is evaluated from time domain perspective. When the peak is found within the last data frame, meaning the trend begin to decrease at the end of odor record, then the phase switches to *zigzag scanning* phase.

During the middle span of *zigzag scanning* and *crosswind tracking* phase, the concentration trend is evaluated from space domain perspective (spatial gradient). The measurement positions during these phases form a straight line. Since tracking node moves at constant speed while measuring odor every constant time interval, in this case the temporal gradient is equivalent to the spatial gradient.

Similarly, during *crosswind tracking* phase, estimation method looks for odor peak. After finding the peak location, the phase switches to *return to the peak location* phase.

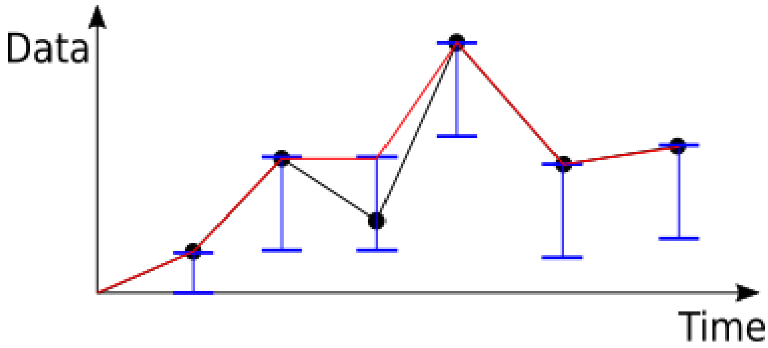

Figure 4.7: Trend estimation using adaptive threshold. The black dots are time series data obtained from sensor measurement. The blue scale is the pair of thresholds. The trend change is indicated by the red line.

4.2.3 Trend estimation using adaptive threshold

This alternative trend estimation method is presented to make comparative evaluation for the trend estimation using regression. Therefore, either regression-based method or adaptive threshold-based method is used as the trend estimation method in the tracking algorithm and the parameters checking for tracking phase switching are modified accordingly. Apart from it, the rest of algorithm is the same.

In this method, iterative checking of newly obtained odor concentration in comparison to a pair of concentration threshold is performed in attempt to estimate the trend of odor concentration over time or space, as illustrated in Figure 4.7. The pair of threshold consists of upper and lower thresholds. The lower threshold is obtained from the upper threshold multiplied with a positive coefficient smaller than one, e.g., (lower threshold) = (upper threshold)$\times$0.7, etc. The upper threshold is updated with the new concentration if the concentration is higher than the threshold or if the concentration is lower than the lower threshold. The pair of threshold is used to manage the sensitivity of the tracking system against concentration fluctuation.

The change of threshold to the higher or lower value is used to determine increasing or decreasing trend of concentration respectively. This trend information is used as parameter to switch tracking phase. During *upwind tracking* or *crosswind tracking* phase, the tracking remains in the same phase when increasing trend is obtained. When the trend turns from increasing to decreasing, if the active phase is *upwind tracking*, the phase switches to *zigzag scanning* or if the active phase is *crosswind tracking*, the phase switches to *return to the peak location*.

4.3 Plume tracking simulation

4.3.1 Methodology

The tracking strategy was tested on the single-obstacle-environment (described in Section 3.1) from time step 700 s to a maximum time (described in Figure 3.4). Here the maximum time is 200 s. Therefore, the tracking node is assumed to find the odor source successfully if it arrives nearby the source location before time limit at 200 s. The nearness criteria is 20 cm from the source location.

In this simulation, the tracking algorithm uses time series information of odor concentration, flow direction and the node location to localize the source. To get this information, the tracking node records odor concentration, flow direction and its location every 1 s while keeps moving at constant speed of 10 cm/s. To carry out these tasks, the tracking node is equipped with an ideal odor sensor to sense any value of odor concentration and follow the concentration change immediately, an anemometric sensor to sense fluid flow direction and a device to record its location coordinate. For obstacle avoidance mechanism, it is also equipped with ultrasonic sensor to detect obstacle within 5 cm proximity at 180° ahead of it.

The tracking not employing concentration trend estimation is implemented by using algorithm of tracking employing the smoothing-trend estimation with frame size 1 data point. By setting the frame size to 1, no smoothing and no trend estimation are applied. Apart from the part for estimation methods and parameters checking for switching tracking phase, the tracking algorithms using regression and adaptive threshold are the same.

Overall performance evaluation of tracking strategy is performed over variation of concentration trend estimation method i.e.: smoothing-regression, regression, smoothing-adaptive threshold, adaptive threshold and without trend estimation. Frame size used for *zigzag scanning* in the tracking strategy employing concentration trend estimation using adaptive threshold is 5 data points as it is the most appropriate frame size for the trend estimation using regression. This selection is determined after the tracking performance evaluation which will be described in Section 4.3.4.

4.3.2 Key parameter selection

The key parameter in zigzag scanning, data smoothing and regression computation is frame size. In this study, the appropriate frame size is selected from options 3, 5, 7 and 9 data points which gives the best tracking performance. The frame size determines how much recent data affect the trend estimation. The shorter size, the more sensitive trend change against the recent fluctuations in odor data. The longer size, the more robust trend change against the recent fluctuations in odor data.

While the key parameter in the trend estimation method using adaptive threshold is threshold coefficient. Similarly, the appropriate threshold coefficient is selected from options 0.6, 0.7 and 0.8 which gives the best tracking performance. Similarly to the frame size effect to the regression-based trend estimation, the threshold coefficient determines sensitivity of the estimated trend against the data fluctuations. The smaller coefficient, the more sensitive the trend change against the fluctuations, and vice versa.

4.3.3 Tracking case studies

Some tracking simulations were performed from initial position (4,2.1) with variation of concentration trend estimation method i.e.: smoothing-regression, regression, smoothing-adaptive threshold, adaptive threshold and without trend estimation. Frame size for smoothing, regression and *zigzag scanning* phase is 5 data points, while the adaptive threshold used coefficient 0.7. Trajectories of the tracking are shown in Figure 4.8.

It is inadequate to evaluate the overall performance of tracking strategy employing different estimation methods solely from these results since each method produces different performance characteristic depending upon the tracking initial position. However, we can compare the performance of tracking employing trend estimation and not employing it and observe the effect of using smoothing on regression and adaptive based trend estimation. Overall performance evaluation of the tracking strategy employing different trend estimation methods will be presented in Section 4.3.4;

Figure 4.8a shows trajectory of tracking employing data smoothing and regression-based (smoothing-regression) trend estimation. The tracking localized the source after some cycles of tracking phases (1. *upwind tracking*, 2. *zigzag scanning*, 3. *crosswind tracking* and 4. *return to the odor peak location*). Figure 4.8b shows trajectory of tracking employing regression trend estimation. Compared to the tracking employing smoothing-regression, it required more cycles of tracking phase before localized odor source.

Figure 4.9a shows trajectory of tracking employing data smoothing and adaptive threshold (smoothing-adaptive threshold) trend estimation. The tracking was able to localize odor source within the first cycle of tracking phase. Figure 4.9b shows trajectory of tracking employing adaptive threshold trend estimation. Compared to the tracking employing smoothing-adaptive threshold, it required more cycles of tracking phase before localized odor source. Tracking without trend estimation failed in following plume dynamics and failed in localizing the source as shown in Figure 4.8c.

From these tracking results, the tracking phase switching were caused by concentration peak detection or equivalently by decreasing concentration trend after an increasing trend previously.

Trend estimations without smoothing detected more peaks due to fluctuation. From comparison between the trend estimation combined with smoothing and without it, the smoothing improves quite significantly the tracking robustness against concentration fluctuation.

While plume tracking not employing trend estimation failed to localized odor source. Since the tracking mission was started when the odor had been approximately distributed over the entire room's floor, the tracking started with *upwind tracking* and kept moving upwind as it always found odor at every odor measurement. This tracking strategy could not sense decreasing concentration trend therefore it could not switch to *zigzag scanning* and so on. So basically, its tracking is based only on simple anemotaxis strategy. However some trackings starting from initial positions near the plume centerline were still able to localize the source.

Figure 4.10 shows the regression fitting to the concentration data obtained from tracking strategy employing smoothing-regression trend estimation starting from initial position (4,2.1) (Figure 4.8a). The regression fitting approximates the latest frame of concentration data iteratively.

4.3.4 Performance evaluation

Performance examination was performed by running the tracking simulation starting from 404 initial positions. The performance of a plume tracking can be measured by time performance i.e., the required time to localize the source. While overall performance of tracking strategy over different initial positions can be measured by average time performance and success rate i.e. the ratio of number of tracking cases that successfully find the odor source before the maximum time of 200 s to the number of all tracking cases i.e. successful and unsuccessful cases. Standard deviation of the time performance is also calculated to measure degree of performance deviation among the cases.

The time performance of tracking starting from an initial position can be represented as color cell at the coordinate of initial position as shown in Figure 4.11. In this context, failure represented as yellow color means that the odor source has not yet been localized when the maximum time (200 s) is over. The figure shows that the successful cases regardless of trend estimation method or without it mainly come from the initial positions which have high odor concentration or near the plume centerline (check the concentration distribution as shown in Figure 3.6a).

The examination result is evaluated in three levels:

- First level, evaluation to determine appropriate value of key parameter for each trend estimation method, i.e., frame size for estimation using regression and threshold coefficient for estimation using adaptive threshold.
- Second level, evaluation to compare within the same trend estimation method (regression or

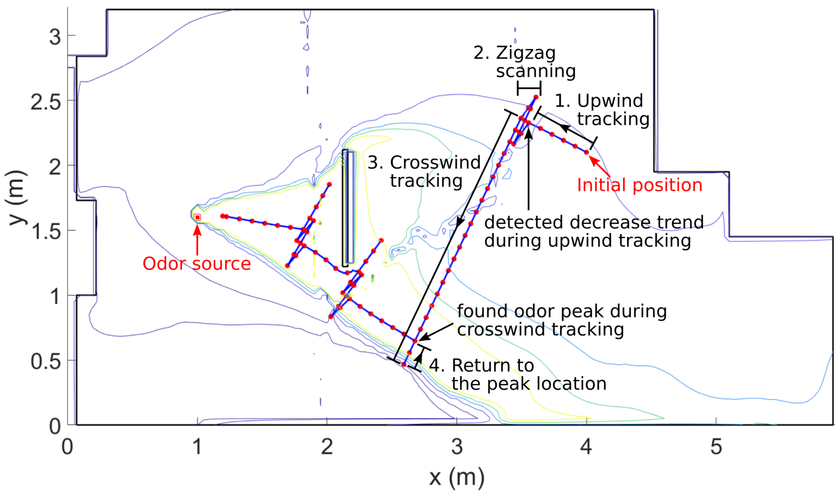

(a) Smoothing-regression with frame size 5 data points.

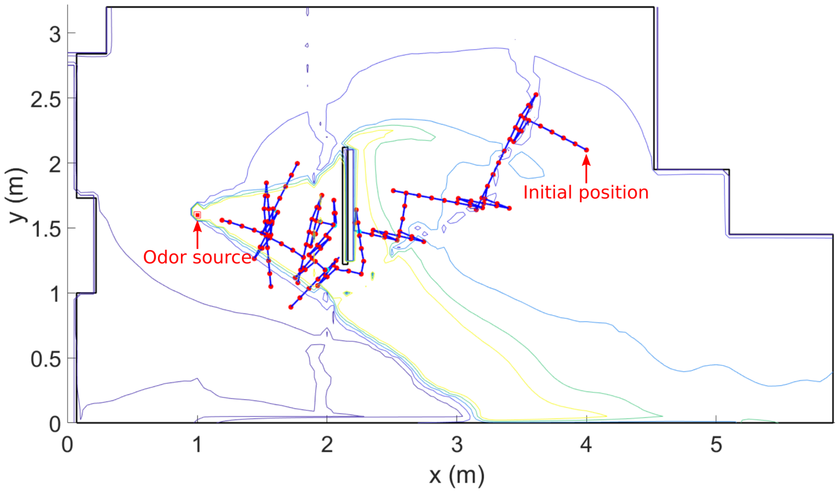

(b) Regression with frame size 5 data points.

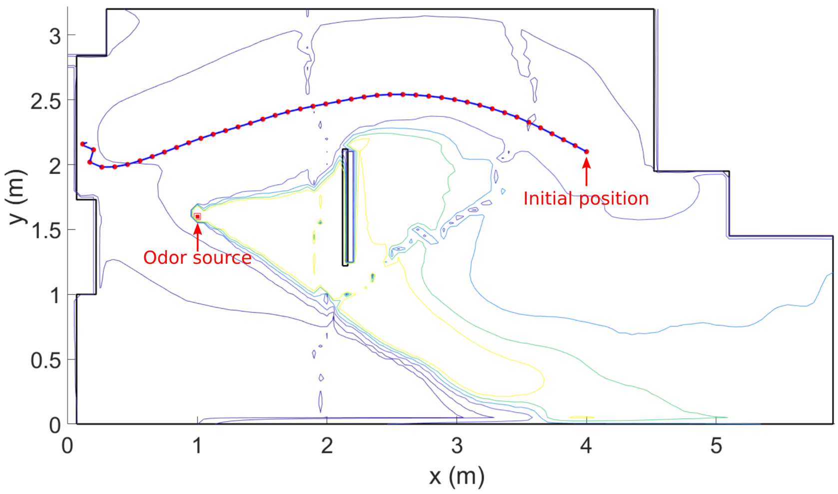

(c) Without trend estimation (frame size: 1 data point).

Figure 4.8: A plume tracking using regression-based trend estimation. The trajectory of plume tracking starting from initial position (4,2.1). The red dots are locations where the node reads odor concentration. Contour line indicates the location with the same concentration.

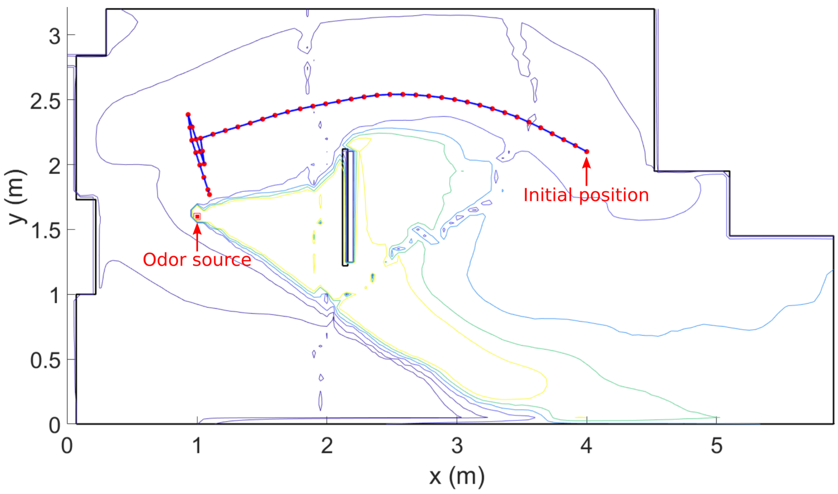

(a) Smoothing-adaptive threshold with frame size 5 data points and threshold coefficient 0.7.

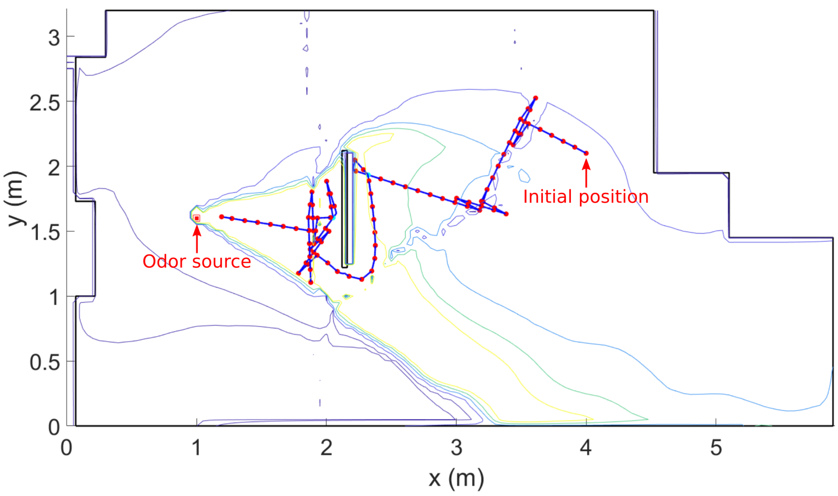

(b) Adaptive threshold with threshold coefficient 0.7.

Figure 4.9: A plume tracking using adaptive threshold-based trend estimation. The trajectory of plume tracking starting from initial position (4,2.1). The red dots are locations where the node reads odor concentration. Contour line indicates the location with the same concentration.

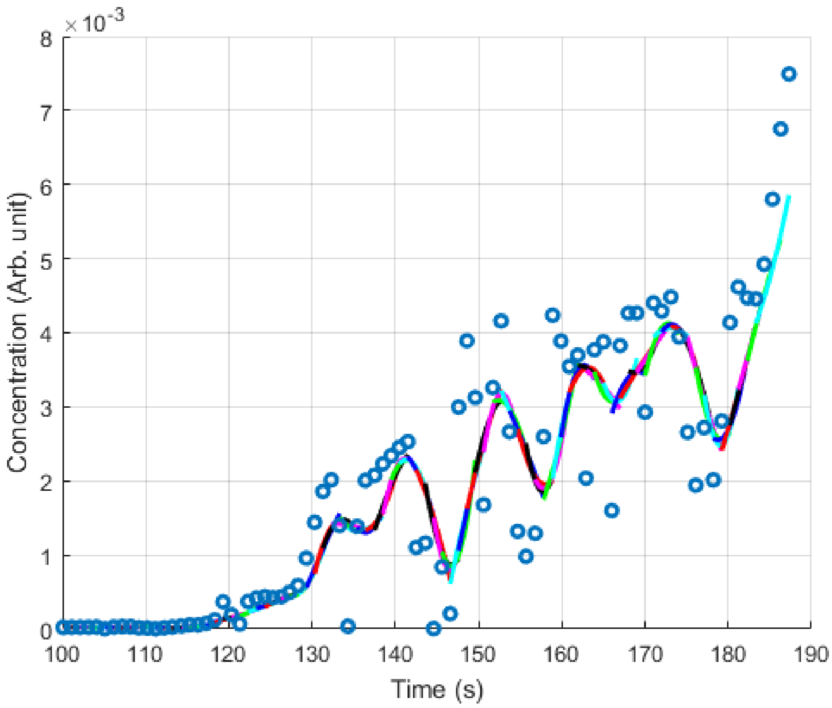

Figure 4.10: Odor concentration record during the tracking (blue circles) and piecewise concentration approximation by regression based on 5 data point (lines varying in colors: blue, red, black, magenta, green and cyan).

adaptive threshold) between the one in combination with smoothing and the one without smoothing.

- Third level, evaluation to compare between the tracking strategy employing trend estimation using smoothing-regression, regression, smoothing-adaptive threshold, adaptive threshold and the one not employing trend estimation.

Statistics of this evaluation result is presented in Table 4.1 and 4.2.

In Table 4.1, tracking strategy not employing trend estimation is obtained by using frame size 1. As shown in the table, the best performance of tracking strategy employing smoothing-regression trend estimation is obtained when using frame size 5 because it resulted in the highest success rate as well as the the minimum average time performance. While the best performance of the strategy employing regression trend estimation is obtained when using frame size 9. Smoothing-regression trend estimation gives better overall tracking performance over different initial positions than the regression trend estimation without smoothing. Thus, this result shows that smoothing improved performance of the estimation for appropriate frame size.

Table 4.1: Overall performance of tracking employing regression based trend estimation for search duration of 200 s.

Method	Frame size	Time performance (s)		Success rate (%)
		Mean	Std. deviation	
Smoothing-regression	3	88.37	49.99	95.04
	5	88.02	53.31	95.79
	7	92.12	71.70	77.47
	9	95.53	74.96	72.77
Regression	3	117.97	64.8	82.43
	5	118.85	64.43	81.68
	7	114.39	61.78	86.88
	9	109.7	61.66	90.59
Without trend estimation	1	129.28	85.19	41.09

Table 4.2: Overall performance of tracking employing adaptive threshold based trend estimation for search duration of 200 s.

Method	Threshold coeff.	Time performance (s)		Success rate (%)
		Mean	Std. deviation	
Smoothing-Adaptive Threshold	0.6	101.34	80.85	62.13
	0.7	97.99	80.25	64.1
	0.8	89.91	76.36	71.53
Adaptive Threshold	0.6	119.03	77.51	57.67
	0.7	128.42	75.67	54.7
	0.8	132.88	74.76	52.72

The performance of tracking strategy not employing trend estimation is significantly lower compared to the performance of the strategy employing estimation. It had high failure rate when the initial position was relatively far from the centerline. Meanwhile tracking starting from around the centerline had good performance because it kept sensing odor and moving upwind without performing *zigzag scanning*, *crosswind tracking* and *return to odor peak location* until it found the source. This resulted in short trajectory toward the source location.

As shown in Table 4.2, the best performance for tracking strategy employing smoothing-adaptive threshold trend estimation is obtained when using coefficient 0.8. While the best performance for the strategy employing only adaptive threshold trend estimation is obtained when using coefficient 0.6. Smoothing-adaptive threshold trend estimation gives better overall tracking performance over different initial positions than the adaptive threshold trend estimation without smoothing. This result also shows that smoothing improved the performance of the estimation significantly for appropriate threshold coefficient.

Among all tested trend estimation method, smoothing-regression trend estimation with frame size 5 data points resulted in the best overall tracking performance as it resulted in the highest success rate and the minimum average time performance.

4.4 Summary

This chapter presented a chemotaxis-anemotaxis based plume tracking strategy to localize the source in realistic turbulent environment using a single tracking node. The strategy was evaluated using ANSYS-MATLAB simulation framework. The framework enables repetitive cycle of development and testing of tracking strategy under unchanged realistic modeled environment.

The modeled environment was built as an asymmetric closed room with a screen inside it. Inside the room, convective process created slow circulating airflow in the room. The screen caused flow fluctuation around it. The airflow transported odor (ethanol) and created turbulent plume. At the start of the source searching mission, odor has been approximately distributed over the entire room's floor. This condition makes tracking based on simple anemotaxis strategy, i.e. moving upwind when detecting odor, does not work effectively as tracking can detect odor almost anywhere on the floor.

In this study, we proposed a combined smoothing-regression trend estimation method of odor concentration profile to improve chemotaxis-anemotaxis tracking strategy for turbulent environment. Performance of the tracking strategy employing this estimation method was compared with the same strategy employing established method of trend estimation using adaptive threshold as well as with the same strategy not employing trend estimation. The odor data smoothing effectiveness on the regression and adaptive threshold was also investigated.

The result shows that the tracking strategy employing concentration trend estimation method performs better than the one not employing it. The utilization of smoothing also improves the estimation method. Selection of key parameter, i.e. frame size for method using regression and smoothing as well as threshold coefficient for the one using adaptive threshold, also affects the performance.

Among the tracking strategy employing different estimation methods, the tracking strategy employing smoothing-regression trend estimation results in the overall best performance indicated by the minimum average time performance and the highest success rate. This result motivates further investigation of the proposed smoothing-regression odor concentration trend estimation method for more complicated turbulent environment.

Because our current environment model does not present heavy temporal and spatial fluctuations, both the environment model and the algorithm should be extended. Moreover, the estimation deteriorates in the upwind side of the source location and at area away from the plume centerline. Thus, this initial study motivates exploration using multiple tracking nodes in more complicated environment.

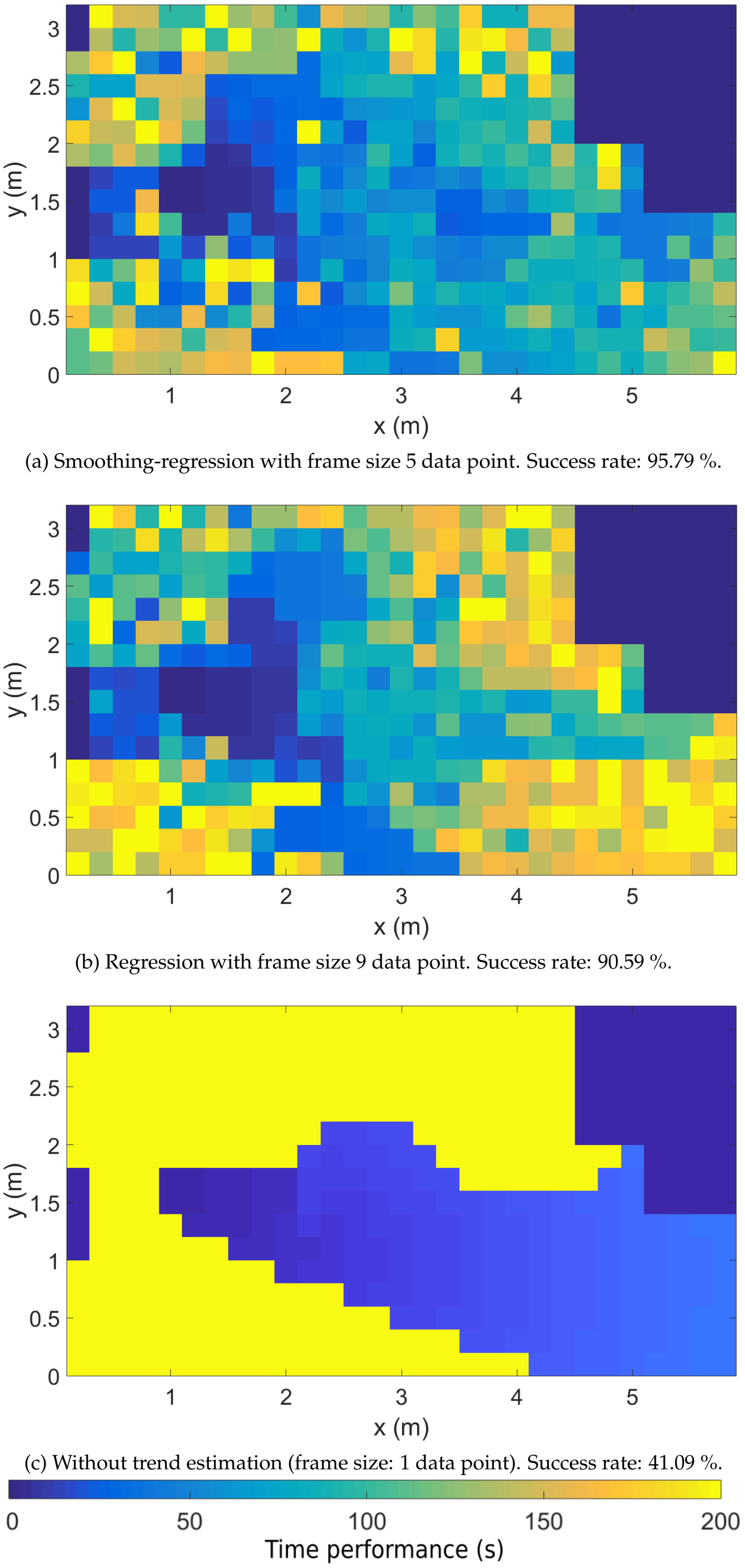

(a) Smoothing-regression with frame size 5 data point. Success rate: 95.79 %.

(b) Regression with frame size 9 data point. Success rate: 90.59 %.

(c) Without trend estimation (frame size: 1 data point). Success rate: 41.09 %.

Figure 4.11: The time performance of tracking strategy using regression-based trend estimation. The cell color represents the required time for tracking starting from the cell position to localize the source.

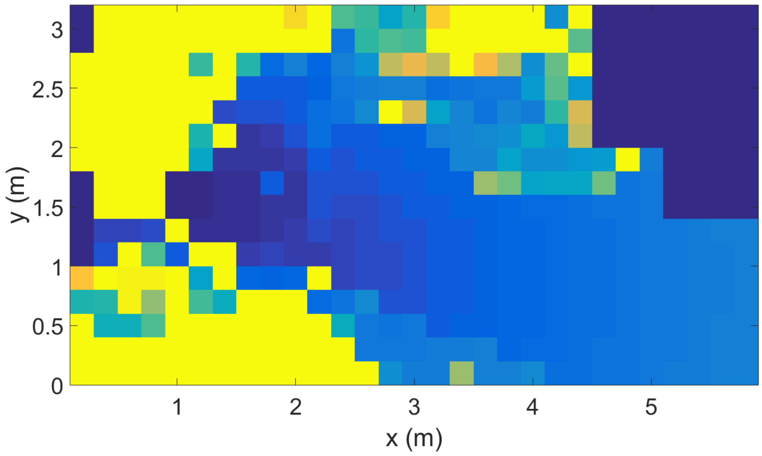

(a) Smoothing-adaptive threshold with threshold coefficient 0.8. Success rate: 71.53 %.

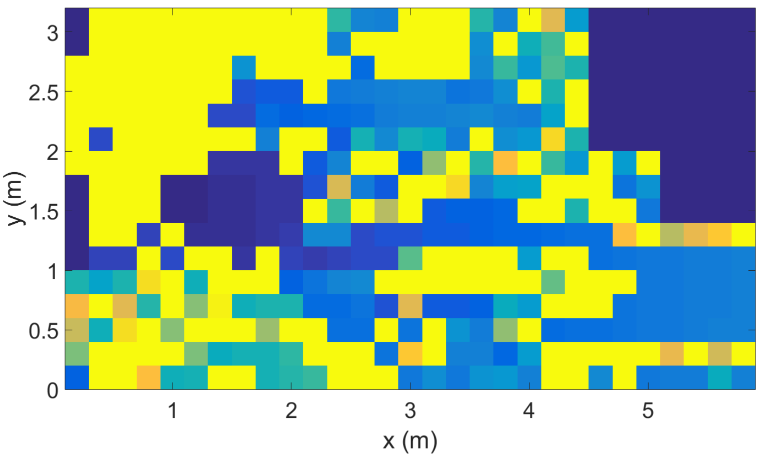

(b) Adaptive threshold with threshold coefficient 0.6. Success rate: 57.67 %.

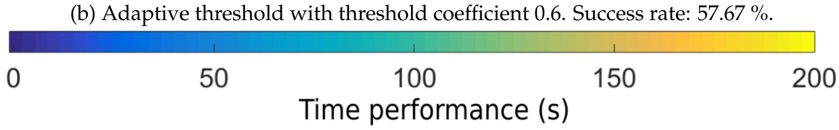

Figure 4.12: The time performance of tracking strategy using adaptive threshold-based trend estimation. The cell color represents the required time for tracking starting from the cell position to localize the source.

Chapter 5

Localization strategy for turbulent environment using an odor sensor with response delay

In this chapter, a new method of plume edge determination in a dynamic turbulent airflow is introduced based on the change in the transient sensor response over time. The strategy utilizes the transient sensor response, which corresponds to odor concentration, and flow direction to track the plume. The odor sensor has a response model derived from an actual semiconductor gas sensor. The novelty of this work is the plume edge detection method which uses gradient sign computed from sensor response function over time. This method detects the start edge of the plume by the negative gradient and the end of the plume by the positive one. There is no requirement of a threshold here, which potentially allows application of this method for plume detection in any environment with any baseline concentration level.

5.1 Sensor model

In this simulation, the sensor node (robot) is modeled a mass point and it can move in any direction on the floor. Thus, it is assumed that the airflow is not disturbed by the sensor node's movement.

The sensor node measures odor concentration and flow direction, and checks for the existence of obstacles every 1 s interval while moving. During this process, necessary data are collected:

- observed sensor response $\{r(x_i, y_i, t_i)\}_{i=1}^{k}$ and
- flow velocity $\left\{u_x(x_i, y_i, t_i), u_y(x_i, y_i, t_i)\right\}_{i=1}^{k}$,

where (x_i, y_i, t_i) is the ith location and time when the data are collected, and u_x andu_y are the airflow velocity in x and y direction respectively. To perform the sensing task, the node is assumed to be equipped with an odor sensor, an anemometric sensor, an ultrasonic sensor, a GPS system and a timer.

The odor sensor has a response model derived from an actual semiconductor gas sensor (TGS822, Figaro Engineering) for a remote sensing source localization system [57]. To simplify the model, the sensor response can be expressed just as a function of time. The steady-state model of sensor response calibration over ethanol concentration is

$$r_0(k) = [1 + 0.2309C_0(k)]^{-0.6705} \tag{5.1}$$

where $r_0(k)$ is the ideal sensor response (ratio of R_{gas} to R_{air}) and $C_0(k)$ is the ethanol concentration in ppm at time k. From this equation, the maximum value of r_0 is equal to unity for zero concentration C_0. For sensor subsequent measurement y at time k and $k+1$, there is a time delay for the sensor response to change from $r_0(k)$ to $r_0(k+1)$. If the delay is described by the first-order discrete-time system, the dynamic sensor response is obtained as

$$r(k+1) = 0.95r(k) + 0.05r_0(k) \tag{5.2}$$

where $r(k)$ and $r(k+1)$ are the observed sensor responses at time k and $k+1$, respectively. Using Equations 5.1 and 5.2, the characteristic of sensor response $r(k)$ with a unit step of odor concentration $C_0(k)$ as the input can be calculated and shown in Figure 5.1. The time constant of Equation 5.2 is 19.5 s.

The sensing method by Eu and Yap [49] requires some input parameters including the transient response and the threshold values for determining a certainty factor of odor detection. This method has complication in selecting the appropriate certainty factors and the threshold values which should be different for different environmental conditions. This could discourage the practical application. The auto-regressive model used in the sensing method by Shigaki et al. [46] is capable of modeling a wide range of non-linear systems. However, the model function could contain excessive number of terms and another method is required to determine the significant terms of this model. In order to comply real-time requirement, the challenge for using this method is to get concise model of the sensor response.

In this study, the response dynamics is modeled based on sensor response characteristic to target chemical and is independent of environmental conditions. Therefore, the model is computed only once for a particular sensor and is applicable for different kinds of environment. This simplicity allows the application of method for any environment with different baseline concentration

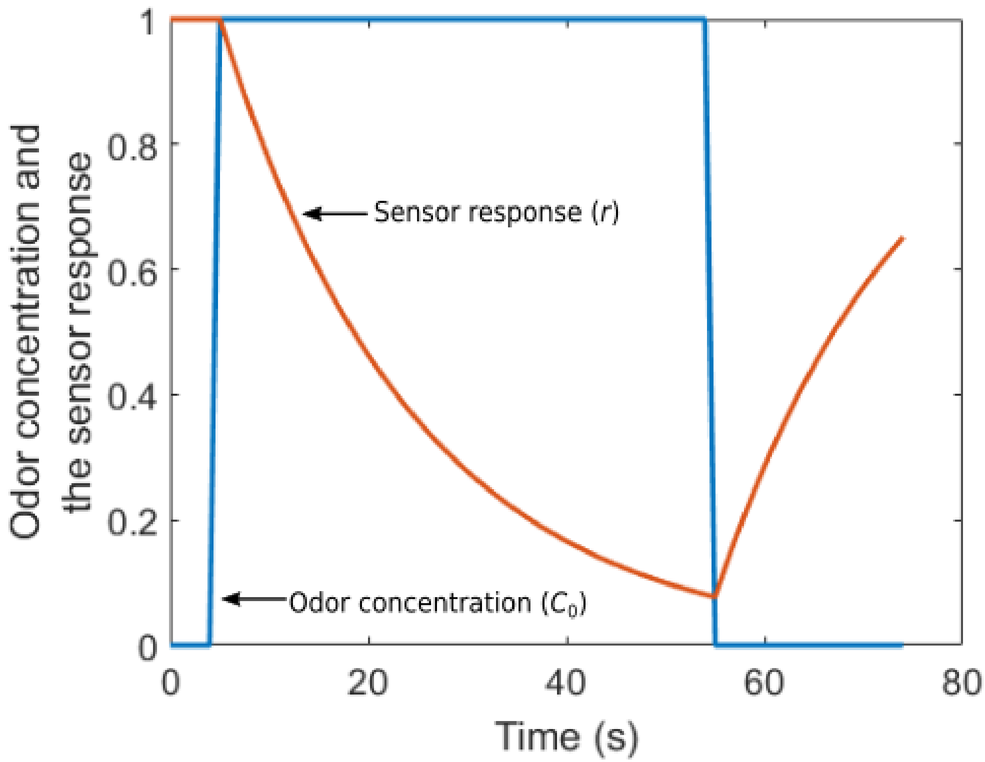

Figure 5.1: Sensor response to a unit step odor concentration signal.

levels and increases the robustness against fluctuations.

An ultrasonic sensor is used to detect an obstacle so that the node can avoid it. It detects the obstacle within a 5 cm proximity in the direction 180° ahead. In general, the obstacle is avoided by turning the tracking direction 90° away from the direction to the obstacle.

5.2 Plume tracking strategy

The main focus of our localization strategy is source searching by tracking the plume. The tracking strategy here is the further development of the strategy we have reported in Chapter 5. In previous strategy, the sensor was assumed to be ideal. It is capable of sensing any value of odor concentration and follow the concentration change immediately. On the other hand, here, a realistic sensor model with sensor response delay is used. When the sensor model with response delay is applied in previous strategy, the zigzag scanning with short zigzag amplitude can not produce reliable direction toward the plume centerline owing to the response delay. Therefore, a new method is required to estimate the plume centerline. This new method is explained in Section 5.2.1 The new centerline estimation method requires new strategy to improve tracking efficiency. This new strategy is explained in Section 5.2.2. The sensor node speed affects the accura of the sensor response. Therefore, two levels of speed is applied in this strategy as explained in Section 5.2.3.

5.2.1 Determination of plume edge and centerline

A real-time method of detecting and tracking a dynamic plume is desirable. However, that is not possible owing to the sensor response delay. The plume is reliably indicated by the ideal sensor response r_0, but it is not accessible during plume tracking. However, the r_0 model can be derived through a calibration experiment [57]. An investigation was performed in MATLAB to understand the correlation between the ideal response $r_0(k)$ and the observed response $r(k)$ by measuring the odor while moving the sensor node through a plume at low speed. In this investigation, the real odor concentration is assumed to be available through the measurement and is used to calculate r_0. An example of the measurement track and the obtained responses are shown in Figure 5.2a and 5.2b respectively. In Figure 5.2b, r_0 and r are shown as the red and blue lines, respectively.

In this strategy, the similar regression-based curve fitting as used in the trend estimation in previous strategy (Chapter 4) is applied to the latest n data points of observed response $\{r(t_i)\}_{i=k-n+1}^{k}$ every time a new response value is obtained to derive a transient sensor response function over time. Since the sensor response dynamics is much less than the corresponding concentration dynamics, a slight change in the sensor response corresponds to a significant change in the concentration. In order to be sufficiently sensitive to this slight change of response, the curve fitting employs third-order polynomial regression. The fitting response function over time for time interval $[t_{k-n+1}, t_k]$ is

$$\left\{\hat{r}(t) = w_3t^3 + w_2t^2 + w_1t + w_0\right\}_{t=t_{k-n+1}}^{t_k} \tag{5.3}$$

where $\hat{r}(t)$ is the expected observed response at time t and w_3, w_2, w_1 and w_0 are coefficients for minimizing the residual. The first derivative of $\hat{r}(t)$ is the gradient function of the observed response for time interval $[t_{k-n+1}, t_k]$, i.e.

$$\left\{r'(t) = d\hat{r}(t)/dt\right\}_{t=t_{k-n+1}}^{t_k} \tag{5.4}$$

This gradient describes the rate of response change over time. The successive plot of $r'(t)$ for $[t_{k-n+1}, t_k]$ is shown as a black curve in Figure 5.2b. This curve shows that a positive r' correlates with an increase in r_0 and a negative r' correlates with a decrease in r_0. From Equation 5.1, we know that high r_0 corresponds to low concentration and low r_0 corresponds to high concentration. As the gradient function is derived every time a new value is obtained at t_k, each data point obtained at time $t_i \geq t_n$ is included in the gradient calculation n times in sequence, resulting in n gradient values corresponding to each value. This repetitive calculation is handled by summing the overlapping gradient values for each data point. The sign of the summed gradient is shown

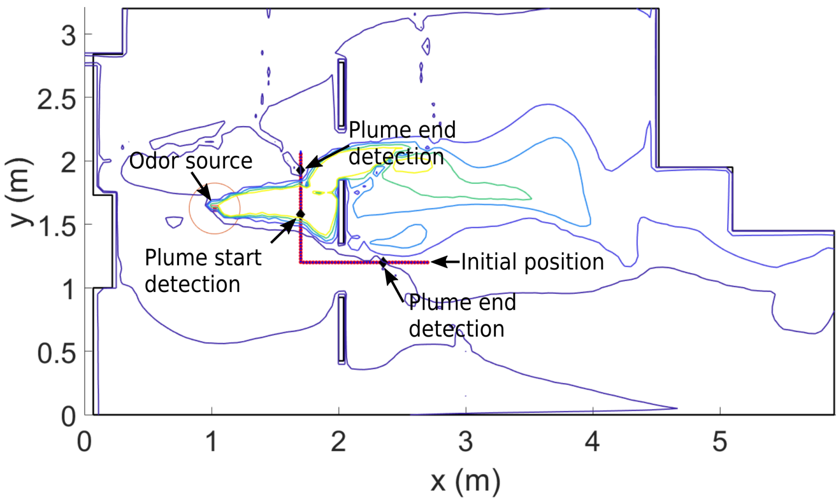

(a)

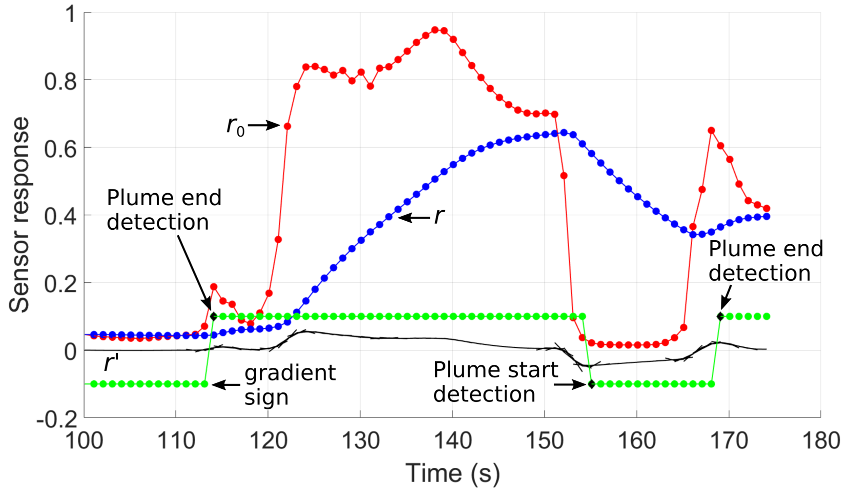

(b)

Figure 5.2: Odor measurement along an L shape track crossing a plume. (a) Measurement track. The contour lines indicate locations with the same concentration. (b) Sensor response during the measurement. The blue and red lines are the observed response (r) and ideal response (r_0), respectively. The black line is the successive plot of gradient function $r'(t)$ for $[t_{k-n+1}, t_k]$. The green line is the sign of the summed gradient multiplied by 0.1 for observation purposes. The black markers in it indicate the detected start and end of the plume.

as the green line in Figure 5.2b. The plume start and end are determined at the start and end of a gradient change to negative and positive, respectively, as marked by black markers in the green line.

The determination of the plume edge is the crucial problem in this strategy for it influences all switching conditions of the phases. Since the gradient is calculated using n data points, at the beginning of tracking, the first calculation is started when the obtained data is equal to n data points. This causes a delay in judging the plume edge by $(n–1)$ data points. Apart from the sensor response delay, another issue in determining the edges is that turbulent airflow can create a pocket of highly concentrated odor separated from the main plume. Odor measurement through this pocket can present a gradient sign change that leads to incorrect determination of the plume edge. This issue can be solved by redundant checking of the gradient sign before declaring the plume edge. The declaration of edge detection is made when the gradient sign is consistent every time new sensor data is obtained for several detections. This method adds more delay in edge detection but can improve its accuracy.

The plume centerline is searched during *crosswind scanning*. We investigate two methods of estimating the centerline. The first is a search for the minimum sensor response that corresponds to the maximum odor concentration within the plume. The second is to calculate the central point between the start and end of the plume.

In this simulation, it is assumed that a GPS system provides an absolute position. The position information is used to pinpoint the estimated centerline location in the end of crosswind scanning. Although the exact requirement for accuracy was not investigated, the acceptable error for the centerline coordinate in crosswind direction should be smaller than half of crosswind width of the plume so that the estimated location is still inside the plume.

5.2.2 Tracking phase

A new simpler strategy than the previous one was developed for localization using an odor sensor with response delay. As described in Figure 5.3, the strategy has 3 phases:

Upwind tracking. A tracking is started in this phase. In this phase, the node moves in the upwind direction. It continues until it is declared that the node is out of the plume and then switches to *crosswind scanning*.

Crosswind scanning. Upon beginning of *crosswind scanning*, the tracking node turns to the direction 90° clockwise or counter clockwise from the upwind direction and then moves straight to search for the plume. The direction of the first turn, either clockwise or counter clockwise, is predetermined because there is no prior information of plume location. However,

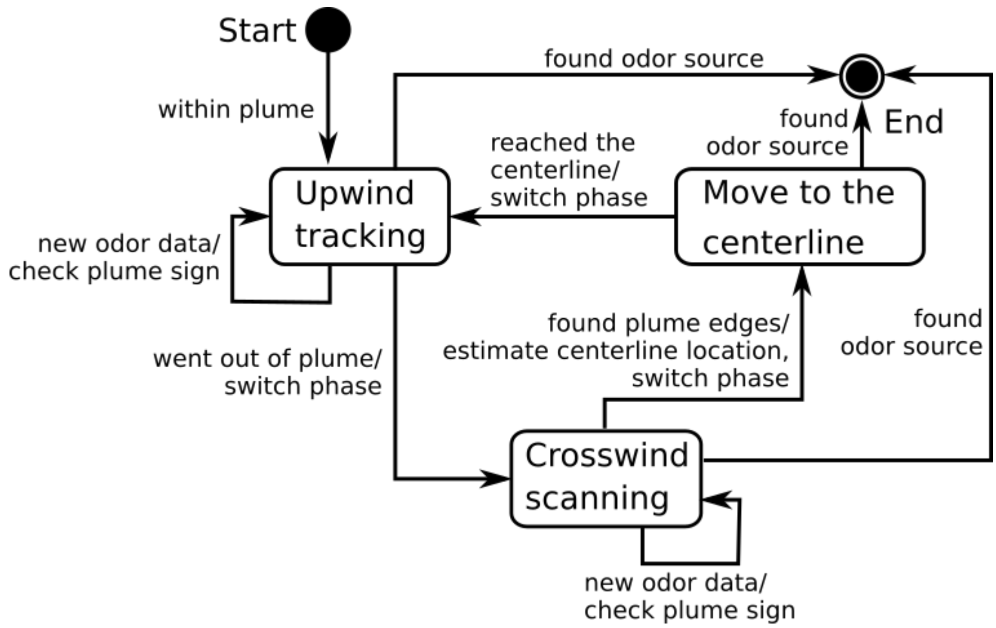

Figure 5.3: Phases of plume tracking strategy.

the second turn onward is determined from the previously obtained plume location. In this phase, the search strategy is similar to the zigzag flying motion of a moth searching for a plume, i.e., the node moves in a crosswind direction for a certain distance to look for a plume edge. When the edge is not found within that distance, it moves in the opposite direction and searches for triple the previous distance and so on. This expanding zigzag search ends when a plume is found. Upon finding the plume, the plume centerline is determined from the minimum response found or the central point between the start and ending edges and then the phase switches to 'move to the centerline'.

Move to the centerline. In this phase, the node simply moves to the estimated centerline. Information on odor concentration and flow velocity is ignored during this phase. When the node has reached the estimated centerline, the phase switches to *upwind tracking*.

Determination of the plume edges and centerline is explained in Section 5.2.1.

5.2.3 Tracking speed

As the sensor has a response delay, the faster the node moves, the less accurate the sensor response data it obtains. To compromise between the demand of fast tracking and appropriately accurate sensor response, we devised the sensor node (robot) with two speeds: high speed and low speed. The high speed is used during 'upwind tracking' and 'move to the centerline', whereas low speed is used during 'crosswind scanning' as a more accurate response is considered necessary in this phase to estimate the centerline.

For selecting reasonable speeds, we took reference from a real experiment [37] using a search robot with the same type of gas sensor as we used here. In that experiment, the robot moves at speed 10-20 cm/s to localize an odor source in indoor space without obstacle. In this study, more complication is provided by turbulence created by the obstacles and the sensor response delay. Therefore, we selected the high speed to be 5 cm/s and the low speed to be 2.5 cm/s. The speed values are indeed subject to optimization. However, the investigation for optimum speeds will be left as a future work.

The obstacle avoidance is prioritized over odor search. When detecting an obstacle, the robot stops searching/tracking for odor and turns 90° and then moves, even if the odor information leads the robot toward the obstacle. This design is reasonable especially when it is known that the sensor response contains delay.

5.3 Plume tracking simulation

5.3.1 Methodology

The tracking strategy was tested on the three-obstacles-environment (described in Section 3.1) from time step 700 s to a maximum time (described in Figure 3.4). Here the maximum time is 500 s. Therefore, the tracking node is assumed to find the odor source successfully if it arrives nearby the source location before time limit at 500 s. The nearness criteria is 20 cm from the source location.

The frame size for the curve fitting of sensor responses is 5 data points. The redundant check of the gradient sign change is performed 5 times. In order to increase the robustness of upwind tracking against eddies and turbulent flow, the upwind direction during 'upwind tracking' is determined by averaging the flow direction of the last 5 data points.

In this simulation, the performances of tracking were compared between the two methods of centerline determination. The overall performance is evaluated by running the tracking simulation starting from 404 initial positions. The performance parameters are the average time required to localize the source, the standard deviation, and success rate, i.e., the ratio of the number of tracking cases in which the odor source was successfully found before the time limit to the total number of tracking cases.

5.3.2 Tracking case studies

A case of plume tracking with centerline estimation by the central point starting from the initial position (2.2,1.2) is shown in Figure 5.4a and the sensor responses is shown in Figure 5.4b. In Figure 5.4a, the directions and sequence of the tracking phases are indicated by black arrows with numbers. The tracking starts with *upwind tracking* (1), then *crosswind scanning* (2), then *move to the centerline* (3), and finally *upwind tracking* (4) until the node arrives within 20 cm of the source location (indicated by red circle around the source location). Another case of plume tracking starting from position (4, 2.1) and the obtained sensor response are shown in Figures 5.5a and 5.5b, respectively.

In Figure 5.4b, The red line is the ideal sensor response (r_0), the blue line is the observed sensor response (r), the black line is the framewise gradient of sensor response (r'), and the green line is the gradient sign multiplied by 0.1 to aid in easy observation. From the green line, the state of the node when the corresponding sensor response is obtained either inside or outside a plume can be observed. The node is assumed to be inside the plume when the line is negative and outside when it is positive. The marker shape on the green line indicates the phase state, i.e., ● for *upwind tracking*, ■ for *crosswind scanning*, and * for *move to the centerline*. As shown in the green line, the tracking phase is not switched at the first plume edge detection, rather after 9 data points owing to the 4-data-points-delay in judging the edge ($n - 1$) and the 5-data-points delay for the redundant check.

5.3.3 Performance evaluation

The overall tracking performances are evaluated and compared for the two centerline determination methods, i.e., phase based on (a) minimum response and (b) central point between the start and ending edges, as shown in Figure 5.6. In the figures, the time performance of tracking starting from an initial position is represented by colored cells at the coordinates of the initial position. In this context, failure, that is, the odor source has not yet been localized by the maximum allowed time, is represented by yellow. The figure shows that the successful cases, regardless of the centerline determination method, have initial positions with high odor concentration or near the plume centerline. However, the determination method using the central point showed better performance for initial positions far from the source at the downwind side. The time performance with initial positions far from the centerline is generally long, typically owing to failure in finding the plume. This failure might correlate with the design selection of the strategy in which tracking starts with *upwind tracking*. The performance when initial positions are at the upwind side of the source is also generally long as this tracking strategy is basically designed only to move crosswind to search for the plume centerline and move upwind along the centerline and does not have a suitable method of searching for the plume in the downwind direction.

The performance statistics of the strategy with and without time delay consideration are shown in Table 5.1. The tracking strategies with response delay consideration perform better as they show significantly higher success rates and lower average times to localize the source than does strategy

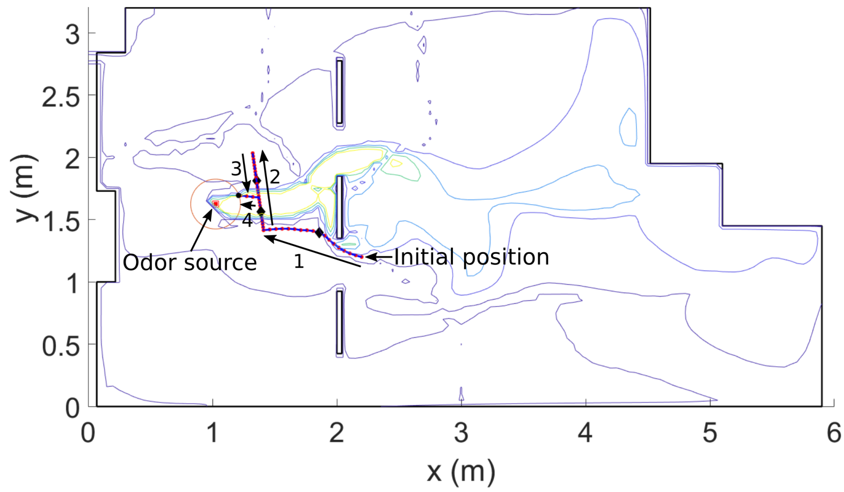

(a)

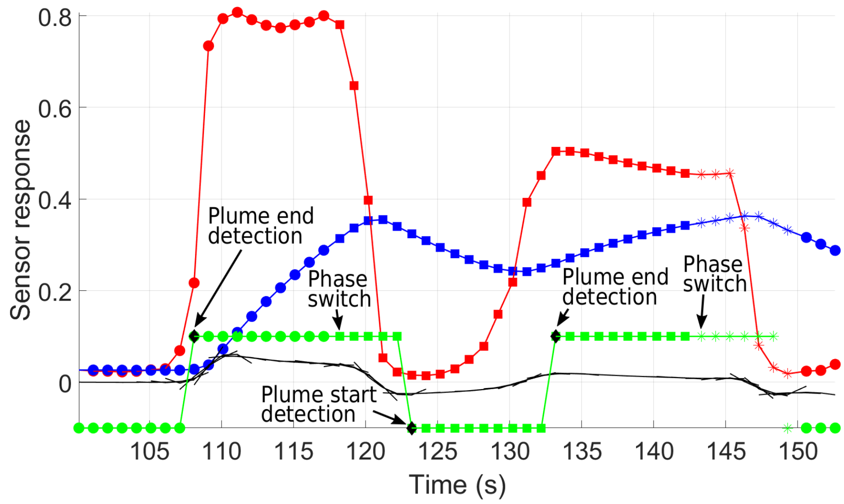

(b)

Figure 5.4: (a) Plume tracking starting from initial position (2.2, 1.2). The contour lines indicate locations with the same concentration. (b) Sensor response recorded during tracking.

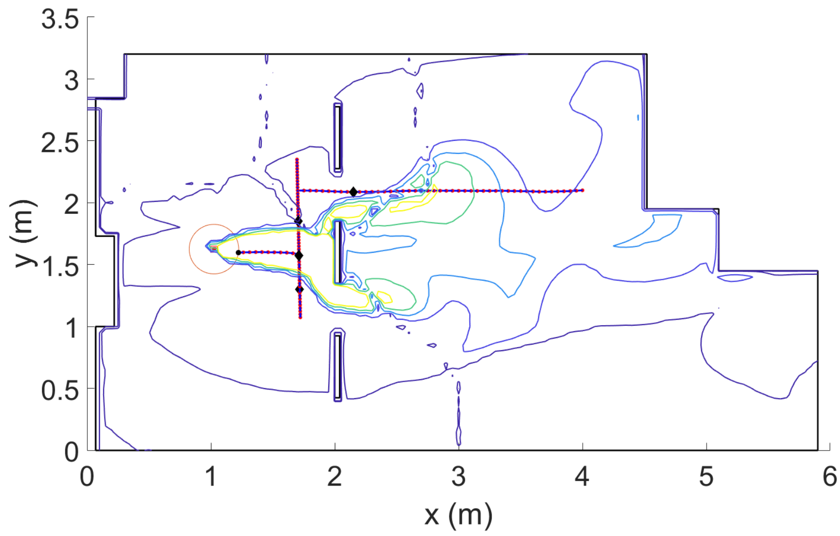

(a)

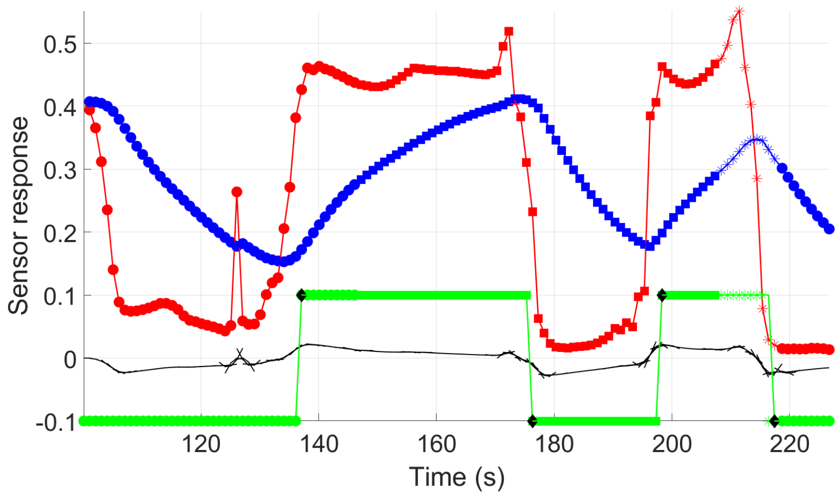

(b)

Figure 5.5: (a) Plume tracking starting from initial position (4, 2.1). The contour lines indicate locations with the same concentration. (b) Sensor response recorded during tracking.

Table 5.1: Performance of tracking with different centerline determination methods. The search was carried out from 404 initial positions and the time limit for each duration is 500 s.

Tracking strategy	Centerline determination by	Time performance (s)		Success rate (%)
		Mean	Std. deviation	
With response delay consideration	Minimum response between two plume edges	287.85	174.00	69.55
	Central point between two plume edges	269.02	169.36	71.53
Without response delay consideration	Minimum response	331.80	161.25	63.61

without delay consideration [44]. Among the strategies considering response delay with different centerline estimation methods, the statistical differences (time performance mean, the standard deviation , and success rate) are quite small. However, by comparing the performance distribution of the tracking strategy with centerline estimation method, as shown in Figures 5.6a and 5.6b, we can conclude that tracking strategy with centerline estimation by the central point has better performance for initial position aways from the source in downwind direction.

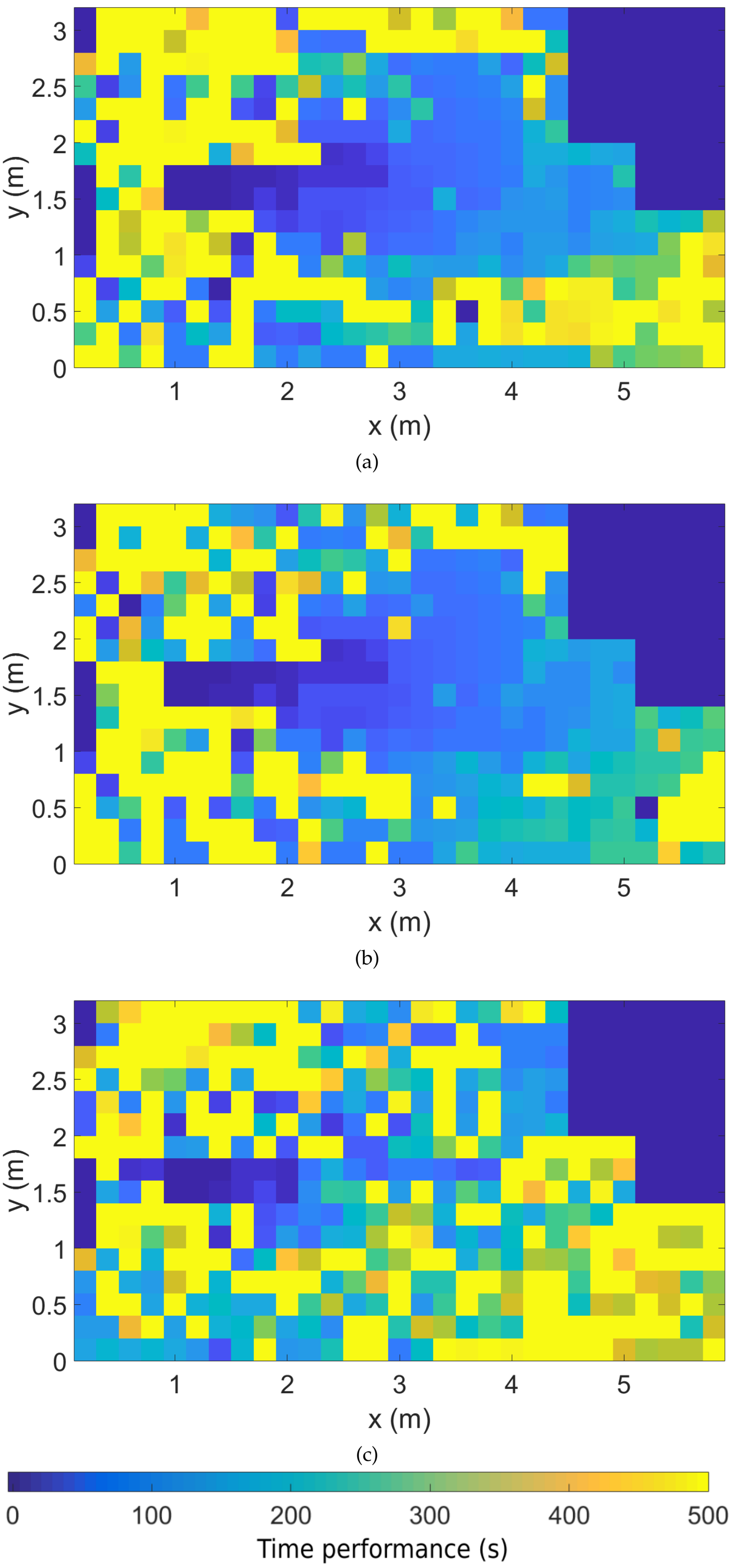

Figure 5.6: Time performance distribution over initial positions. The tracking strategy with response delay consideration. The centerline is estimated during *crosswind scanning* based on: (a) minimum response and (b) central point between start and ending edges. (c) The tracking strategy without response delay consideration. The centerline is estimated during *crosswind tracking* based on minimum response.

5.4 Summary

The strategy plume for tracking in a turbulent environment using an odor sensor with a time constant was developed and evaluated under a CFD simulation framework. The sensor response delay makes the observed response value unreliable in representing odor concentration dynamics. Therefore, the transient characteristic of sensor response data was investigated to identify a plume. The transient characteristic was observed by calculating the gradient of the data. From this observation, it was found that the gradient sign of a curve-fitted time series response is sufficiently reliable to detect a plume edges. The problem of inaccurate plume identification owing to plume dynamics was addressed by incorporating redundant check of the gradient sign. This plume edges detection was used for switching conditions of the tracking phases during *upwind tracking* and *crosswind scanning*, and for the centerline estimation. Evaluation of centerline estimation using different method, by the central point and by the minimum response, results in quite small performance difference. Using either of these centerline estimation method, the tracking strategy considering the response delay in turbulent environment results in a promising success rate at around 70%. The success rate is quite high considering the complexity of the environment and that many initial positions of the evaluation are near walls and at the upwind side of the source which are significant disadvantages for source localization.

The failures were frequent when tracking began at initial positions far from the centerline and at the upwind side of the source. Therefore, further improvement should be made by including a strategy for tracking from these areas. The performance of a plume tracking strategy without response delay consideration was also presented here for comparison. The statistical difference between the performance of the strategy with response delay consideration and without it may not wide but it is significant and helpful since any actual chemical sensor has response delay. Considering that the statistical result is obtained from sufficient number of tests covering the entire search area, the proposed delay consideration strategy is likely to consistently provide clear advantage for different environmental conditions. The difference is expected to be enhanced the faster the sensor node moves. Although actual sensors are not used in our work, the strategy described here is applicable to a sensing system to search for an odor source.

Chapter 6

Conclusions and future work

6.1 Conclusions

This PhD research topic was motivated by a demand on a robotic odor source localization system. This localization system gains increasing interest in our modern life for various application such as to cope with an increasing threat owing to dangerous chemicals or to help in a rescue operation in disaster situations. To date, the developments and testings of odor source localization strategies in real experiment are limited to simplified environments. Building a real testing environment is typically expensive and cumbersome. Whereas, a localization strategies needs a realistic testing environments being targeted by the strategies, such as a collapsed building, a factory with a chemical leakage, and any other harmful environments. A CFD framework gives a solution to this problem by enabling convenient and fast development of realistic virtual environment at low cost, that is, at the cost of computational resources and memory, and probably the software license as well.

This thesis was focused on development and evaluation of chemotaxis-anemotaxis-based odor source localization strategies under CFD framework. There have been numerous studies used chemotaxis-anemotaxis for odor source localization. These strategies which is reported to work well in turbulent environment. However this general strategy typically needs specific methods to tackle issues regarding with environmental conditions and hardware specification. In this study, the issues are:

- First, an environment with a dynamic turbulent airflow. This airflow transports the odor resulting in dynamically complex plume shape.
- Second, increasing concentration level owing to accumulating odor, thus using a fixed threshold value for detecting plume is not effective.

- Third, sensor response delay which disturbs plume detection.

To tackle the issues, this thesis work was carried out gradually in three development phases. The first phase was to develop a strategy for a static environment assuming a Gaussian odor distribution. By assuming a simple environment, the development could be focused in devising a strategy employing multiple search robots (sensor nodes). Optimal arrangement of sensor nodes was investigated which was then incorporated into the multiple-sensor-nodes strategy adopting an approach of zigzag search of odor plume and upwind surge. The strategy assigned two cooperative roles for each node: a leading node whose priority to search for the source by moving upwind along the plume and supporting nodes which follow behind the leading node while moving zigzag to collect odor information. However, the effectiveness of this strategy has not been tested in a realistic environment.

The second phase was to develop a strategy for a dynamic turbulent environment simulated under CFD framework. The simulated environment was a closed room that contain a natural convective airflow and an obstacle which disturb the airflow. The strategy comprises 4 phases: *upwind tracking*, *zigzag scanning*, *crosswind tracking*, and *return to the peak location*. The strategy uses a single sensor node equipped with an ideal odor sensor. An odor gradient estimation method based on second-order polynomial regression was employed to search for the plume centerline by a concentration peak. Although gradient following method is not new in the field of odor source localization, to the best of author's knowledge, this regression-based gradient calculation using a frame of time-series data points is the first application in this field. This method liberates from the necessity for a threshold value which is commonly used in determining a plume. For comparative evaluation, an gradient estimation using adaptive threshold was developed. The evaluation resulted two main conclusions: First, this strategy is effective for a turbulent environment even when the plume is irregular. Second, the gradient estimation based on regression outperforms that based on adaptive threshold.

The third phase was to extend the second strategy to address more realistic environment and an odor source with a response delay. The sensor response has a time constant around 20 s. The complexity of the testing environment was increased by adding the number of obstacles and reducing the odor emission rate. The strategy was simplified from the previous one comprising 3 phases: *upwind tracking*, *crosswind scanning*, and *move to the centerline*. In this strategy, the plume centerline was determined by determining the plume edges along crosswind direction. Having found the edges, the centerline can be determined at the central position between the edges or at the position of the highest concentration between them. Performance evaluation showed that the centerline determination by the central position between the plume edges is more accurate than by the position of the highest concentration between them.

The strategy resulted from the last phase of development has taken into account common issues of real application in the real-world environment. It is capable of tracking a dynamic plume in an indoor environment with obstacles using an odor sensor with response delay. The strategy however does not include a plume searching toward downwind direction. Some limitations are also imposed by the environmental setting, sensor model and simplifying assumptions such as the tracking robot as a mass point body.

6.2 Future work

We have developed the localization strategy to tackle all those issues mentioned in Section 6.1 and demonstrate the applicability in a computer simulation. It is possible that the plume tracking pass the source location in upwind direction and arrive at the upwind side area of the source, or it is started from an initial position at the upwind side of the source. Therefore, the strategy should include a strategy to search for the plume in downwind direction. Some limitations of this strategy may appear for different environmental conditions, sensor model, and assumptions. Therefore, the strategy needs to be evaluated under variations of environmental conditions, sensor model, and assumptions.

The CFD parameters selection, such as meshing method, physical parameters, flow model, etc., should be validated with the real experiment to get sufficiently accurate model parameterization. The developed strategy using multi sensor nodes needs to be tested in a dynamic environment under CFD framework. This odor source localization simulation also employs some assumptions related with odor and ultrasonic sensors, and GPS system, therefore the strategy resulted from it needs to be evaluated in the real experiment. The validation experiment will be useful to make better assumptions and considerations for the next simulations.

This PhD thesis investigated only bio-inspired odor source localization strategies. Another strategies should also be investigated under the CFD framework. Different strategies may work best for different environmental conditions. Therefore, the comprehensive investigations of various strategies can helps in determining the best strategy for a targeted environment.

Bibliography

[1] X. Liu, S. Cheng, H. Liu, S. Hu, D. Zhang, H. Ning, A survey on gas sensing technology, Sensors 12 (7) (2012) 9635–9665. doi:10.3390/s120709635.

[2] T. Nakamoto, H. Ishida, H. Matsukura, Multiple Sensorial Media Advances and Applications: New Development in MulSeMedia, IGI Global, 2012, Ch. Olfactory Display Using Solenoid Valves and Fluid Dynamics Simulation, pp. 140–163.

[3] G. Kowadlo, R. A. Russell, Robot odor localization: a taxonomy and survey, The International Journal of Robotics Research 27 (8) (2008) 869–894. doi:10.1177/0278364908095118.

[4] J. Basil, J. Atema, Lobster orientation in turbulent odor plumes: Simultaneous measurement of tracking behavior and temporal odor patterns, The Biological Bulletin 187 (2) (1994) 272–273. doi:10.1086/bblv187n2p272.

[5] N. J. Vickers, Mechanisms of animal navigation in odor plumes, The Biological Bulletin 198 (2) (2000) 203–212. doi:10.2307/1542524.

[6] T. D. Wyatt, Moth flights of fancy, Nature 369 (6476) (1994) 98–99. doi:10.1038/369098a0.

[7] A. D. Hasler, A. T. Scholz, Olfactory imprinting and homing in salmon, The Quarterly Review of Biology 59 (4) (1984) 508.

[8] K. Mjos, F. Grasso, J. Atema, Antennule use by the american lobster, *Homarus americanus*, during chemo-orientation in three turbulent odor plumes, Biological Bulletin 197 (1999) 249–250.

[9] J. Atema, Eddy chemotaxis and odor landscapes: exploration of nature with animal sensors, The Biological Bulletin 191 (1) (1996) 129–138. doi:10.2307/1543074.

[10] A. Lilienthal, A. Loutfi, T. Duckett, Airborne chemical sensing withmobile robots, Sensors 6 (11) (2006) 1616–1678. doi:10.3390/s6111616.

[11] H. Ishida, Y. Wada, H. Matsukura, Chemical sensing in robotic applications: a review, IEEE Sensors Journal 12 (11) (2012) 3163–3173. doi:10.1109/jsen.2012.2208740.

[12] H. Ishida, K. Suetsugu, T. Nakamoto, T. Moriizumi, Study of autonomous mobile sensing system for localization of odor source using gas sensors and anemometric sensors, Sensors and Actuators A 45 (1994) 153–157. doi:10.1016/0924-4247(94)00829-9.

[13] H. Ishida, Y. Kagawa, T. Nakamoto, T. Moriizumi, Odor-source localization in clean room by autonomous mobile sensing system, in: Proceedings of the International Solid-State Sensors and Actuators Conference - TRANSDUCERS '95, IEEE, 1995, pp. 783–786. doi:10.1109/sensor.1995.717349.

[14] H. Ishida, Y. Kagawa, T. Nakamoto, T. Moriizumi, Odor-source localization in the clean room by an autonomous mobile sensing system, Sensors and Actuators B: Chemical 33 (1-3) (1996) 115–121. doi:10.1016/0925-4005(96)01907-7.

[15] R. A. Russell, Laying and sensing odor markings as a strategy for assisting mobile robot navigation tasks, IEEE Robotics & Automation Magazine 2 (3) (1995) 3–9. doi:10.1109/100.414920.

[16] C. Lytridis, G. S. Virk, Y. Rebour, E. E. Kadar, Odor-based navigational strategies for mobile agents, Adaptive Behavior 9 (3-4) (2001) 171–187. doi:10.1177/10597123010093004.

[17] A. T. Hayes, A. Martinoli, R. M. Goodman, Distributed odor source localization, IEEE Sensors Journal 2 (3) (2002) 260–271. doi:10.1109/jsen.2002.800682.

[18] D. Zarzhitsky, D. F. Spears, W. M. Spears, D. R. Thayer, A fluid dynamic approach to multi-robot chemical plume tracing, in: Proc. The 3rd International Joint Conference on Autonomous Agents and Multiagent Systems (AAMAS), 2004.

[19] S. Pang, J. A. Farrell, Chemical plume source localization, IEEE Transactions on Systems, Man and Cybernetics, Part B (Cybernetics) 36 (5) (2006) 1068–1080. doi:10.1109/tsmcb.2006.874689.

[20] J. Farrell, S. Pang, W. Li, R. Arrieta, Chemical plume tracing experimental results with a REMUS AUV, in: Oceans 2003. Celebrating the Past ... Teaming Toward the Future (IEEE Cat. No.03CH37492), IEEE, 2003. doi:10.1109/oceans.2003.178458.

[21] H. Ishida, T. Nakamoto, T. Moriizumi, Remote sensing and localization of gas/odor source and distribution using mobile sensing system, in: Proceedings of International Solid State Sensors and Actuators Conference (Transducers '97), IEEE, 1997. doi:10.1109/sensor.1997.613711.

[22] L. Marques, A. T. D. Almeida, Electronic nose-based odour source localization, in: Proc. 6th International Workshop Advanced Motion Control., 2000. doi:10.1109/amc.2000.862822.

[23] R. A. Russell, Tracking chemical plumes in constrained environments, Robotica 19 (04). doi:10.1017/s0263574700003283.

[24] G. Kowadlo, R. Russell, Naïve physics for effective odour localisation, in: Proc. Australasian Conference on Robotics and Automation, 2003.

[25] A. J. Lilienthal, F. Streichert, A. Zell, Model-based shape analysis of gas concentration gridmaps for improved gas source localisation, in: Proc. IEEE International Conference on Robotics and Automation (ICRA), 2005.

[26] R. A. Russell, A. Bab-Hadiashar, R. L. Shepherd, G. G. Wallace, A comparison of reactive robot chemotaxis algorithms, Robotics and Autonomous Systems 45 (2) (2003) 83–97. doi:10.1016/s0921-8890(03)00120-9.

[27] R. A. Russel, A ground-penetrating robot for underground chemical source location, in: Proc. Intelligent Robots and Systems (IROS), IEEE/RSJ International Conference on Intelligent Robots and Systems, 2005.

[28] L. Marques, U. Nunes, A. T. de Almeida, Olfaction-based mobile robot navigation, Thin Solid Filmsdoi:10.1016/s0040-6090(02)00593-x.

[29] A. Lilienthal, T. Duckett, Building gas concentration gridmaps with a mobile robot, Robotics and Autonomous Systems 48 (1) (2004) 3–16. doi:10.1016/j.robot.2004.05.002.

[30] G. Ferri, E. Caselli, V. Mattoli, A. Mondini, B. Mazzolai, P. Dario, SPIRAL: a novel biologically-inspired algorithm for gas/odor source localization in an indoor environment with no strong airflow, Robotics and Autonomous Systems 57 (4) (2009) 393–402. doi:10.1016/j.robot.2008.07.004.

[31] S. M. Mamduh, K. Kamarudin, S. M. Saad, A. Y. M. Shakaff, A. Zakaria, A. H. Abdullah, Braitenberg swarm vehicles for odour plume tracking in laminar airflow, in: 2013 IEEE Symposium on Computers & Informatics (ISCI), IEEE, 2013. doi:10.1109/isci.2013.6612365.

[32] Y. Takei, Y. Shimizu, K. Hirasawa, H. Nanto, Braitenberg's vehicle-like odor plume tracking robot, in: IEEE SENSORS 2014 Proceedings, IEEE, 2014. doi:10.1109/icsens.2014.6985243.

[33] A. Lilienthal, T. Duckett, Experimental analysis of gas-sensitive Braitenberg vehicles, in: Proc. Advanced Robotics, Vol. 18, Informa UK Limited, 2004, pp. 817–834. doi:10.1163/1568553041738103.

[34] R. P. Croll, Gastropod chemoreception, Biological Reviews 58 (2) (1983) 293–319. doi:10.1111/j.1469-185x.1983.tb00391.x.

[35] R. Matsuo, S. Kobayashi, M. Yamagishi, E. Ito, Two pairs of tentacles and a pair of procerebra: optimized functions and redundant structures in the sensory and central organs involved in olfactory learning of terrestrial pulmonates, The Journal of Experimental Biology 214 (6) (2011) 879–886. doi:10.1242/jeb.024562.

[36] A. Gomez-Marin, M. Louis, Active sensation during orientation behavior in the Drosophila larva: more sense than luck, Current Opinion in Neurobiology 22 (2) (2012) 208–215. doi:10.1016/j.conb.2011.11.008.

[37] H. Ishida, G. Nakayama, T. Nakamoto, Controlling a gas/odor plume-tracking robot based on transient responses of gas sensors, IEEE Sensors Journal 5 (3) (2005) 537–545. doi:10.1109/JSEN.2004.839597.

[38] T. Lochmatter, X. Raemy, L. Matthey, S. Indra, A. Martinoli, A comparison of casting and spiraling algorithms for odor source localization in laminar flow, in: Proc. IEEE International Conference on Robotics and Automation, California, USA, 2008. doi:10.1109/robot.2008.4543357.

[39] T. Lochmatter, A. Martinoli, Simulation experiments with bio-inspired algorithms for odor source localization in laminar wind flow, in: Proc. Seventh International Conference on Machine Learning and Applications, California, USA, 2008. doi:10.1109/icmla.2008.128.

[40] M. Awadalla, T.-F. Lu, Z. F. Tian, B. Dally, Z. Liu, 3D framework combining CFD and MATLAB techniques for plume source localization research, Building and Environment 70 (2013) 10–19. doi:10.1016/j.buildenv.2013.07.021.

[41] B. Gao, H. Li, F. Sun, 3D moth-inspired chemical plume tracking, in: Proc. IEEE Conference on Robotics and Biomimetics, 2015. doi:10.1109/robio.2015.7419031.

[42] Y. Tian, W. Li, A. Zhang, J. Yu, Q. Zhang, Y. Li, From simulation to validation: moth-inspired chemical plume tracing with an autonomous underwater vehicle, in: 2014 Oceans - St. John's, IEEE, 2014. doi:10.1109/oceans.2014.7002997.

[43] N. Voges, A. Chaffiol, P. Lucas, D. Martinez, Reactive searching and infotaxis in odor source localization, PLOS Computational Biologydoi:10.1371/journal.pcbi.1003861.

[44] M. Muhtadi, T. Nakamoto, Optimal estimation method of temporal odor concentration profile for plume tracking in dynamic turbulent environment, IEEJ Transactions on Sensors and Micromachines 138 (1) (2018) 15–22. doi:10.1541/ieejsmas.138.15.

[45] A. Marjovi, L. Marques, Multi-robot olfactory search in structured environments, Robotics and Autonomous Systems 59 (2011) 867–881. doi:10.1016/j.robot.2011.07.010.

[46] S. Shigaki, T. Sakurai, N. Ando, D. Kurabayashi, R. Kanzaki, Time-varying moth-inspired algorithm for chemical plume tracing in turbulent environment, IEEE Robotics and Automation Letters 3 (1) (2018) 76–83. doi:10.1109/LRA.2017.2730361.

[47] T. Nakamoto, H. Ishida, T. Moriizumi, An odor compass for localizing an odor source, Sensors and Actuators B: Chemical 35 (1-3) (1996) 32–36. doi:10.1016/s0925-4005(96)02009-6.

[48] P. Neumann, V. H. Bennetts, A. J. Lilienthal, M. Bartholmai, J. H. Schiller, Gas source localization with a micro-drone using bio-inspired and particle filter-based algorithms, Advanced Robotics 27 (9) (2013) 725–738. doi:10.1080/01691864.2013.779052.

[49] K. S. Eu, K. M. Yap, Chemical plume tracing: a three-dimensional technique for quadrotors by considering the altitude control of the robot in the casting stage, International Journal of Advanced Robotic System 15 (1) (2018) 1–21. doi:10.1177/1729881418755877.

[50] T. Lochmatter, A. Martinoli, Theoretical analysis of three bio-inspired plume tracking algorithms, in: Proc. IEEE International Conference on Robotics and Automation, Kobe, Japan, 2009. doi:10.1109/robot.2009.5152686.

[51] M. Muhtadi, T. Nakamoto, Plume tracking strategy in turbulent environment using odor sensor with time constant, Sensors and Materials 30 (9) (2018) –.

[52] J. A. Farrell, J. Murlis, X. Long, W. Li, R. Carde, Filament-based atmospheric dispersion model to achieve short time-scale structure of odor plumes.doi:10.21236/ada399832.

[53] Y. Tian, W. Li, A. qun Zhang, A lagrangian particle random walk model for simulating a deep-sea hydrothermal plume with both buoyant and non-buoyant features, China Ocean Engineering 27 (2) (2013) 215–230. doi:10.1007/s13344-013-0019-7.

[54] A. Lilienthal, T. Duckett, Creating gas concentration gridmaps with a mobile robot, in: Proc. IEEE/RSJ Intl. Conference on Intelligent Robots and Systems, 2003.

[55] A. Loutfi, S. Coradeschi, A. J. Lilienthal, J. Gonzalez, Gas distribution mapping of multiple odour sources using a mobile robot, Robotica 27 (2009) 311–319.

[56] J. Hinze, Turbulence, McGraw - Hill, New York, 1975.

[57] H. Ishida, T. Nakamoto, T. Moriizumi, Remote sensing of gas/odor source location and concentration distribution using mobile system, Sensors and Actuators B: Chemical 49 (1-2) (1998) 52–57. doi:10.1016/s0925-4005(98)00036-7.

[58] J. Kowalik, M. R. Osborne, Methods for unconstrained optimization problems, Elsevier, New York, 1968.

[59] R. F. Stengel, Stochastic optimal control, Wiley, New York, 1986.

[60] J. Kennedy, R. Eberhart, Particle swarm optimization, in: Proc. IEEE International Conference on Neural Networks, 1995.

[61] W. Jatmiko, K. Sekiyama, T. Fukuda, A PSO-based mobile robot for odor source localization in dynamic advection-diffusion with obstacles environment: theory, simulation and measurement, IEEE Computational Intelligence Magazine 2 (2) (2007) 37–51. doi:10.1109/mci.2007.353419.

[62] W. Jatmiko, P. Mursanto, B. Kusumoputro, K. Sekiyama, T. Fukuda, Modified PSO algorithm based on flow of wind for odor source localization problems in dynamic environments, WSEAS Transactions on Systems.
URL `http://dl.acm.org/citation.cfm?id=1455982.1455991`

[63] W. Jatmiko, A. Nugraha, R. Effendi, W. Pambuko, R. Mardian, Localizing multiple odor sources in a dynamic environment based on modified niche particle swarm optimization with flow of wind, WSEAS Transactions on Systems.

[64] W. Jatmiko, F. Jovan, R. Y. S. Dhiemas, M. S. Alvissalim, M. I. Fanany, A. Febrian, T. Fukuda, K. Sekiyama, Robots implementation for odor source localization using PSO algorithm, WSEAS Transactions on Circuits and Systems.

[65] A. Marjovi, L. Marques, Swarm robotic plume tracking for intermittent and time-variant odor dispersion, in: 2013 European Conference on Mobile Robots, IEEE, 2013. doi:10.1109/ecmr.2013.6698871.

[66] M. Vergassola, E. Villermaux, B. I. Shraiman, 'Infotaxis' as a strategy for searching without gradients, Nature 445 (7126) (2007) 406–409. doi:10.1038/nature05464.

[67] J.-G. Li, Q.-H. Meng, Y. Wang, M. Zeng, Odor source localization using a mobile robot in outdoor airflow environments with a particle filter algorithm, Autonomous Robots 30 (3) (2011) 281–292. doi:10.1007/s10514-011-9219-2.

[68] J. A. Farrell, S. Pang, W. Li, Plume mapping via hidden Markov methods, IEEE Transactions on System, Man, and Cybernetics-Part B: Cybernetics 33 (6) (2003) 850–863. doi:10.1109/tsmcb.2003.810873.

[69] Q.-H. Meng, W.-X. Yang, Y. Wang, M. Zeng, Collective odor source estimation and search in time-variant airflow environments using mobile robots, Sensors 11 (11) (2011) 10415–10443. doi:10.3390/s111110415.

[70] M.-L. Cao, Q.-H. Meng, B. Luo, M. Zeng, Experimental comparison of random search strategies for multi-robot based odour finding without wind information, Austrian Contributions to Veterinary Epidemiology 8. doi:10.5281/zenodo.33822.

[71] Z. Pasternak, F. Bartumeus, F. W. Grasso, Lévy-taxis: a novel search strategy for finding odor plumes in turbulent flow-dominated environments, Journal of Physics A: Mathematical and Theoretical 42 (43) (2009) 434010. doi:10.1088/1751-8113/42/43/434010.

[72] R. Emery, F. Rahbar, A. Marjovi, A. Martinoli, Adaptive levy taxis for odor source localization in realistic environmental conditions, in: 2017 IEEE International Conference on Robotics and Automation (ICRA), IEEE, 2017. doi:10.1109/icra.2017.7989407.

[73] A. Marjovi, L. Marques, Optimal swarm formation for odor plume finding, IEEE Transactions on Cybernetics 44 (12) (2014) 2302–2315. doi:10.1109/tcyb.2014.2306291.

[74] W. J. Bell, T. R. Tobin, Chemo-orientation, Biological Reviews 57 (2) (1982) 219–260. doi:10.1111/j.1469-185x.1982.tb00369.x.

[75] H. Schöne, Spatial Orientation: The Spatial Control of Behavior in Animals and Man, Princeton, NJ, Princeton University Press, 1984.

[76] L. Davidson, Fluid mechanics, turbulent flow and turbulence modeling, Lars Davidson, Division of Fluid Dynamics, Department of Applied Mechanics, Chalmers University of Technology, SE-412 96 Göteborg, Sweden, 2018.
URL $www.tfd.chalmers.se/\ lada/postscript\_files/solids - and - fluids\_turbulent - flow\_turbulence - modelling.pdf$

[77] MRIGlobal, Chemical sensor market survey, Tech. rep., MRIGlobal (September 2013).

[78] A. Ponzoni, E. Comini, I. Concina, M. Ferroni, M. Falasconi, E. Gobbi, V. Sberveglieri, G. Sberveglieri, Nanostructured metal oxide gas sensors, a survey of applications carried out at SENSOR Lab, Brescia (Italy) in the security and food quality fields, Sensors 12 (12) (2012) 17023–17045. doi:10.3390/s121217023.

[79] J. Hodgkinson, R. P. Tatam, Optical gas sensing: a review, Measurement Science and Technology 24 (1) (2013) 1–59.
URL http://iopscience.iop.org/article/10.1088/0957-0233/24/1/012004/pdf

[80] J. W. Strutt, B. Rayleigh, The theory of sound, Vol. 1, Maccmillan and Co, London, 1987.

[81] F. A. Angona, The absorption of sound in gas mixtures, Tech. Rep. V, Dept. Physics, University of California (1953).

[82] S. Phillips, Y. Dain, R. M. Lueptow, Theory for a gas composition sensor based on acoustic properties, Measurement Science and Technology.

[83] Linde Gases Division, Linde AG, Gas chromatography. With HiQ(R) specialty gases.
URL `http://hiq.linde-gas.com/en/analytical_methods/gas_chromatography/index.html`

[84] R. E. Cavicchi, Calorimetric sensors, Chemical Science and Technology Laboratory, National Institute of Technology, Gaithersburg, MD 20899 301 975 3970, USA.

List of publications

Paper

1. M. Muhtadi, T. Nakamoto, “Plume Tracking Strategy in Turbulent Environment using Odor Sensor with Time Constant”, Sensors and Materials, Vol. 30, No. 9.

2. M. Muhtadi, T. Nakamoto, “Optimal estimation method of temporal odor concentration profile for plume tracking in dynamic turbulent environment”, IEEJ Transactions on Sensors and Micromachines, Vol. 138, No. 1, pp. 15-22, 2018.

International conference

1. **Oral presentation**: M. Muhtadi, T. Nakamoto, “Odor Source Localization Strategy using Multiple Sensor Nodes in Dynamic Turbulent Environment”, Digital Olfactory Society, December 2016.

2. **Poster presentation**: M. Muhtadi, T. Nakamoto, “Odor Source Localization Strategy using Multiple Sensor Nodes for Dynamic Simulated Environment”, International Symposium on Biomedical Engineering, November 2016.

3. **Oral presentation**: M. Muhtadi, T. Nakamoto, “Combined Chemotaxis-infotaxis Strategy for Odor Source Localization Using Mobile Sensor Nodes”, The 11th Annual IEEE International Conference on Nano/Micro Engineered & Molecular Systems, April 2016.

Domestic conference

1. **Poster presentation**: M. Muhtadi, T. Nakamoto, “Odor source localization strategy under environment with obstacles and dynamic turbulent airflow”, Sensor Symposium, October 2017.

2. **Oral presentation**: M. Muhtadi, T. Nakamoto, "Odor Source Localization Strategy using Multiple Sensor Nodes under Simulated Dynamic Turbulent Environment", The 2017 annual meeting record of IEE Japan, March 2017.

3. **Oral presentation**: M. Muhtadi, T. Nakamoto, "Combined Chemotaxis-infotaxis Strategy for Odor Source Localization Using Mobile Sensor Nodes", The 2016 annual meeting record of IEE Japan, March 2016.